Final Report 2000-10

Research

Analysis of Electrical Capsule Pipeline Systems

Technical Report Documentation Page

1. Report No.	2.	3. Recipient's Accession No.
MN/RC - 2000-10		

4. Title and Subtitle	5. Report Date
ANALYSIS OF ELECTRICAL CAPSULE PIPELINE SYSTEMS	March 2000
	6.

7. Author(s)	8. Performing Organization Report No.
Yiyuan J. Zhao, Thomas S. Lundgren and John M. Sampson	

9. Performing Organization Name and Address	10. Project/Task/Work Unit No.
University of Minnesota Department of Aerospace Engineering and Mechanics 110 Union Street, S.E. Minneapolis, MN 55455	11. Contract (C) or Grant (G) No. c) 74708 wo) 51

12. Sponsoring Organization Name and Address	13. Type of Report and Period Covered
Minnesota Department of Transportation 395 John Ireland Boulevard St. Paul, Minnesota 55155	Final Report
	14. Sponsoring Agency Code

15. Supplementary Notes

16. Abstract (Limit: 200 words)

This report discusses the major technical issues, environmental impacts, and economic factors for the design and analysis of the electrical pipeline system.

Researchers reviewed the history and related work on pipeline transportation, as well as linear electric motors, analyzed basic components for an electrical pipline system, and devised and compared se veral possible system configurations. They selected a moving-primary linear induction motor configuration for medium-0to long-range freight transportation.

For this system configuration preliminary designs are conducted on capsule structure, linear induction motor units, and pipe tubes. A comprehensive computer simulation program is coded based on governing equations of motion. Researchers conducted system operation design and simulations by using the computer program.

17. Document Analysis/Descriptors		18. Availability Statement
Freight pipelines		No restrictions Document available from:
Tube transportation	Capsules	National Technical Information Services,
Linear electric propulsion	Aerodynamics	Springfield, Virginia 22161

19. Security Class (this report)	20. Security Class (this page)	21. No. of Pages	22. Price
Unclassified	Unclassified	128	

ANALYSIS OF ELECTRICAL CAPSULE PIPELINE SYSTEMS

Final Report

Prepared by

Yiyuan J. Zhao and Thomas S. Lundgren
Department of Aerospace Engineering and Mechanics
University of Minnesota

and

John M. Sampson
Office of Environmental Services
Minnesota Department of Transportation

Published by

Minnesota Department of Transportation
Office of Research Services
First Floor
395 John Ireland Boulevard, MS 330
St Paul, Minnesota 55155

March 2000

Disclaimer

Acknowledgments

This project is supported by the Minnesota Department of Transportation. The authors would like to acknowledge and thank the following individuals for their participation on the Technical Advisory Panel for this project and contributions to this document:

Jay Koski	Mn/DOT Office of Research Administration
Greg Paul Busacker	Mn/DOT Environmental Services

Mr. W. Vandersteele at Ampower, Inc. provided many valuable comments during the course of the research.

TABLE OF CONTENTS

List of Tables

List of Figures

Executive Summary

Pipeline transportation systems have many distinct advantages. These systems eliminate potential dangers to human presence and relieve surface congestion. Underground pipeline systems have little impact on environmental surroundings. In addition, a pipeline system can be fully automated, and operated around the clock and regardless of weather conditions. In comparison with a subway system, a pipeline system is easier to build and to maintain.

For the last 150 years, pneumatic pipeline systems have been used to provide highly reliable and safe transportation of mail, documents, cash, and tools. Pneumatic pipelines employ air pressure difference to propel capsules. As a result, pneumatic pipelines suffer from short haul range, high noise level, and poor energy efficiency. Coupled with technological limitations in construction in the past, large scale pneumatic pipeline systems have been considered infeasible and dubbed the name of "pipe dream".

Over the last half century, great advances have been made in linear electric motors, construction equipment, and computers. As a result, a pipeline system powered by linear electric motors and automated by on-board computers has become feasible. This system can be designed to be highly safe and reliable, energy-efficient, and friendly to the environment. It can be fully automated and operated over a long distance. Such a system, called an electrical pipeline system, represents a promising mode of transportation for the 21st century.

This report discusses major technical issues, environmental impacts, and economic factors for the design and analysis of an electrical pipeline system. Specifically, history of and related work on pipeline transportation as well as linear electric motors are reviewed. Basic components for an electrical pipeline system are analyzed. Several possible system configurations are devised and compared. A moving-primary linear induction motor configuration is selected for medium to long range freight transportation. For this system configuration, preliminary designs are conducted on capsule structure, linear induction motor units, and pipetubes. Governing equations of motion are developed from which a comprehensive computer simulation program is coded. System operation design and simulations are conducted using the computer program.

1. Introduction

The last several decades have witnessed significant increase in both surface and air traffic. Today, most human movement is achieved with a combination of personal automobiles and air flight, whereas freight transportation is mainly achieved by long overhaul trucks. At this point, both the highway system and air traffic system are approaching saturation. Based on a linear projection of 1960-1992 data, it was estimated that truck traffic will increase by 50% over the 1990 level by the year 2020 [1]. Efforts are being made to enhance the capacities of existing transportation infrastructures. At the same time, such a significant projected traffic increase calls for the examination of new transportation infrastructure concepts.

Recognizing the potential problem, the U.S. Congress enacted an inter-modal transportation act in 1991 [2], stating the importance of developing transportation systems that are economically profitable, environmentally sound, and can move people and goods in an energy-efficient manner.

Any future alternative transportation system should take advantage of technological advances in the last several decades. Such a system should have some or all of the following qualities. (1) A candidate system should be able to provide highly reliable, safe, and secure transportation of people and/or freight. (2) Such a system should be able to be operated with full automation, and regardless of weather conditions. (3) It is preferable that such a system use electric power, and produce little pollution and intrusion to the environment. (4) System operation should be energy-efficient. (5) Finally, any proposed system should decrease the current ground/air traffic congestion.

This report examines a pipeline transportation system that can potentially achieve these qualities. In such a system, capsules are propelled through pipelines by linear electric motors. To distinguish from traditional pneumatic pipeline systems, the pipeline system directly powered by linear electric motors will be called **electrical pipelines**. Figure 1.1 shows a schematic drawing of an electrical pipeline system.

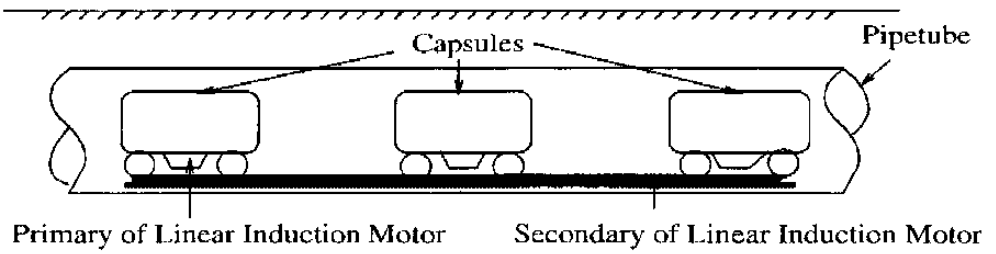

Figure 1.1 An Electrical Capsule Pipeline System

There are other transportation systems that contain the pipeline name. Examples of these systems include oil and gas pipelines, water and sewer pipelines, pipelines for coal and other slurry commodities, and hydro capsule pipelines that use water or other fluid to propel capsules through the pipes. Capsule pipeline systems studied here are distinguished by the close fit between capsules and pipeline tubes. As such, capsule pipeline systems also differ from underground subway systems.

1.1 Pipeline Transportation

Human kind has been fascinated for a long time by the security and full automation potential that a pipeline transportation system offers. George Medhurst seems to be the first person who systematically proposed and documented pneumatic pipeline systems both for freight transportation and for passenger movement [3]. Since that time, pipeline systems of different sizes have been used for various applications even to this day.

All historical pipeline systems were pneumatically powered and often referred to as pneumatic capsule pipelines. In pneumatic capsule pipelines, capsules are propelled by differential air pressure. These systems have been providing reliable freight transportation around the world for over 150 years [4]. Among various possible applications, pneumatic pipelines can be used for rapid movement of high priority documents. Such systems are called *pneumatic dispatch systems*, and use pipelines with diameters ranging from one and half inches to six inches. Pneumatic dispatch systems have been used to move telegraphs and messages, and to transmit mail. Some pneumatic systems were used to transmit

cash, and to transfer paper documents, small tools, etc. The Federal Aviation Administration used pneumatic dispatch to move flight strips from towers to en-route controllers. Pneumatic pipeline systems have also been used for bulk material handing and for package/mail delivery. These systems generally have diameters between 20 to 40 inches, and employ wheels on capsules. These systems continue to be used today, especially in the United States, Japan, and Russia.

Unfortunately, pneumatic capsule pipelines have some serious disadvantages that have prevented large diameter pneumatic pipelines (with diameters ranging between 6 to 15 ft) from being widely used. These systems could potentially be used for both freight transportation and passenger movement. In a pneumatic pipeline system, aerodynamic drag on a capsule is the driving force. This would require a tight seal between capsules and interior surfaces of pipelines. Air leakage necessitates the use of booster pumps to transport cargos beyond a distance of several miles. Since capsules cannot go through the pumps, it becomes necessary to interpose a set of valves and airlocks through which the capsules can bypass the booster pumps. In addition, pneumatic pipelines suffer from low energy efficiency and high noise level. Coupled with the fact tunneling construction was very expensive and challenging until recently, these system concepts were deemed impossible and were dubbed "pipe dreams."

Over the last several decades, great technological advances have been made. In particular, advances in linear electric motors, computer technologies, and construction equipment have made a fully automated electrical capsule pipeline concept feasible and attractive. We now briefly examine developments and applications of linear electric motors.

1.2 Development of Linear Electric Motors

Linear electric motors use principles of electromagnetic interactions and convert electrical energy into linear translational motion. The first concept of linear electric motors was patented in 1841 [5]. Since then, numerous innovations have been made in the design and construction of linear motors until several decades ago [6]. The basic configurations

of electric machines have remained essentially the same for the past several decades and will most likely remain so for many years to come. On the other hand, technologies of solid-state semiconductors, which can be used to control electric machines efficiently, have made significant progress over the last several decades.

There are two basic types of linear motors: linear induction motors (LIM) and linear synchronous motors (LSM). Both types of linear motors have been used in transportation systems. Table 7 in Ref. [7] contains a detailed list of transportation projects that employ linear motors. These applications show that linear motor technologies are mature for transportation systems. Among these applications, the Urban Transport Development Corporation of Canada developed a LIM-propelled rapid transit system with steel wheels on a steel rail track suspension [8]. Three such systems have been employed at Toronto Greater Metro in 1985, Vancouver in 1985, and Detroit in 1987. A top speed of 24 m/s or 54 mph can be achieved by supplying the LIM from a 0-60 Hz alternating current input, with a nominal air gap of 8 to 11 mm.

In another example, the Maglev transit link between Birmingham Airport and Birmingham International Railway Station has been in continuous use since 1984. This system uses a single-sided, short stator LIM for propulsion and attractive direct current electromagnetic levitation. Power is supplied through 600 V direct current power rails and current collectors. On-board power is then used to supply both the levitation magnetic control circuit and the LIM variable frequency supply inverter [9-11]. A speed of 15 m/s (33.5 mph) can be achieved, and a nominal air gap of 15 mm is required.

Japan Airlines in cooperation with Sumitomo Electric Industries developed a 16 ton, 48 passenger Maglev vehicle called HSST 03 [12]. The propulsion forces in this system are provided by six short-stator single-sided LIMs, supplied via power rails and current collectors. Suspension is provided by a set of attractive dc electromagnets.

In yet another example, a prototype Maglev system using a long stator linear synchronous motor (LSM) has been developed at Emsland, Germany. This system, better known as TRANSRAPID, uses an active track where primary windings are mounted on

the ground track. The use of an active track simplifies on-board power requirements, at the expense of a large impedance of the active track and the need for a vehicle position detection winding along the track [13].

In the United States, research on high-speed trains essentially stopped at early 1970's and seems to be reviving now. Currently, several maglev projects are on the drawing boards in Nevada, California, Florida, Maryland and Pennsylvania [14].

1.3 Main Features of Electrical Pipeline Systems

Linear electric motors can be used in capsule pipeline systems to power capsule motions, as shown in Figure 1.1. The use of electric motors would retain all the advantages of a pipeline system and yet eliminate disadvantages of pneumatic propulsion. Advantages of an electrical pipeline system that can be achieved by its very nature and by proper design are summarized below.

(1) Such a system would provide a highly reliable, safe, and secure mode of transportation, absent of external intrusions. Historically, pneumatic freight pipeline systems have had high operational reliability and essentially no accidents. Linear electric motors can be used for thrusting as well as braking, which offers another degree of operational safety. The concealed pipeline environment does not cause any traffic accidents with other traffic or dangers to human presence. Pipeline systems are closed and can thus be operated regardless of weather conditions. This is an important advantage compared to air and surface transportation.

(2) Such a system provides an energy-efficient way of transportation. Linear motors can be designed to be highly efficient compared to other modes of transportation. Regenerative braking in linear motors converts capsule kinetic energy into electricity. In addition, linear electric motors in general require low maintenance effort.

(3) An electrical pipeline system can be fully automated. The controlled pipeline environment, without weather effect and external intrusion, is ideal for automated operation. Linear motors can be efficiently controlled through solid-state semiconductor devices.

The recent advances in radar, moving vehicle position detection, and computer technology can all be employed to develop a fully automatic, around the clock pipeline system.

(4) An electrical pipeline system is friendly to the environment. The use of electric power produces little direct air and noise pollution. Pipelines buried underground would have little effect on the surroundings once installed. In addition, capsules and pipelines can be designed properly to shield electromagnetic wave radiation.

(5) The concealed system does not interfere with surface human movement and can reduce the current surface/air traffic congestion. If the proposed system were to replace trucks, it can alleviate the highway congestion problem partially caused by trucks, and reduce the wear-and-tear of trucks on highways and the associated maintenance costs. Compared to subway systems, concealed pipeline systems do not need to be buried as deep and are less costly.

The coming of the computer age and information superhighways has presented many opportunities as well as challenges. Many people have already used the world wide web on the Internet for shopping and information search. This trend will definitely increase with time. The effective use of the Internet will place high demands on reliable, weather-proof, intrusion-proof, and on-time freight delivery. An electrical pipeline system has the potential to be part of this system.

The proposed electrical pipeline system also has two potential problems. (1) A significant problem in the concealed pipeline system is the heat generated by losses in electric motor windings, mechanical friction, and aerodynamic resistance. Especially with closely-spaced multiple capsules operating at high speeds, heat ventilation and cooling will become crucial. (2) The proposed electrical pipeline system is a high capital, low operating cost system. Substantial initial investment on the infrastructure is needed.

1.4 Related Work

The idea of electrical capsule pipeline transportation is not completely new. In 1984, Ampower Corporation of Alpine, New Jersey proposed and patented a capsule pipeline system powered by linear induction propulsion [15], with a pipeline diameter of 2 meters and a speed of 60 mph. Economic analysis was conducted to demonstrate the feasibility of the proposed system. Swiss researchers proposed a cross-country high-speed pipeline transportation system for passengers, powered by linear induction motors and magnetic levitation. This system would use a 4.5 meter diameter pipeline and operate at a speed of 250 to 300 km/hr. Air resistance is reduced through evacuation of the tunnel [16]. The NASA "New Millienium Transportation System" proposes a hypervelocity underground system operating in vacuum tunnels at speeds up to 4000 mph [17]. Researchers in the Netherlands are also developing an electrical capsule pipeline system for transporting freight out of the Amsterdam International Airport to a suburban warehouse [18]. However, little technical detail is known at this time for any of these systems. In particular, the potential heating problem was not discussed.

Recently, Japanese researchers have constructed and tested a prototype pipeline transportation system powered by linear synchronous motors [19, 20]. This system has a pipeline diameter of 300 mm or 500 mm and operates at a maximum speed of 10 m/s or 22 mph. This system is used for material handling within a certain range. It is the first demonstrated design and testing of an electrical capsule pipeline system. Apparently, heating is not a problem because the system transports a single capsule or two connected capsules at a time, and the capsule speed is low.

1.5 Potential Applications

Before proceeding to technical studies on electrical pipeline systems, we will now discuss some potential applications of such a system concept. Different applications would have different requirements on the electrical system and thus would result in different

designs. In particular, freight transportation and human movement have different characteristics. While safety is important for all systems, moving people requires flexibility, convenience, and speed; transporting freight requires cost-effectiveness, on-time delivery, and security in transit. The separation of freight transportation from human movement will increase the efficiency and safety of both [21]. Based on the spirit of separation of freight transportation from passenger movement, the proposed electrical pipeline system can be used in the following scenarios.

(1) The electrical pipeline system can be used in freight transportation over short corridors, such as airports to distribution centers. In this case, operating speed is not too high. Continuous windings of electrical wires are feasible. High operating efficiency is desirable.

(2) The electrical pipeline system can be used to handle sensitive materials over short distances and/or within the same department. This application includes material movement in a hospital, or in a large complex. In this case, the operating speed is limited while low vibration and secure movement are required. Again, continuous wire winding is feasible but high operating efficiency is not crucial.

(3) Electrical pipelines can be used for freight transportation over city pairs, such as Minneapolis/St. Paul to Duluth or to Chicago. This type of system has a medium to high operating speed, and prefers high operating efficiency. The long distance makes continuous wire winding too costly.

(4) Electrical pipelines can be used for a nation-wide network of underground freight pipelines similar to the highway system for freight transportation. Such a transportation infrastructure will greatly increase the cargo delivery capability throughout the nation. In this case, both high operating speed and high operating efficiency are desirable. A continuous wire winding is completely impractical. Therefore, a moving primary configuration should be used. Capsule switching and routing will be important issues. If desired operating speed exceeds a certain limit, some evacuation of pipelines may be needed.

(5) The proposed system concept can also be used for human movement. A human movement system needs to have smooth accelerations/decelerations, and has special requirements on capsule structures.

2. Component Modeling

In Appendix A, a capsule free-body diagram is presented and equations of capsule motion are derived. In this chapter, models of basic forces in an electrical pipeline system are examined. Forces acting on a capsule include (1) aerodynamic forces (lift, drag, and moment), (2) electric motor forces (thrust and normal force), (3) mechanical friction, (4) normal support force, and (5) gravity force. In order for capsules to move at a specified speed, the electric motor thrust must overcome aerodynamic drag on the capsule, mechanical friction on the wheels, and slope grade changes.

2.1 Capsule Aerodynamics

Effects of aerodynamic forces on a capsule can be expressed by lift, drag, and moment. Aerodynamic drag is the most important component of the three. It constitutes a major force on a capsule.

2.1.1 Aerodynamic Drag on a Capsule

Air pressure drag plays a different role in a pneumatic pipeline versus in an electrical pipeline system; causing many differences in the design of capsules and pipelines in the two systems. In a pneumatic pipeline system, capsules are moved by drag forces created by blowers. In an electrical pipeline system, on the other hand, capsules are moved by electric propulsion and capsule drag becomes a resistance to capsule motion. Therefore, it is important to minimize aerodynamic drag in capsule design.

The aerodynamic drag on a capsule is given by

$$D = \frac{1}{2}\rho(V - w)^2 A C_D \tag{2.1}$$

where ρ is the air density, V is the capsule speed, w is the flow speed, A is the capsule cross-sectional area, and C_D is the capsule drag coefficient. Detailed derivation of the capsule drag coefficient is given in Appendix B. The final result is given by

$$C_D = \frac{\beta}{(1-\beta)^2} + \frac{(1+\beta^{1/2})}{(1-\beta)^3}\frac{2l}{R}C_{fg} \tag{2.2}$$

where the friction coefficient is given approximately by the Blasius formula [22] [23].

$$C_{fg} = .316/4R_{eg}^{1/4}, \quad R_{eg} = \frac{2(R_T - R)v}{\nu} = \frac{2R_T(V-w)}{\nu(1+\beta^{1/2})} \tag{2.3}$$

Schlichting [23] favorably compares the Blasius friction coefficient formula with experiments for turbulent flow in pipes of noncircular cross section for a broad range of Reynolds numbers based on mean velocity and hydraulic diameter, and for Mach numbers up to one. Values of the drag coefficient obtained from Eq. (2.2) are very close to experimental results reported by Tsuji [24].

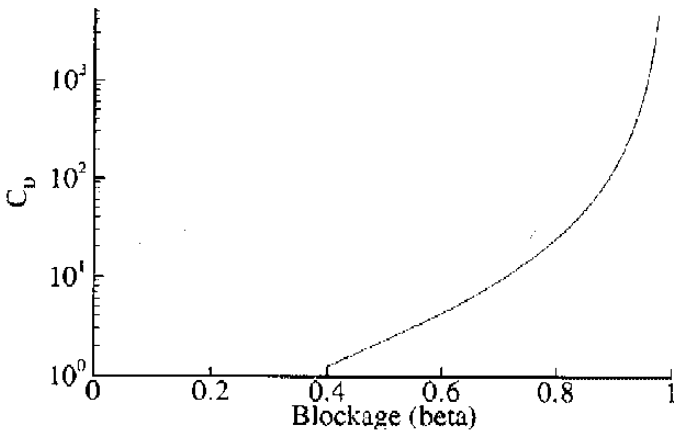

Figure 2.1 Capsule Drag Coefficient versus Blockage Ratio, $V - w = 25$ m/s.

The drag coefficient depends on the relative velocity $(V - w)$ through the friction coefficient. The drag coefficient is plotted versus β in Figure 2.1. It should be noted that when β is near one (full blocking) the drag coefficient can be 1000 or more. This does not necessarily mean that the drag itself is large because $(V - w)$ can become small enough to compensate for the large C_D.

2.1.2 Choking Phenomenon

The above drag coefficient was derived for incompressible flow. While in most cases the capsule has a fairly low velocity compared to the speed of sound, the velocity in the

gap is much larger and can approach sonic if the gap is small. If this occurs the analysis must be modified to account for the compressibility of air. When the gap velocity reaches the speed of sound, the mass flow through the gap is restricted and the flow is said to be "choked" [25]. Calculations reported by Hammitt [26] show that the drag coefficient stays close to the incompressible value until the gap Mach number nearly reaches one and then rapidly increases to a value which is easily double the incompressible value. This can occur at moderate capsule speeds if the gap is small.

Flow choking should be avoided during normal capsule operation. As a result, the gap must be large enough for high speed capsule operation. Correspondingly, capsule design speed is limited by a maximum value for the blockage area ratio. On the other hand, the choking phenomenon may be used as an aerodynamic braking technique. Specifically, fins that can be extended may be mounted on the capsule surface. These fins are held under the capsule surface during normal operation and can be extended to stop the capsule when necessary. The extensions can be controlled remotely in a central station, or triggered by a sensor mounted on the capsule nose to avoid collisions. This concept of aerodynamic braking is similar to the concept discussed in Tsuji, Morikawa & Seki [27].

2.2 Linear Electrical Propulsion

Electric machines operate based on two phenomena. (1) When a conductor is placed in a magnetic field with changing flux or is moved in a magnetic field, an electric voltage is induced on the conductor, as shown in Figure 2.2 (a). (2) When a current-carrying conductor is placed in a magnetic field, the conductor experiences a mechanical force, as shown in Figure 2.2 (b).

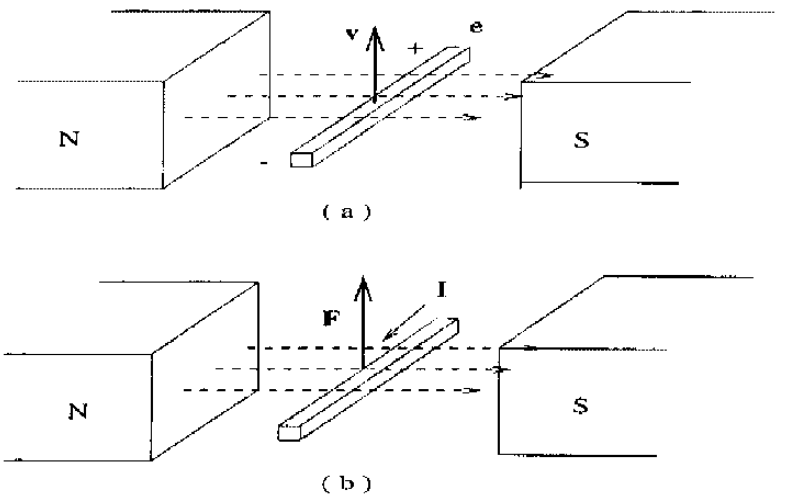

Figure 2.2 Basic Phenomena of Electromagnetic Interaction

A wide range of electric machines have been designed by using the above two principles. An electric machine that converts mechanical energy into electrical energy is called a generator, whereas an electric machine that converts electrical energy into mechanical energy is called a motor. Three types of electrical machines have been widely used for electromagnetic energy conversion: induction machines and synchronous machines that use alternating current (ac) supply, and direct current (dc) machines [28-31].

2.2.1 Rotary Electric Machines

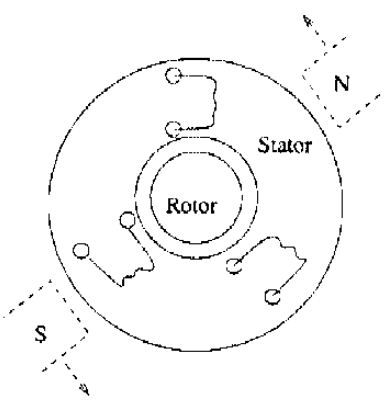

Figure 2.3 A Three-Phase Induction Machine

Figure 2.3 shows a three-phase induction machine. A three-phase winding is put in slots cut on the inner surface of the stator frame. The rotor consists of laminated ferromagnetic material with slots cut on the outer surface. In a squirrel-cage induction machine, aluminum or copper bars are embedded in the rotor slots and shorted at both ends by aluminum or copper end rings. The rotor can also be made of windings just like the stator, and is called a wound rotor. The squirrel-cage induction machine is simpler, more economical, and more rugged than the wound-rotor type. In an actual induction machine, the three-phase winding is distributed around the circumference of the stator or rotor. The end of the three-phase windings on the stator can be connected in a wye or a delta connection, depending on the requirement on input line voltage.

When connected to a three-phase alternating current supply, each phase produces a sinusoidally distributed magnetic field in space, pulsating along the phase axis and having a peak located along the axis. In each cycle of the current variation, the resultant magnetic field rotates in the air gap of the machine. This in effect creates a pair of magnets (for a two-pole machine) rotating in the air gap [Figure 2.3]. By the first basic phenomenon stated above (Faraday's law), this varying magnetic field will induce an electrical voltage thus create current in the rotor. By the second basic phenomenon stated above, interaction of the rotor that now contains induced voltage and current with the magnetic field will produce a force on the rotor; causing the rotor to rotate in the direction of magnetic field rotation.

Windings on the stator can be made to produce more than two poles. For a p-pole induction machine connected with a three-phase current of frequency f Hz, the revolutions per minute n (rpm) of the traveling magnetic field is

$$n_s = \frac{120f}{p}$$

This speed is called the *synchronous speed* of the machine. The rotor steady-state speed n is less than the synchronous speed. The *slip* s is defined as

$$s = \frac{n_s - n}{n_s}$$

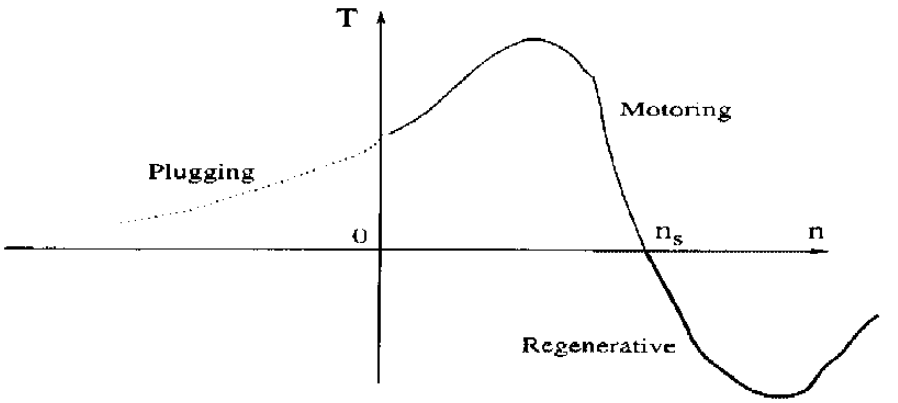

Figure 2.4 Induction Machine Torque-Speed Curve

Figure 2.4 shows a typical relationship between the torque an induction machine generates and the corresponding rotor speed. An induction machine can be operated in three modes: motoring, generating, and plugging. If the stator terminals are connected to a three-phase supply, the rotor will rotate in the direction of stator rotating magnetic field at a steady-state speed n that is less than the synchronous speed n_s. If the rotor rotates faster than the synchronous speed (or the synchronous speed is smaller than the current rotor speed), the induction machine operates as a generator and produces a generating torque. This mode can be used to provide *regenerative braking*. Finally, if the stator winding polarity is reversed, the induction machine will generate a torque opposite to the direction of rotor rotation. This torque is a braking torque.

Speed of an induction motor can be controlled by (1) changing the stator winding to alter the number of poles, (2) varying the input voltage, (3) varying the input frequency, and/or (4) varying the rotor resistance. Changing the input voltage can change the magnetic field intensity. Changing the input frequency can change the magnetic field intensity as well as the synchronous speed. Varying the rotor resistance can change the shape of the torque-speed curve and the maximum torque available.

In the electric machine terminology, field winding refers to the winding that generates the first magnetic field, whereas a voltage is induced in the armature winding. In an

induction machine, the stator winding is the field winding. The rotor winding, if it exists, is the armature winding. It is the opposite on a synchronous machine.

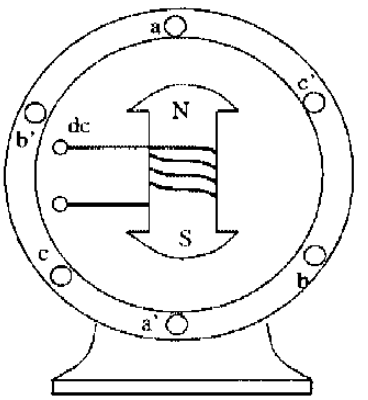

Figure 2.5 A Three-Phase Synchronous Machine

Figure 2.5 shows the basic structure of a three-phase salient-pole synchronous machine. The stator of a three-phase synchronous machine has a three-phase distributed winding similar to that of a three-phase induction machine. The stator winding is connected to a three-phase alternating current supply and is sometimes called the armature winding. In comparison, the rotor has the field winding that carries a direct current. The field winding on the rotor is normally fed from an external direct current source through slip rings and brushes. The field winding can also be replaced by permanent magnets.

Unlike induction machines, the rotating magnetic field in the air gap and the rotor in a synchronous machine rotate at the same speed (thus the name synchronous machine). A synchronous machine can be used either as a generator or a motor. When it is used as a generator, the rotor is rotated by a prime mover and the field current in the rotor winding establishes a revolving magnetic field in the air gap. The rotating flux so produced will change the flux linkage of the armature windings and will induce voltages in these stator windings. These induced voltages on different phases have the same magnitudes but are phased-shifted by 120 electrical degrees. The rotor speed and frequency of the induced voltage are related by

$$n_s = \frac{120\ f}{p} \tag{2.4}$$

where n_s is the rotor speed in rpm and p is the number of poles. When a synchronous machine is used as a motor, the stator winding is connected to a three-phase alternating current supply. If the rotor has started rotating at a speed close to the synchronous speed, the magnetic fields of the rotor and the stator will tend to align up with each other; causing the rotor to rotate at the synchronous speed, as shown in Figure 2.6.

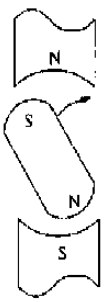

Figure 2.6 Principle of Synchronous Motor

However, a synchronous motor is not self-starting. This is because the rotating magnetic field produced by stator currents normally rotates very fast in the air gap, such as 3600 rpm. It is difficult for a rotor with a certain inertia to catch up automatically. One way of starting a synchronous motor is to use a frequency converter to control the synchronous speed in Eq. (2.4) so that the synchronous speed can be increased gradually. In another approach, a synchronous motor can be started as an induction motor. This approach requires additional winding on the rotor [28].

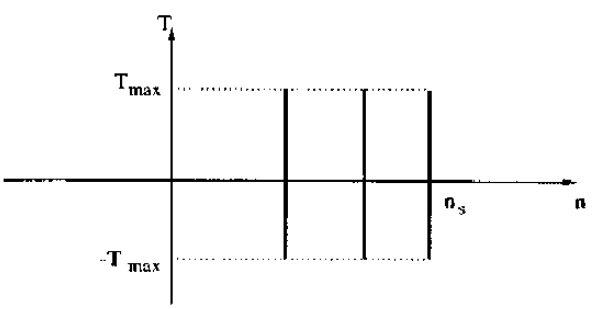

Figure 2.7 Synchronous Motor Torque-Speed Curve

A synchronous motor tends to lose synchronism under shock loads. Therefore, feedback control of rotor speed may be needed. On the other hand, a synchronous motor rotates at a constant speed even under load variation and voltage fluctuation, as long as the maximum required torque stays within a certain limit. Figure 2.7 shows a typical torque-speed curve for a synchronous motor. Synchronous motor speed can be controlled by varying the frequency on the stator winding.

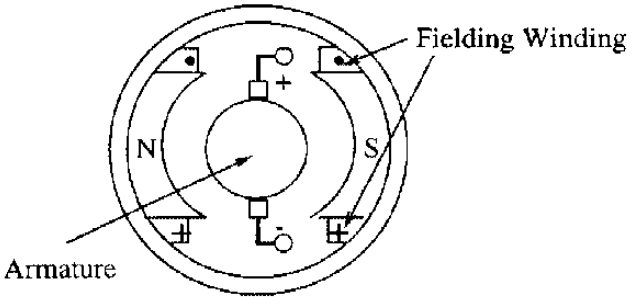

Figure 2.8 A DC Machine

Finally, dc machines convert direct current electrical energy into rotational mechanical motion or vice versa. In a dc machine, the field winding is placed on the stator and the armature winding on the rotor, as shown in Figure 2.8. A dc current is passed through the field winding to produce magnetic flux in the machine. Voltage induced in the armature winding is alternating. A mechanical commutator and a brush assembly are needed as a rectifier or inverter, which makes the armature terminal voltage unidirectional. When a dc machine is used as a generator, it is driven by a primer mover at a constant speed. Output from the armature terminals is dc electrical power. When a dc machine operates as a motor, the armature windings are connected to a dc supply. The rotor will develop a mechanical torque and power. In any case, a dc current is needed in the field winding on the stator.

All three types of rotary machines have been widely used for different applications. For transportation system drives such as transit systems or locomotive drives, dc motors have been used traditionally for many years, because dc motors offer easy speed control

over a wide range. However, dc motors require frequent maintenance (on brushes and commutators) and are expensive. Both induction motors and synchronous motors have fewer maintenance problems than dc motors. In addition, dc motors have been controlled by inserting resistance in series with motors and changing the resistance to regulate speeds. This method of speed control is not efficient because the extra resistance wastes some electrical energy. In comparison, the use of solid-state semiconductor devices for speed control consumes very little energy. Recent advances in solid-state semiconductor devices have made the speed control easy and inexpensive for both induction and synchronous motors.

The choice between an induction motor and a synchronous motor depends on desired operating speed and power level. Because of their higher initial cost compared to induction motors, synchronous motors are not suitable for applications at high speed or below 50 HP in the medium-speed range. For low-speed and high power applications, an induction motor is not necessarily cheaper than a synchronous motor due to its large amount of iron required to establish a high air gap flux density. Under similar conditions, induction motors are more rugged and less expensive than synchronous motors. On the other hand, induction motors require a more complex inverter control circuit, and have lower efficiency and lower power factors compared to synchronous motors. Synchronous motors are especially desirable for constant-speed operations. Permanent magnets can also be used on a synchronous motor, which will make the motor more rugged.

2.2.2 Linear Electric Motors

Conceptually, any rotary machine may be "unrolled" to yield a linear machine. In addition, linear machines can be built for which a rotary version is not feasible [29-34]. Linear electric machines are almost exclusively used as motors. Polyphase synchronous motors and induction motors both use alternating current as the input electricity source and represent the economically feasible choices for a pipeline system.

A linear induction motor (LIM) can be imaginatively obtained by unrolling a rotary induction motor. As shown in Figure 2.9, the stator is now called "primary" and rotor is called "secondary". Depending on the relative length of the primary and the secondary, a linear induction motor can be called a short-primary or a short-secondary LIM. Different from its rotary counterpart, a LIM can have either a moving primary or a moving secondary. Secondaries can be either plate or sheet (sometimes backed by ferromagnetic materials, called back iron), or the usual cage type. A wound-type secondary is rare. Stator windings of a LIM are similar to those of a rotary induction machine, except that often a primary of an LIM has half-filled end slots [29].

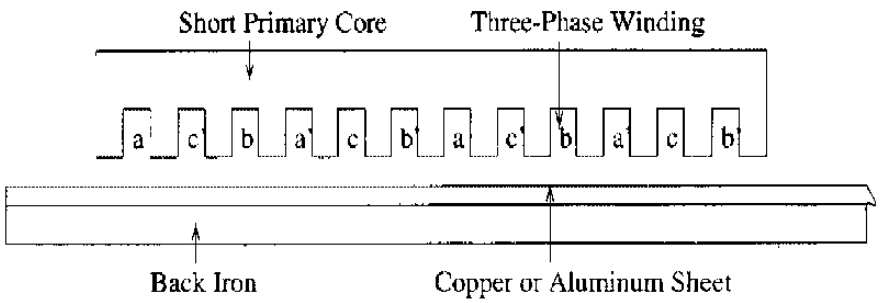

Figure 2.9 A Single-Sided Linear Induction Motor

A linear induction motor can also be obtained imaginatively by crushing a rotary motor. This linear induction motor would have two primaries and is called a double-sided linear induction motor (DSLIM, Figure 2.10). In comparison, Figure 2.9 shows a single-sided induction motor (SLIM). Both DSLIM and SLIM are called flat LIMs. There are also tubular LIMs. In addition, magnetic flux can be designed to be along the longitudinal or transverse directions.

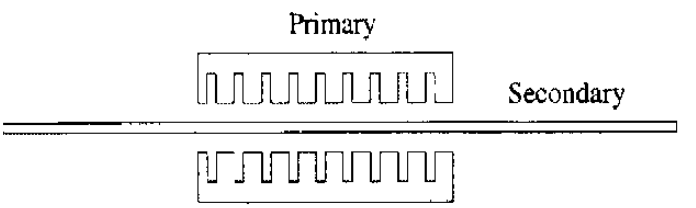

Figure 2.10 A Double-Sided Linear Induction Motor

The operating principle of a linear induction motor is similar to that of a rotary induction motor. When connected to a three-phase alternating current supply, the primary windings produce a magnetic field in the air gap traveling at a speed known as the synchronous speed

$$V_s = 2\tau f$$

where τ is the pole pitch (distance between two poles). Note that the synchronous speed does not depend on the number of poles. At steady-state, the secondary moves with respect to the primary at a speed V, which is smaller than the synchronous speed.

The thrust-velocity characteristic of a LIM is basically similar to the torque-speed characteristic of a rotary induction motor shown in Figure 2.4. However, a linear induction motor requires a larger air gap, typically 15-30 mm, whereas the air gap for a rotary induction motor is on the order of 1-1.5 mm. A LIM also operates at a larger slip, typically 0.15-0.2 compared with 0.02-0.05 in rotary motors. These differences result in lower power factors and a larger secondary loss (thus lower efficiency) in a linear motor. These effects result in a slightly different slope of the force-speed curve around the synchronous speed. In addition, end effect produces extra resistive loss and reduces the maximum thrust a rotor can produce [Figure 2.11].

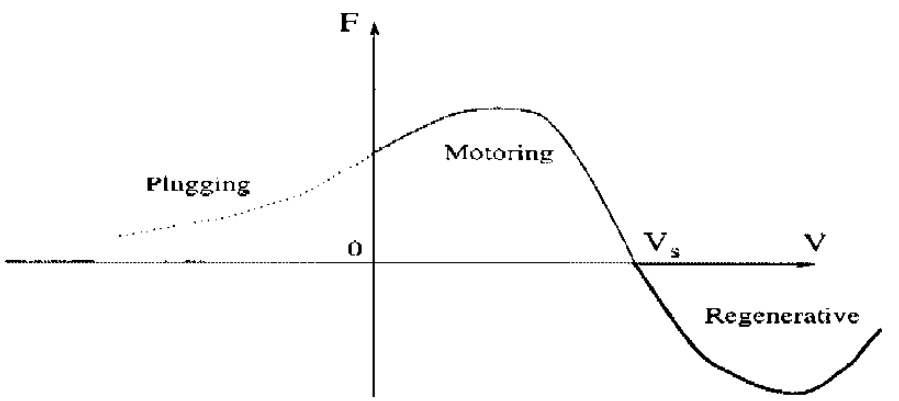

Figure 2.11 A Typical Linear Induction Motor Force-Speed Curve

In a single-sided linear induction motor, there is also a normal force between the primary and the secondary. This normal force is significant compared with the thrust

force. It is attractive for steel secondaries and can become repulsive at high slip for aluminum sheet secondaries [7, 29, 31].

A linear synchronous motor (LSM) has a similar operating principle as a rotary synchronous motor. Figure 2.12 shows a schematic drawing of a LSM, in which the primary has a three-phase winding. The secondary can have electromagnets (dc field winding), permanent magnets, or superconducting magnets. When the primary windings are connected to a three-phase ac supply, a traveling magnetic flux will be generated in the air gap that moves along the length of the primary. This air gap magnetic field will travel at a speed known as the synchronous speed

$$V_s = 2\tau f$$

where τ is the pole pitch, and f is the frequency of the ac supply. In steady-state operations, the magnets on the secondary will be synchronously locked with the traveling wave.

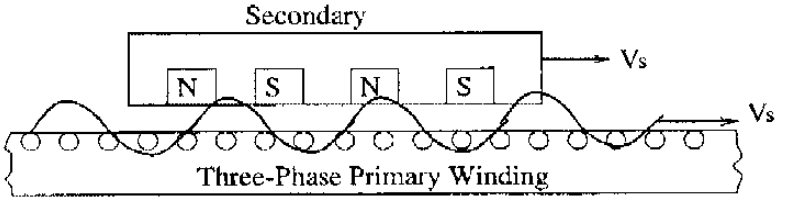

Figure 2.12 A Salient-Pole Linear Synchronous Motor

LSM is a constant speed machine in the presence of load variations and voltage fluctuations, if the required maximum thrust is within limits. The force-speed curve of a LSM is very similar to the torque-speed curve of a rotary LSM shown in Figure 2.7. In principle, a LSM could have either a moving field winding or a moving armature winding. In practice, a moving field winding with dc supply or permanent magnet is more practical. In other words, the three-phase primary winding is usually fixed. A LSM can operate at a leading power factor and better efficiency compared to a LIM. If powerful magnets such as superconducting magnets are used, a LSM can operate at a higher air gap. On the other hand, a LSM may lose synchronism in shock loads just as a rotary synchronous motor

would. At present, LSM has not been used as widely as LIM. On the other hand, LSM has a great potential in high-speed transportations, where a large air gap clearance is needed. In many countries, research is underway in developing high-speed vehicles with speeds up to 500 km/h. In short, the choice between LIM and LSM depends on many factors in a specific application.

Finally, linear levitation machines (LLM) are often used in conjunction with LIM or LSM to provide sufficient normal forces between primary and secondary for suspension. The so called "maglev" machines are based on the principle that, if a magnet moves over a conducting sheet, the eddy currents induced in the sheet will cause a normal force of repulsion between the magnet and the sheet. This principle can also be used to provide lateral guidance for a traveling vehicle.

2.2.3 Advantages of Linear Motors over Rotary Motors

Either LIM or LSM can be used for the proposed electrical pipeline system. Actually, rotary electric motors may also be used to drive capsules if the operating speed is low. In this case, rotary motors can either be used on the vehicle to drive the wheels or mounted on the ground to drive a conveyor belt.

In general, linear motors have two significant deviations from rotary machines. These deviations can be drawbacks at times. (1) In linear motors, normal forces do not automatically cancel out as in rotary machines. These normal forces may be attractive or repulsive, can vary in variable speeds LIM, and can be significant compared to thrust forces. Normal forces can sometimes be used to advantage. When normal forces are not desirable, proper designs can be used to minimize them. (2) There are end effects in linear motors because of the limited length of the primaries. As a result, operating efficiency of a linear motor is generally lower than its rotary counterpart.

On the other hand, linear motors have some unique advantages over rotary machines. (1) There is no need for a gearbox or rotary-to-linear conversion. Linear motors provide cleaner configurations and are easier to maintain than rotary motors. In particular, thrust

forces produced by rotary motors depend on the adhesion between the wheels and rail tracks, and are affected by the pipeline grade and external temperature. In addition, rotary motors on a capsule will make the useful capsule volume small. In contrast, linear motors generate direct propulsion, and can be used over steep grades or even vertically oriented pipelines. The use of linear motors reduces the wear-and-tear on wheels and tracks, and can withstand a hostile environment. This is especially desirable in a North America climate. (2) Linear motors can provide high direct acceleration and deceleration, and are especially suited for high speed motion. (3) Finally, linear motors provide convenient control of thrust and speed. Careful designs can be made to increase operation efficiency.

When all factors are considered, efficiencies of linear motors can be comparable to or even better than rotary motors in a pipeline system. Therefore, we will assume the use of linear motors in the electrical pipeline system.

2.2.4 Basic Relations in Linear Induction Motors

In the next chapter, several electrical pipeline system configurations using linear motors are compared, and a single-sided moving primary linear induction motor design is selected for a medium to long range electrical pipeline system. Here, some fundamental relations of linear induction motors are reviewed.

For a linear induction motor, the synchronous speed is a fundamental variable. The synchronous speed produced by a three-phase primary winding is given by,

$$V_s = 2\tau\ f \tag{2.5}$$

This is the speed with which the electromagnetic wave produced by the primary winding travels. At steady-state operations, the secondary moves with respect to the primary at a speed $V < V_s$. The *slip* is defined as

$$s = \frac{V_s - V}{V_s} = 1 - \frac{V}{V_s} \tag{2.6}$$

The *electromagnetic power* transmitted from the primary through the air gap to the secondary is

$$P_{\text{elm}} = P_{\text{out}} + \Delta P_2 = F\ V_s \tag{2.7}$$

where the mechanical output power of a LIM is

$$P_{\text{out}} = F\ V \tag{2.8}$$

From these relations, we have

$$P_{\text{out}} = \frac{V}{V_s} P_{\text{elm}} = (1-s) P_{\text{elm}} \tag{2.9}$$

$$\Delta P_2 = s P_{\text{elm}} \tag{2.10}$$

The total power input to a LIM consists of

$$P_{\text{in}} = \Delta P_1 + \Delta P_{\text{core}} + \Delta P_{\text{end}} + \Delta P_{\text{edge}} + P_{\text{elm}} \tag{2.11}$$

where ΔP's are various losses in a linear induction motor. The efficiency of a LIM operation can be defined as

$$\eta_e = \frac{P_{\text{out}}}{P_{\text{in}}} = \frac{(1-s)P_{\text{elm}}}{\Delta P + P_{\text{elm}}} \tag{2.12}$$

where ΔP represents all other losses except for the secondary loss. Appendix C provides an approximate expression for the LIM efficiency.

If the primary winding resistance is negligible and the magnetic circuit is unsaturated, the thrust force developed by a LIM can be predicted by the Kloss' formula

$$F = \frac{2F_{\text{max}}}{s/s_{sr} + s_{sr}/s} \tag{2.13}$$

where F_{max} is the maximum motor thrust, and s_{cr} is called critical slip. At $s = s_{cr}$, $F = F_{max}$.

For a flat LIM with a secondary that contains a ferromagnetic core, the normal force is given by

$$F_N = \frac{B_{\text{mz}}^2}{4\mu_0} A - \frac{B_{\text{mx}}}{B_{\text{mz}}} T \tag{2.14}$$

where $F_N > 0$ represents an attraction force. In this equation, the first term is caused by the attraction between the primary and the secondary ferromagnetic cores. The second term is an electromagnetic repulsive force and is caused by the action of eddy currents induced in the secondary conductors on the primary magnetic field. This second term is proportional to the thrust.

The effects of LIM normal force depend on specific applications. In the current application, normal forces affect capsule operations through rolling friction. Since the rolling friction coefficient is small for a metal wheel on a metal rail configuration and capsule weights are in general much larger than motor normal forces, the effects of motor normal forces are neglected in the current study.

2.2.5 Linear Induction Motor Speed Control

Control of the LIM speed can be achieved by changing the pole pitch τ, input voltage U, and/or input frequency f. A change in the pole pitch can be achieved in a discrete way by either designing two or more independent windings with different pole pitches or by reconnecting various parts of one winding. As a result, pole pitch change can provide two or more discretely different operating speeds. For a given linear induction motor, its operating speed can be changed by varying the input voltage U and/or the input frequency f. For a constant input voltage, a higher input frequency results in a smaller maximum thrust $F_{\max}$ and a larger synchronous speed. For a fixed input frequency, a higher input voltage results in a larger maximum thrust without changing the synchronous speed. Finally, the maximum thrust can be kept constant by keeping U/f at a constant.

For LIM speed control, a variable-frequency converter is needed as an interface between the utility power system (e.g. 60 Hz, 408 V) and a certain phase of induction motor primary winding. Variable-frequency converters can be divided into two categories. Indirect converters change an ac supply first into dc and then back to ac source (ac→dc→ac). Direct converters, on the other hand, change an ac supply of a fixed frequency directly

into an ac source of specified frequency (ac→ac). Direct converters are also called cyclo-converters.

Variable-frequency converters can be implemented by using solid-state semiconductor devices. These devices provide unidirectional flow of electrical current controlled either by the circuit or a control signal. Solid-state semiconductor devices can be classified into three groups: (1) diodes in which on and off states are controlled by the circuit, (2) thyristors, which are latched on by a control signal but must be turned off by the circuit, and (3) controllable switches, which are turned on and off both by control signals. The required control signals are usually very small. Typical response time constants for these devices are around 10^{-6} seconds. As a result, these devices can be used to control motions of linear motors easily and inexpensively. Further advances are still being made in these devices. Coupled with advances in feedback control theories, full capabilities of linear induction motors can now be utilized.

2.3 Friction Forces

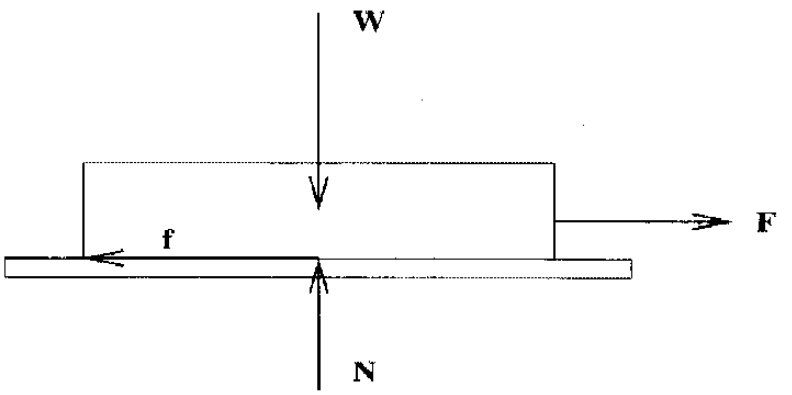

Figure 2.13 Definition of Sliding Friction

Mechanical friction exists in all physical systems [35-39]. A simple form of friction is called sliding friction. Friction force is defined as the resisting force tangential to the interface between two bodies when, under the action of an external force, one body moves

or tends to move relative to the other. In Figure 2.13, f represents the sliding friction and N is the normal force.

The use of wheels on a rail track can greatly reduce sliding friction. In pure rolling, the point of contact of the cylinder on the base plane remains stationary. If the cylinder and plane were both perfectly rigid, there would be a single point of contact. Frictional force would not consume any energy and the cylinder would continue to roll indefinitely in the lack of air resistive forces. However, there will be a slight ridge of contact points in real systems. A driving force must be applied to overcome another form of resistance to maintain motion. This resistance is called rolling friction (Figure 2.14).

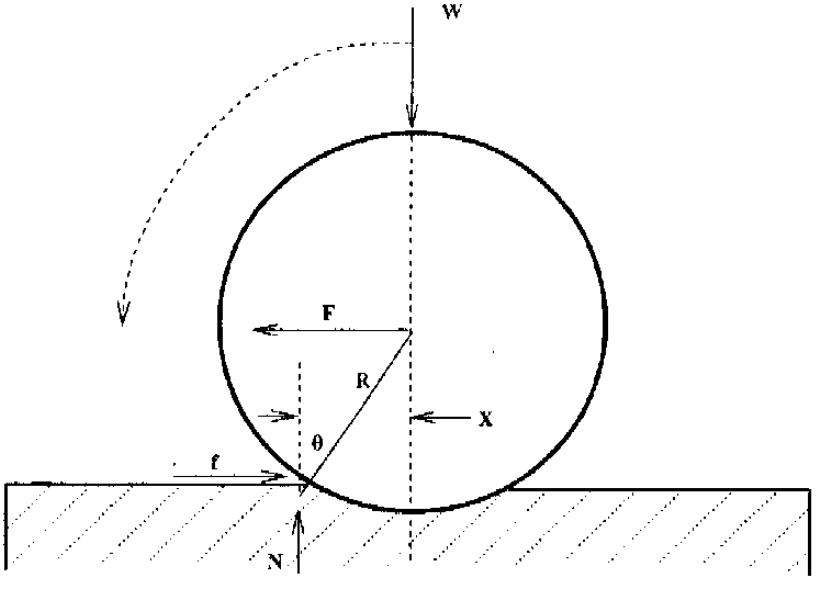

Figure 2.14 Rolling Friction

In early research, rolling friction was treated as a mechanical process in which the interaction of rough surfaces of absolutely rigid solid bodies was considered. Coulomb was the first to introduce the hypothesis of the dynamic nature of friction during rolling. In the classical equation

$$f = \mu_r \frac{N}{R} = f_r N \tag{2.15}$$

μ_r is the coefficient of rolling friction having the dimension of length, N is the normal load, R is the radius of the rolling body, and f_r is a dimensionless coefficient of rolling friction.

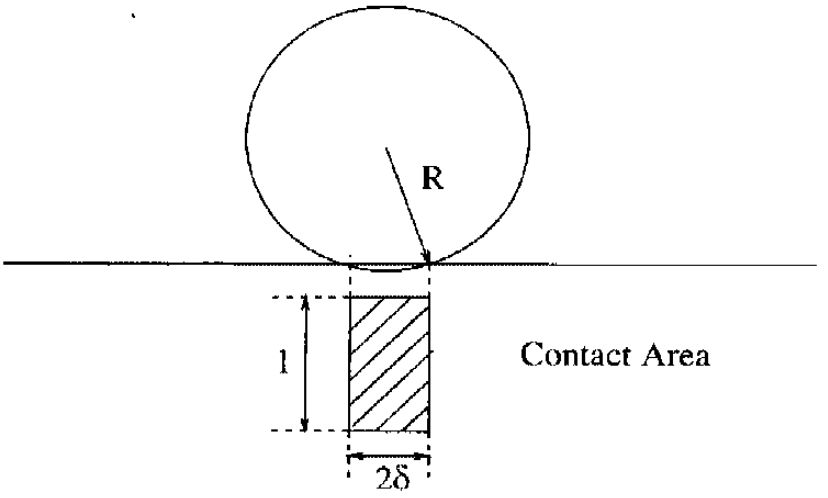

Figure 2.15 Coefficient of Rolling Friction

In Ref. [36], an expression is derived for the coefficient of rolling friction for a cylinder rolling on a plane surface under free rolling. In free rolling, pure rolling is assumed to occur without sliding or traction. Rolling friction is caused by the deformation of contacting surfaces during the process of rolling motion. Referring to Figure 2.15, the result is given by

$$f_r = \frac{f}{N} = \frac{2\epsilon\delta}{3\pi R} \tag{2.16}$$

where δ is the contact area semi-width, and ℓ is the contact area length, and ϵ accounts for the energy dissipation due to the elastic hysteresis loss occurring in the complex straining of the material which must occur during the rolling process. An approximate estimate of the hysteresis loss coefficient ϵ is that it should be three times the loss factor measured in a simple tension test. The value of the contact semi-width δ is given by

$$\delta = \sqrt{\frac{4NR}{\pi\ell}\left(\frac{1-\nu_1^2}{E_1} + \frac{1-\nu_2^2}{E_2}\right)} \tag{2.17}$$

where ν is the Poisson's ratio, E is Young's modulus, the suffixes denote the two contacting bodies.

2.4 Capsule Braking Methods

There are basically four available methods for slowing down and stopping a capsule. They are aerodynamic braking, electrical braking, mechanical braking, and grade braking. All methods are based on converting capsules' kinetic energy into some other energy form.

(1) The aerodynamic drag on a capsule is proportional to the square of its speed relative to the air flow and to the cross-sectional area (Eq. (2.1)). If the cross-sectional area is expanded, the capsule drag will increase drastically and can be used to slow down the capsule. Figure 2.16 demonstrates a mechanism that can potentially be used to stop a capsule in emergency. In aerodynamic braking, capsules kinetic energy is converted into kinetic energy of the air mass by increasing the air temperature. Essentially, capsule kinetic energy is converted into heat.

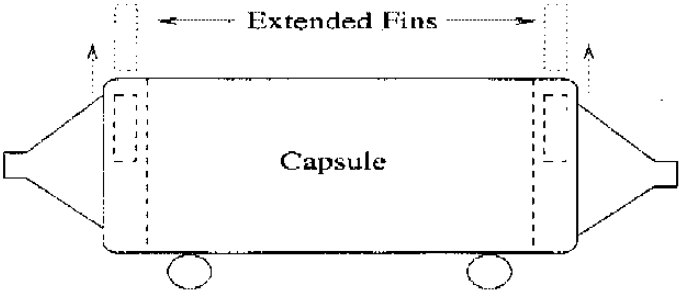

Figure 2.16 Aerodynamic Braking

(2) Electrical braking occurs when the thrust is in the opposite direction of capsule velocity. There are three electrical braking methods available on a linear induction motor: regenerative braking, plugging, and dynamic braking. Figure 2.11 shows the motor thrust force versus capsule speed in three braking modes. (a) *Regenerative braking* occurs when the speed of the LIM is greater than the synchronous speed, i.e. $V > V_s$. In this case, the LIM operates in a generator mode and thus extracts energy from the moving capsule. Therefore, the capsule's kinetic energy is mainly converted into electrical energy. (b) *Plugging* is obtained by reversal of the primary winding connections while the LIM is

running. When the plugging method is used, the input voltage is often reduced to avoid excessive primary current. This method of braking is similar to braking a direct current motor by reversing the input voltage while it's running. In this method, both input electrical energy and capsule's kinetic energy will be converted into heat. (c) Finally, *dynamic braking* occurs when the primary windings are excited by direct current immediately after their disconnection from the three-phase source. This method is similar to braking a direct current motor by disconnecting it from the voltage source and closing the circuit with a resistor. The capsule's kinetic energy is dissipated as heat in the circuit.

The regenerative braking method is the easiest and the most energy efficienct to use. It can be implemented by decreasing the synchronous velocity below the motor's speed gradually through normal capsule speed control and does not require any additional switching logic. In comparison, the plugging method may produce excessive current and can be used to stop capsules in an emergency. The dynamic braking method produces very small braking forces at low velocities. Regenerative braking and plugging methods are sufficient for the proposed electrical pipeline system.

(3) Mechanical braking requires pushing a brake pedal against wheels or some other ground-attached surface. It uses friction to convert the capsule's kinetic energy into heat. Mechanical braking cause serious wear-and-tear on vehicle wheels and rail tracks.

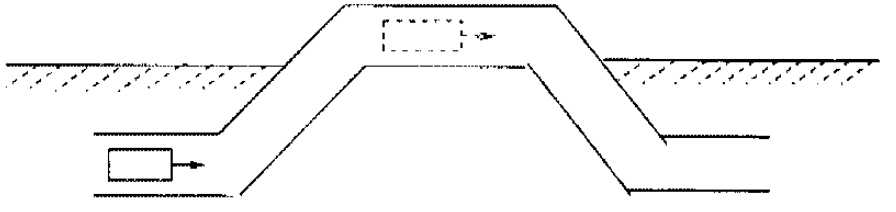

Figure 2.17 Grade Braking

(4) Finally, pipeline grade changes can be designed to slow a vehicle down. Figure 2.17 shows a capsule loading station that is higher than the average pipeline level line. In a grade braking, the vehicle's kinetic energy is converted into potential energy. The

mechanism of grade braking is also favorable to starting a capsule motion, since the higher potential energy can be used to jump start a capsule.

Of the four braking methods, electrical regenerative braking and grade braking convert capsule kinetic energy into either electrical or potential energy. These two methods make the system energy efficient and environmentally friendly. Therefore, a combination of regenerative braking and grade design should be used during normal capsule operations. Plugging can be used in an emergency when electricity is available, and aerodynamic braking may be used in an emergency in the event of a power failure. Proper designs of the capsule and pipeline can be made so that mechanical braking is not necessary. Capsules can be secured into position by mechanical locks at loading stations.

2.5 Efficiency of Linear Electric Propulsion

In a pneumatic system, simply stated, a pump/blower raises the pressure on one end of the tube and blows the capsules through the tube. Under ideal operating conditions the capsules are moving at the same speed as the pumped air and there is no aerodynamic drag on the capsules. The pressure difference required across the ends of the tube is the same as required to pump air at that speed, namely

$$\Delta p A_T = \frac{1}{2}\rho V^2 2\pi R_T C_f \tag{2.18}$$

where Δp is the pressure difference, A_T is the tube area, ρ the density of air, V the capsule speed, R_T and L_P the pipetube radius and length and C_f is a friction coefficient. The power required is

$$P_{pn} = \frac{1}{2}\rho V^3 2\pi R_T C_f \tag{2.19}$$

This is independent of the number of capsules in the tube. This formula neglects rolling friction, which would require an additional pressure drop across each capsule to overcome this friction, and a consequent air speed in the tube which is greater than the capsule speed.

In an electrical pipeline system, each capsule is individually driven by the motor force and is resisted by aerodynamic drag. In a tube, which is open to the atmosphere at both ends, the moving capsules force part of the air to pass through the gap between the capsule and the tube wall and also force some air to flow through the tube. The balance between these effects is determined by the size of the gap. If the gap is very small more air is pushed through the tube. In this sense the linear electric motor takes the place of the pump in the pneumatic system. The pressure distribution in the tube, proceeding in the direction of motion, consists of pressure increases across each capsule and pressure drops between the capsules because of the air friction with the tube walls.

The force on a single capsule is given by Eq. (2.1)

$$\frac{1}{2}\rho(V-w)^2 AC_D \tag{2.1}$$

It may be shown that

$$V - w = \frac{V}{(1+\phi)} \tag{2.20}$$

where

$$\phi = \sqrt{\frac{\beta}{2}\frac{R_T}{L_P}\frac{nC_D}{C_f}} \tag{2.21}$$

Here n is the number of capsules in the tube and $\beta = A/A_T$ is the blockage ratio. The formula takes into account the frictional resistance of the pushed air, which depending on parameters, can offer less resistance than forcing the air through the gap.

The total power required to drive n capsules is

$$P_{li} = \frac{1}{2}\rho V^3 AnC_D/(1+\phi)^2 \tag{2.22}$$

and therefore the two power requirements may be compared by the efficiency ratio

$$\frac{P_{li}}{P_{pn}} = \frac{\phi^2}{(1+\phi)^2} \tag{2.23}$$

where ϕ is the relative friction parameter defined above. This ratio is always less than one. Under maximum traffic conditions (large n) it approaches one. However, when there are only a few capsules in the tube, it becomes much smaller than one. This is because the pneumatic blower has to maintain the same power independently of the number of capsules, in order to keep the speed up. One may therefore conclude that the linear electrical system is always more efficient, and can be much more efficient when the traffic is light.

3. Electrical Pipeline System Conceptual Design

3.1 Design Considerations

A key objective in a transportation system is to provide reliable delivery of freight or timely movement of people. In addition, any acceptable system design should be technically sound, economically profitable, and environmentally friendly.

(1) From a technical point of view, a system should be able to operate within a specified range of speeds, with acceptable performance in acceleration, deceleration, and normal operations. Special design features should consider potential emergency cases, such as power failure or maintenance needs. An electrical pipeline system concept is inherently safe, reliable, and secure. Therefore, the system design process should emphasize on system controllability and safe operations in emergencies.

In addition, it is highly desirable in the system design phase to allow for easy expansion in the future. For example, a system may be designed at one time for a certain speed range and a certain maximum number of capsules. Future needs may desire higher operating speeds and/or a larger number of capsules. Development of infrastructures requires a substantial amount of capital; thus any subsequent changes will likely be costly.

(2) Economic factors include initial development cost, operating cost, and maintenance cost. Initial development cost consists of expenses for manufacturing capsules, electric motor parts, and pipetubes, as well as system installations (construction).

System installation requires connecting and burying pipeline segments underground. There are two basic methods of installing pipelines underground: tunneling and trenching (cut and cover). Construction is more expensive for larger diameter tubes. Statistics roughly show that for pipelines with diameters 6 to 8 feet or less, an order of magnitude cost for excavation and pipeline installation is approximately $800 per linear foot, in 1993 dollars. The costs per linear foot of tunnel normalized to 15 ft diameter exhibits wide scatters. From a minimum of just under $1,400 to almost $7,000 per linear foot, the

average cost is about $3,200. Construction technologies have improved tremendously over the last several decades. It is expected that construction costs will decrease modestly over the coming years [4]. Construction cost affects the choice of pipeline diameters.

The use of linear motors can provide operation efficiency comparable to or better than existing modes of freight transportations. In addition, proper designs of linear motor parts and speed control networks can further increase the operating efficiency. Necessary maintenance efforts depend on pipeline system configuration and specific design of linear induction motor parts. System configurations can be selected to require low maintenance efforts.

(3) Consideration of environmental impact has become increasingly important in the design of transportation systems. There are four relevant potential types of environmental pollutions from an electrical pipeline system: air pollution, noise pollution, surface intrusion, and electromagnetic radiation pollution. The use of electric motors produces little direct air and noise pollution, and little intrusion to the surface environment. In addition, pipelines and capsules can be designed to effectively shield the effects of electromagnetic radiation. (Electromagnetic radiation represents a serious environmental concern in the proposed TRANSRAPID high-speed transportation system [14]).

Choices of capsule support mechanisms depend on desired ranges of capsule operating speeds. The wheels-on-rails configuration can be used for low to moderate speed capsule operations, with a maximum speed about 250 to 300 km/h. Beyond this speed, construction and maintenance cost will increase drastically. As a result, magnetic suspension is needed for higher speeds (say 500 km/h). There are basically two types of magnetic suspensions: electromagnetic levitation and electrodynamic levitation. Electromagnetic levitation employs attraction, and electrodynamic levitation employs repulsion.

3.2 Comparison of Several Electrical System Layouts

In this report, we assume that capsules operate with speeds less than 200 miles per hour and the wheels-on-rails configuration is used. The best design configuration depends

on the requirements of a specific application. In order to determine a good system configuration for an electrical pipeline system, we first sketch out possible configurations that use either linear induction motors or linear synchronous motors. These different configurations are then compared in terms of initial development cost, system operating efficiency, maintenance cost, ac supply requirement, capsule speed control requirement, requirements on capsule-ground communications, and future expandability. One design is recommended as a good solution for a medium to long range freight pipeline system.

There are four basic configurations of electrical pipelines using either a linear induction motor or synchronous motor, as shown in Figures 3.1 through 3.4. Specifically, the system can have either a moving primary or a moving secondary, using either a linear induction motor or a linear synchronous motor. Main characteristics and possible variations of each system configuration are now discussed below.

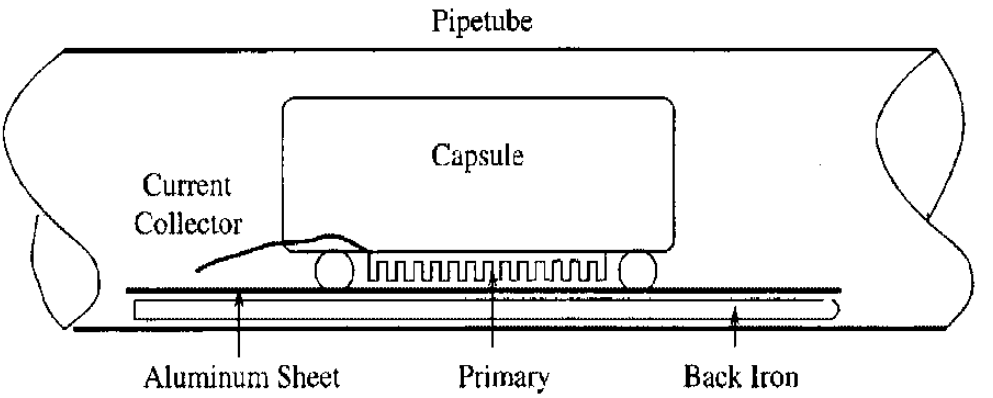

Figure 3.1 A Moving Primary Linear Induction Motor System (MPLIM)

(1) In a moving primary linear induction motor system (MPLIM) as shown in Figure 3.1, three-phase primary windings are mounted on capsules, whereas a secondary metal sheet and ground ac supply are placed on the pipeline (passive guideway). Power supply to the moving capsule is from a variable-frequency converter, which receives electricity from the ground via a current collector. The ground ac supply can be a fixed voltage, fixed frequency standard industrial electricity source (408 V, 60 Hz, three phase). The variable-frequency converter, together with on-board radar unit, capsule speed detector,

and computer, serves as the capsule speed control unit. On-board radar can detect the relative distance between one capsule and the capsule ahead, and speed control can be adjusted automatically to avoid collisions with the capsule ahead. A desired steady-state operating speed can be pre-set in the on-board computer, before the capsule is injected into the pipeline.

Primary windings often use copper wires, whereas the secondary is often made of aluminum or copper sheet, backed by an iron sheet or steel plate. As a result, this arrangement has relative low initial development cost, low maintenance cost, but a modest operating efficiency. Capsule primary windings can be designed to increase the operating efficiency at the expense of increased capsule cost. On-board capsule speed control can automatically achieve a specified operating speed and avoid collisions without changing the voltage or frequency of the ac supply at the ground. This moving primary LIM concept is the basis of the Japanese HSST 03 system, the maglev transit link in Birmingham, and the transit system in Vancouver.

If the system contains many capsules distributed over a range of pipeline length, each capsule can control its own speed. A close spacing can be achieved to take advantage of the drafting effect without physical chains, so that each capsule has the freedom to head for different destinations when necessary.

Since specific capsule designs greatly affect the speed and controllability of a capsule, this system is easily expandable. The range of speeds depends on both primary windings and secondary structure. Therefore, the plate thickness in the secondary should be selected to accommodate possible speed increase and different capsule designs in the future. The minimum possible spacing between two capsules depends on the response time of capsule speed control and will most likely be improved over time.

The system shown in Figure 3.1 has one possible variation, in which a double-sided primary may be used. In a double-sided configuration, the secondary metal sheet is placed vertically between two primary units on the capsule. The double-sided configuration has a higher demand on the accuracy of capsule position with respect to the guideway, but has

the advantage of canceled normal force. Single-sided LIM configurations are superior to double-sided configurations in terms of interaction with guideways: it simplifies switching, and allows for simpler and more economical guideway construction.

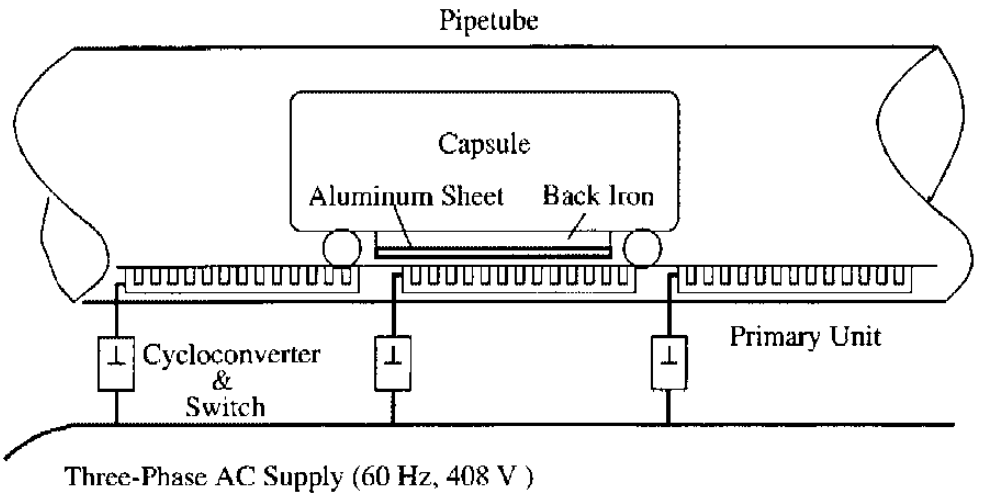

Figure 3.2 A Moving Secondary Linear Induction Motor System (MSLIM)

(2) Figure 3.2 shows a moving secondary linear induction motor system (MSLIM). In this system, three-phase primary windings are placed on the pipeline tubes (active guideway), and a capsule contains the moving secondary. The moving capsule only needs to contain a metal sheet at the bottom without any windings. The three-phase primary windings on the ground are divided into a series of winding segments for the purpose of capsule speed control and for the reduction of primary winding resistance. Spacing of these segments is usually small to generate continuous thrust for traveling capsules. Each segment connects to a fixed voltage, fixed frequency ground ac supply via a variable-frequency converter. Capsule speed control is achieved by varying voltage/frequency on the ground segments that are around the current capsule position. Therefore, sensing devices are needed on the ground to detect capsule position and speed. Signals from these devices are used to switch on the segments ahead and around the current capsule position, and switch them off after the capsule passes.

This system configuration does not require any current collectors that transfer electric power from the ground to capsules. On the other hand, the initial development cost is high because of the almost continuous primary windings on the ground. The maintenance cost is higher than the MPLIM configuration because of the multiple segment primary windings and the many cycloconverter units. In a multiple capsule scenario, sufficient separations between two capsules are necessary for the ground switch units to control their speeds separately and to maintain inter-capsule separations. In fact, the system is unstable in multiple-capsule operations if sufficient inter-capsule separations are lost, as will be discussed in Chapter 6. Therefore, capsules cannot be put very close to each other without the use of chains. The operating efficiency of this configuration is medium. Expandability of this system is limited, because of the difficulty to change the primary windings on the ground once installed and the requirement on sufficient inter-capsule separations.

The MSLIM configuration also has a double-sided primary variation, in which the moving capsule has a vertically oriented secondary.

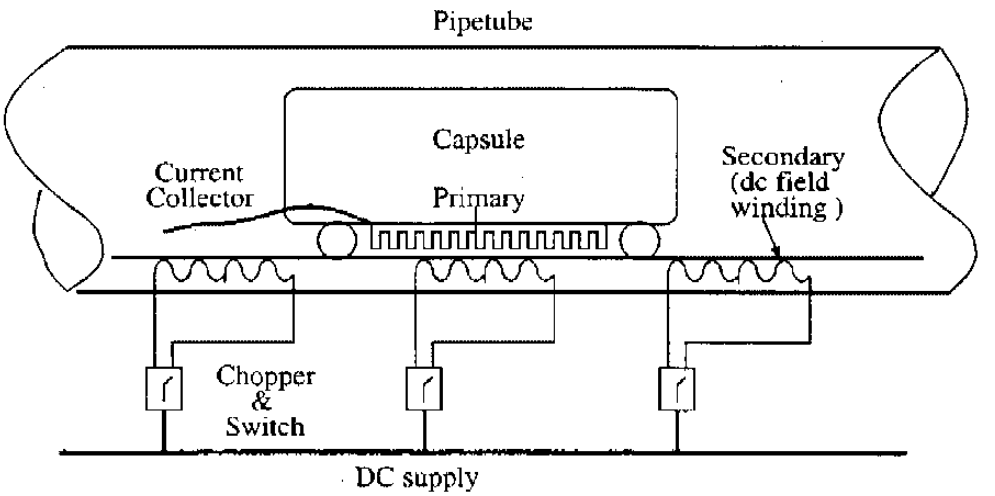

Figure 3.3 A Moving Primary Linear Synchronous Motor System (MPLSM)

(3) A moving primary linear synchronous motor (MPLSM) system as shown in Figure 3.3 is similar to a moving primary LIM system in Figure 3.1, except that the secondary on the pipeline in a MPLSM needs to contain direct current field windings. Power input to

the moving capsule requires an ac current collector, which is connected to a fixed voltage, fixed frequency ground electricity supply. Capsule speed control is achieved via a frequency converter on the capsule, which connects the current collector to the primary winding on the capsule. For additional control authority over capsule speed and to reduce dc winding resistance, the ground-based dc field windings are divided into a series of segments. Each segment connects to a fixed voltage dc supply via a chopper, which changes a fixed voltage dc source into a variable voltage dc supply.

Compared with the moving primary linear induction motor (MPLIM) design, this arrangement can achieve a higher operating efficiency at the expense of a higher initial development cost due to the dc field windings on the ground and a higher maintenance cost for these dc field windings. Similarly to MPLIM, the capsule speed control requires an on-board radar unit to avoid collisions with capsules ahead, an on-board speed sensor for feedback control of capsule speed, and an on-board computer to perform all necessary calculations. Speed control for a linear synchronous motor requires the change of input frequency and is usually simpler thus less expensive than that for a linear induction motor. DC voltage from choppers to dc field windings can also be changed to control capsule speed and to regulate power factors. The system expandability is good. Ground-based dc windings can be designed to allow for possible increase in speed in the future.

There are several variations of this system concept. First, the dc field windings may be replaced by permanent magnets. The use of permanent magnets reduces the need for dc windings. For high-speed high-load pipeline applications, it seems from past applications that dc field windings are more practical. Linear reluctance motor is another variation of the LSM concept, in which both the three-phase winding and the dc field winding are placed on the primary, whereas the secondary consists of notched ferromagnetic materials that provide variable reluctance. Linear reluctance motors achieve a cleaner secondary design at the expense of larger motor sizes.

(4) Finally, capsules can be the moving secondaries in a linear synchronous motor (MSLSM) system. In a MSLSM configuration, three-phase primary windings are placed

on the ground pipeline (active guideway). The capsule secondary requires dc supply thus needs a current collector to connect with the ground. Ground primaries are made of a series of segments, and capsule speed control is achieved via a variable-frequency converter. Similarly to MSLIM, spacing of these segments is usually small to generate continuous thrust for traveling vehicles. Ground sensing devices are needed to measure capsule speeds. DC choppers that connect the dc field winding with the dc current collector may also be used to control capsule speed and power factors.

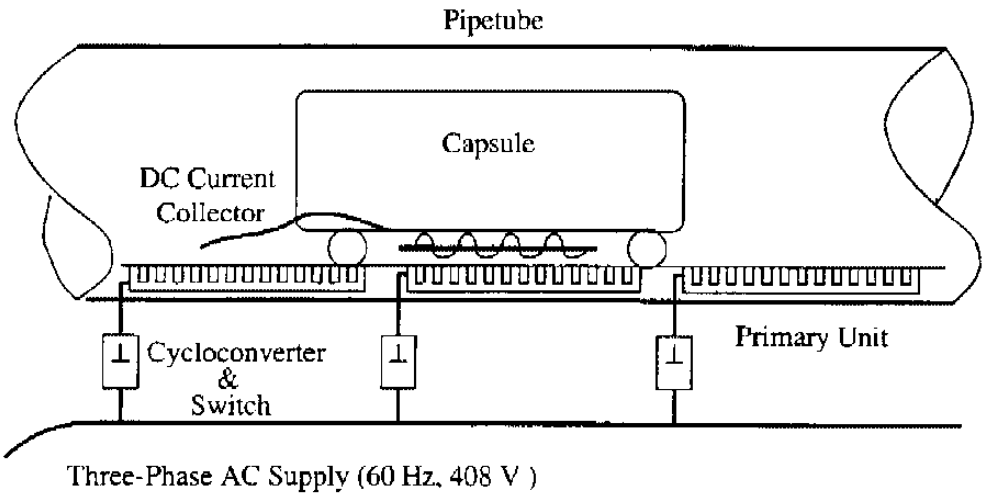

Figure 3.4 A Moving Secondary Linear Synchronous Motor System (MSLSM)

This active guideway concept is the basis of the TRANSRAPID system being developed in Europe. For a single vehicle or sufficiently-spaced vehicles, this active guideway LSM system is efficient and provides precise speed control. If the travel distance is long, however, the primary winding can be very costly both in terms of initial development and maintenance efforts. It is difficult in this system to control individual speeds of a series of closely-spaced capsules. The future expandability of the system is poor, also because of the ground-based primary windings. For some applications, permanent magnets can be used on the secondary to replace dc field windings, as in the Japanese linear tube project [19, 20].

3.3 A Short-Primary Linear Induction Motor System

Table 3.1 summarizes the advantages and disadvantages of the four basic system configurations. Clearly, the best system depends on requirements of specific applications. For a medium to long range electrical pipeline system, continuous primary windings can be very costly to develop and to maintain. For the convenience and flexibility in capsule travel, capsules should be allowed to enter the pipeline system at their best times. These capsules in general head for different locations, and thus should not be chained together. At the same time, closely-spaced capsules can use less average thrust by taking advantage of drafting effect. Therefore, the system should allow for separate speed control of capsules. Finally, system expandability should be considered for such a high initial capital and low operating cost system.

Table 3.1. Comparison of System Configurations

Layout	Initial Cost	Operating Efficiency	Maintenance	Capsule control	Expandability
MPLIM	Excellent	Good	Excellent	Excellent	Excellent
MSLIM	Poor	Good	Poor	Poor	Poor
MPLSM	Good	Excellent	Good	Excellent	Good
MSLSM	Poor	Excellent	Poor	Poor	Poor

The above considerations lead to the choice of a moving primary linear induction motor system. In this system, individual capsules can control their own speeds through some automatic algorithms. A linear induction motor secondary is usually a solid-iron sheet, and is very rugged and robust. This pipeline system requires the least amount of initial investment and maintenance. Capsule primaries can be designed to operate sufficiently efficient. This system configuration also has the largest freedom in the future. If a higher operating speed is desirable at some future time, one only needs to change the primary design on the capsule. The pipeline secondary can be designed in the initial investment to be flexible for a foreseeable range of speeds.

3.3.1 Primary Construction

Unlike that of a polyphase rotary induction motor, the air gap magnetic field of a LIM often has a forward component, a backward component, and a pulsating component. The forward component dominates, but the presence of other components is not desirable. Design and construction of LIM primaries are therefore based on tradeoffs between manufacturing costs and the quality of the airgap magnetic field.

LIM primary is made of a laminated core with open slots in which the three-phase windings are placed, as shown in Figure 2.9. Many winding layouts are possible. In Ref. [29], four different winding layouts are compared in terms of manufacturing costs and quality of the air gap field distribution. The most suitable configuration in high-thrust applications is a two-layer winding with odd number of poles and half-filled end slots, as shown in Figure 3.5. This configuration produces a purely traveling-wave airgap field in the central zone [$(2p-1)$ poles in length] whereas pulsating components occur only along the marginal, half-wound poles. In comparison, other configurations, such as a one-layer winding with even number of poles and a three-layer winding with even number of poles, exhibit notable pulsating components besides the traveling wave.

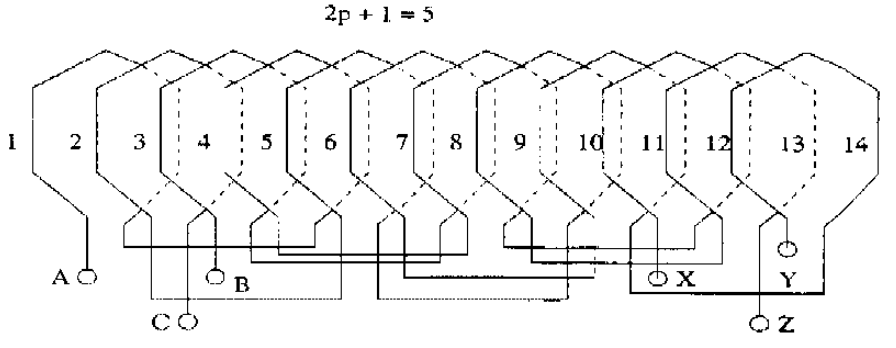

Figure 3.5 A Two-Layer LIM Primary Winding

Figure 3.5 shows a 5-pole winding configuration. The length of a capsule allows for many more poles to the placed. A high number of poles reduces the end effects and thus increases the efficiency of system operation.

3.3.2 Secondary Construction

In general, the secondary of a flat LIM may be of an aluminum (or copper) sheet with or without a solid back iron plate. In special cases, a laminated slotted core with a ladder secondary may be used. Figure 3.6 compares the three configurations. Configurations (a) and (b) are less expensive to manufacture but have poorer energy conversion performance compared with the ladder secondary (c).

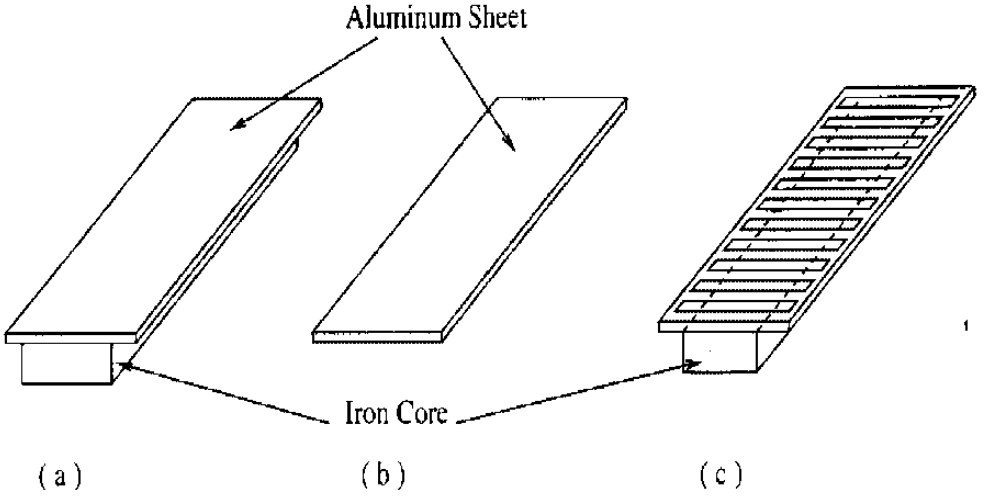

Figure 3.6 Configurations of Linear Induction Motor Secondary

For the short-primary LIM pipeline system, the secondary is designed to be made of either an aluminum sheet with back iron (a) or a ladder aluminum with back iron (c), depending on the construction cost. A continuous secondary along the pipeline is recommended.

3.3.3 Pipeline Network Design

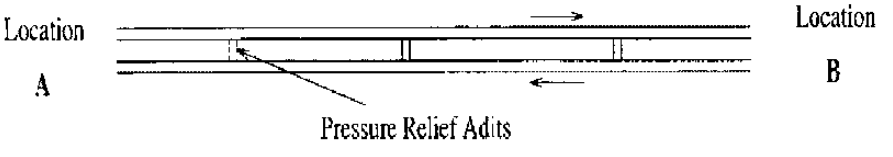

Figure 3.7 Pipeline System Between Two Fixed Locations

For transportation needs between two fixed locations, a two-bore pipeline system can be used. Each pipeline has a fixed direction of capsule motion, as shown in Figure 3.7.

For transportation needs among several fixed locations, a network of dual pipelines can be used as shown in Figure 3.8. Each location has a loading/unloading station, at which capsules can also be re-routed into another direction. A national pipeline system can be built as a network of dual pipelines.

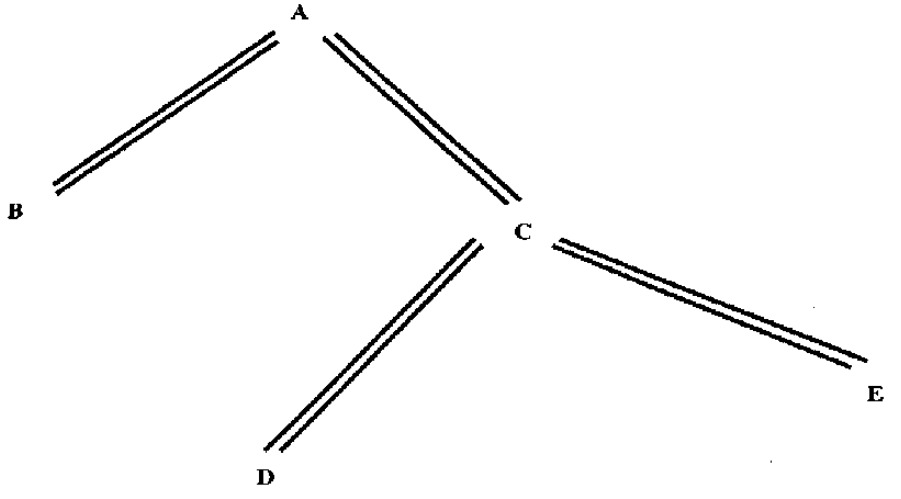

Figure 3.8 A Pipeline Network Among Several Locations

3.4 Heating Problem

For a closed pipeline system, the ventilation and control of heat need to be addressed in the pipeline design process. Currently achievable overall efficiency of LIM operation is around 50%. Therefore, a substantial amount of electrical energy is converted into heat. Excessive heating increases air temperature, and high air temperature affects the performance of linear motors.

The seriousness of the heat problem depends on the density of capsules in the system and capsule operating speed. If the pipeline operates at a low capacity, there is sufficient time for natural heat ventilation and dissipation. On the other hand, active ventilation and cooling may be necessary if the pipeline operates at a high capacity and high speeds.

The determination of exact relations among LIM power losses, heat, and temperature variations inside the pipetube requires careful analytical studies and experiments. Should high temperature occurs due to heating, there are basically three schemes to decrease the high temperature: ventilation, active cooling, and heat energy reuse.

Ventilation methods rely on circulation and natural cooling of the air to prevent temperature from building up. Pipeline configuration, therefore, should be designed to enhance the air flow. Air fans may also need to be used. Figure 3.9 shows the use of adits in a dual pipeline system. Adits connect pipelines of two directions and thus increase the air circulation. In addition, the use of adits can also reduce aerodynamic drags on capsules. This is because adits allow air to circulate among different pipetube sections as shown in Figure 3.9; thus reducing capsule's relative speed with respect to air flow. In addition to the use of adits, ventilating outlet windows (vents) may be placed on pipelines that lead to outside.

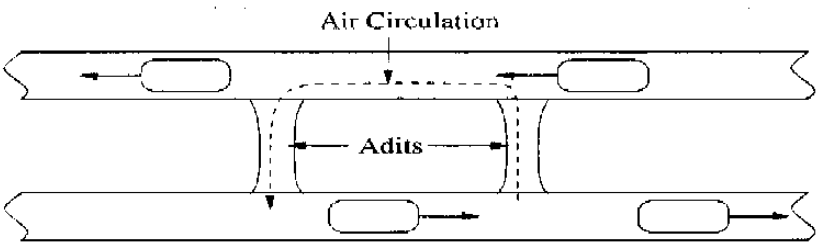

Figure 3.9 Pipeline System with Adits

If ventilation is not sufficient in controlling air temperature, active cooling through air conditioning needs to be used. This may especially be true in hot ambient temperatures, such as in hot summer. Active cooling increases the cost of system operation. For installing air conditioning unit, extra space must be reserved in pipeline tubes and ventilation outlet windows must be constructed from pipelines to surface level.

Finally, temperature rise inside pipelines due to heating may be reused for other purposes, such as water heating. This approach is appealing from both an energy point of view and an environmental point of view. To use the heat from power losses to heat

water, separate small pipelines are needed inside the pipetube to carry circulating waters. More creative designs are still needed to effectively use heat from power losses.

3.5 Electromagnetic Radiations

The operation of linear electric motors produces an electromagnetic field that travels with a capsule. This field can be very strong for high-thrust applications and is considered by some to be a key deterring factor for the proposed magnetic levitation high-speed transportation system [14]. If unshielded, this electromagnetic field may adversely affect sensitive cargos transported in the capsules, and people/animals nearby the pipelines.

Fortunately, electromagnetic field dissipated very quickly in conductors. Faraday cage, a closed metal box, can be used to shield materials inside the box from electromagnetic field outside the box or vice versa. Specifically, a concept of skin depth (or depth of penetration) can be defined as follows for good conductors for which $\sigma \gg 2\pi f\epsilon$ in the range of practical frequencies [40].

$$\delta = \frac{1}{\sqrt{\pi f \mu \sigma}} \tag{3.1}$$

where σ is the conductivity of the conductor medium in Siemens per meter (S/m), f is the frequency of the electromagnetic wave in Hertz (or 1/second), μ is the mobility of the conductor medium in Henry per meter, ϵ is the permittivity of the conductor medium in Farads per meter, and $\pi = 3.14$. At one depth of penetration into a conductor, the field is attenuated to $e^{-1} = 36.8\%$ of its initial value. At 5δ, the field is practically zero. Table 3.2 lists the depth of penetrations in different conductor materials. At high temperatures, μ and σ both decrease, so skin depth will increase.

Table 3.2. Skin Depths for Several Conductors at $f = 60$ Hz

Medium	Conductivity σ	Mobility μ	Skin Depth
Aluminum	38.2 MS/m	$4\pi \times 10^{-7}$ H/m	10.5 mm
Copper	58 MS/m	$4\pi \times 10^{-7}$	8.5 mm
Silver	61.7 MS/m	$4\pi \times 10^{-7}$	8.3 mm

In fact, the shielding conductor box does not need to be a solid box. A conductor mesh box can sufficiently shield an electromagnetic field, as long as the mesh grid size is significantly smaller than the wavelength of the electromagnetic field. Wavelength λ for an electromagnetic wave is defined as

$$\lambda = \frac{V}{f} \tag{3.2}$$

where f is the frequency of the wave in Hertz, and V is the speed with which waves travel. The velocity of the electromagnetic wave in free space is given by

$$V_o = \frac{1}{\sqrt{\epsilon_0 \mu_0}} \tag{3.3}$$

For $\epsilon_0 = 8.8547 \times 10^{-12}$ and $\mu_0 = 4\pi \times 10^{-7}$, we have

$$V_0 = 2.99784 \times 10^8 \quad \text{m/s} \tag{3.4}$$

Phase velocity of electromagnetic waves in a material medium is

$$V = \frac{1}{\sqrt{\epsilon \mu}} = \frac{V_0}{\sqrt{\epsilon_r \mu_r}} \tag{3.5}$$

which is less than V_0. In air, $V \approx V_0$. For $f = 60$ Hz, in air, the wavelength of an electromagnetic field is

$$\lambda = 5.0 \times 10^6 \text{ m} = 5000 \text{ km}$$

Therefore, the necessary grid size can be vary large. On the other hand, a conductor mesh box can only shield objects outside the box against electromagnetic field inside or vice versa. In the following, metal frames are used on pipelines to provide both structural integrity and electromagnetic field shielding.

3.6 Capsule Design

The structure and material choice for a capsule can be designed by iterating over the following factors. (1) Capsule interior design should allow the capsule to contain all specified cargos or passengers. (2) Capsule exterior design should allow the capsule to be

propelled in an energy efficient manner, and should provide sufficient structural integrity and protections against heat and electromagnetic radiation. (3) Capsule door design should allow for easy loading and unloading of transported cargos or passengers. (4) Sufficient room should be reserved on a capsule for speed control, radar unit, computer, and power supply unit. (5) Special considerations should be made for capsule safety in both power-on and power-off emergencies. These factors are the same for freight capsules and for passenger-moving capsules. In the following, these factors are discussed in detail for a freight-carrying capsule.

3.6.1 Capsule Interior Design

The size and shape of capsule interior should be selected to contain all specified cargos. For most freight transportation, a rectangular interior cross-section is preferred. One can also design capsules for special needs, such as for liquid transportation. A cylindrical interior cross-section could be used for liquid transportation. Materials for capsule interior should be selected to provide cushion for cargos and should be rugged for repeated uses. For example, a layer of rubber or plastic materials may be used for the interior shell of a capsule.

3.6.2 Capsule Exterior Design

Capsule exterior should be designed to reduce aerodynamic drag and mechanical friction, and to ensure the efficiency of linear motors. Results in Chapter 2 indicate that capsule drag is affected by blockage ratio, which is the ratio of exterior capsule cross-sectional area over the interior pipetube cross-sectional area. The smaller the blockage ratio, the smaller the aerodynamic drag under equal conditions. Therefore, exterior shape design should minimize the exterior cross-sectional area, given a specified size and shape of capsule interior, subject to some practical constraints. For a rectangular interior section, a rectangular exterior shape is better than a cylindrical cross-section. Aerodynamic considerations also require the use of round nose and tail sections to reduce pressure drag. Preferably, nose and tail section should be designed with the same configuration (capsule

symmetry) so that capsules can be moved in either direction. Finally, exterior surface of a capsule should be smooth to reduce skin friction drag.

Low frictions are accomplished by selecting proper wheels on a capsule. Basically, there are two types of wheel selections: metal wheels moving on rail tracks and rubber tires moving on the inside walls of the pipetube. Metal wheels on metal rail track configuration is desirable for two reasons. This configuration has a much smaller rolling friction than tire on a hard surface design. In addition, metal wheels on metal track can provide much more accurate air gap than rubber tires on a hard surface. Usually, a smaller air gap results in a higher efficiency of linear motor operation, and a constant air gap is desirable. Practical range of air gaps is 10 to 30 mm in order for linear motors to be effective. Some rubber tires on capsule sides may be used to secure capsules inside pipelines for better clearance, cushion, and controlled air gap. For very high speed operations, there is also an option of magnetic levitation, in which capsules are suspended by electromagnetic forces. For very high speed operations, vacuum pipeline should be considered to reduce aerodynamic drag. From low speed to a significantly high speed (e.g. 250 mph), metal wheels on rail track seem to be more energy-efficient than maglev, as suggested by some experimental results.

In addition, capsule exterior shell should provide structural integrity and insulations against direct electricity contact, heat, and electromagnetic waves. The most external surface for a capsule should be made of dielectric materials. This surface also needs to provide insulation against heat. Combined considerations of these two factors favor materials such as ceramic materials, plastics, rubbers, or other composite materials. Rubber has the added advantage of vibration reduction. The need for shielding the electromagnetic field requires a layer of conductor sheet or mesh around the capsule. This can be done by having a middle layer between the rubber or plastic interior, and the dielectric exterior. This layer can be made of either solid aluminum sheet or aluminum mesh.

3.6.3 Capsule Door Design

For the structural integrity and low manufacturing cost of a capsule, one door on each capsule should be sufficient. The capsule door size must be sufficiently large to allow for easy loading and unloading of cargos. This door should almost cover one complete side of a capsule. There are several possible mechanisms of door opening. The door can open sideways (like car door or a sliding Dodge caravan door), open up (like car hatch back), or open down (like some small airplane doors). Up-opening mechanism requires hydraulic system to support opening doors, whereas down-opening mechanism requires soft support on the ground when doors are open. Both up and down opening mechanism takes extra space along the diameter direction of a pipeline. For the first design, a sliding door mechanism is recommended.

3.6.4 Capsule Speed Control Units

Capsule operation and speed control require on board the capsule a current collector, a cycloconverter unit, a proximity sensor (such as radar), a capsule speed sensor, and a computer. These systems can be installed inside the nose/tail cone created to reduce aerodynamic drags. On-board radar system is now feasible and has been used on some experimental cars (for additional cost of several hundred dollars).

Information on capsule destination, desired operating speed, transportation needs, and capsule identification can be coded onto a sticker plate/transmitter placed on the outside of a capsule. Capsule speed can also be fed into this sticker/transmitter plate and detected from a series of sensors placed on the inside wall of the pipetube. These information can be used in a central station for capsule position monitoring and capsule traffic flow management. Actually, the capsule transmitter and pipetube detector can work both ways to transmit speed commands from a central station to a traveling capsule.

3.6.5 Emergency Considerations

In the event of system malfunction, capsules should not collide with each other and should come to a stop. If electricity is available, plugging method can be used to stop the capsule. In case of electric power failure, aerodynamic braking can be used. In this case, the proximity sensor can trigger an automatic fanning mechanism to extend. It is necessary that these extendible fans can be retracted once the emergency is gone, either automatically when the proximity sensor is off alarm, or remotely by central control. Because pipelines are concealed, the ability to start motion again after an emergency stop is crucially important.

All of the technologies and mechanisms discussed above are readily available. Therefore, electrical pipeline system is technically feasible. Efforts can be made at detailed design phase to reduce potential manufacturing cost and maintenance cost. Manufacturing costs depend on materials for capsules, materials for the LIM, and capsule shapes.

The cost of pipeline guideway construction needs to be considered in determining the specific sizes of capsule interior. There are two general tube sizes to consider. Tubes and capsules on the order of 6-8 feet in diameter are small enough to achieve significant cost reduction in tunneling and guideway construction. They also represent a reasonable lower limit to capsule volume and carrying capacity, and are probably still large enough to efficiently transport bulk commodities. On the other hand, a larger tube size [12-15 feet in diameter] can easily integrate into the existing shipping container industry. Standard eight and one half feet high by eight feet wide shipping containers could be accommodated on such a tube system, with obvious savings in reduced handling and packing of freight. However, infrastructure costs per unit length would increase dramatically, and one would essentially be recreating a conventional railroad.

3.6.6 A Candidate Capsule Design

Based on the above discussions, we have the following candidate design for freight carrying capsules.

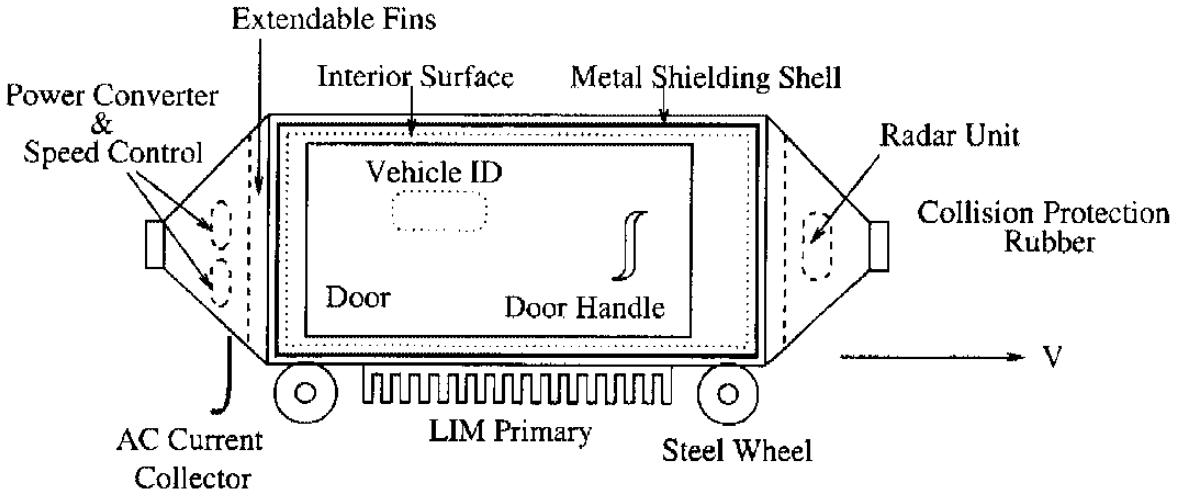

(a) Side View

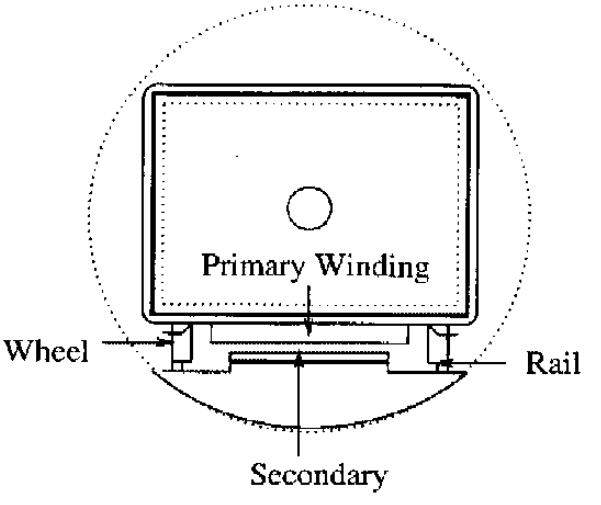

(b) Rear View

Figure 3.10 A Candidate Capsule Design

3.7 Tube Design

An entire pipeline system consists of a series of pipetube segments. A pipetube segment can be designed by considering factors similar to those for a capsule design. (1) A pipetube segment interior needs to provide ac electrical power to capsules through current collector, houses secondary plates, and provides sufficient clearance between capsules and

its own inside walls. In addition, a pipetube structure should allow for ventilation and heat circulation. (2) Pipetube structure should provide a meshed conductor box for shielding the outside environment from the electromagnetic field. This can be done by using conductor metal bars as structural stiffeners as well as for electromagnetic field shielding. (3) Segmentation of pipelines should allow for easy maintenance access, pipetube segment connections, and easy installations, and should provide sufficient structural strengths for each segment. The connection of pipetube segments should provide water-tight seals. Figure 3.11 sketches a candidate design for a pipetube segment.

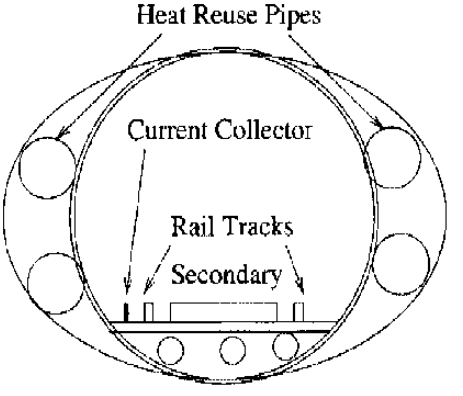

(a) Cross-Section

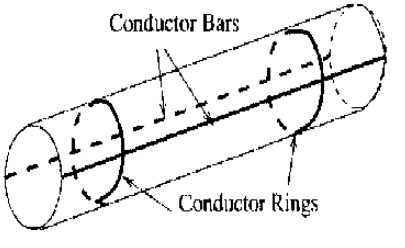

(b) Conductor Bars and Rings

Figure 3.11 A Candidate Pipetube Design

4. Equations of Motion and Cost Measures

We consider a two-bore freight pipeline system consisting of parallel tubes, connected at regular intervals by pressure relief tunnels (Figure 4.1). These tunnels can be opened up to external environment as vents or just adits. The capsules are driven automatically by linear induction motors. The moving capsules cause flow in the tubes and through the adits. The part of pipeline between two adits is called a section.

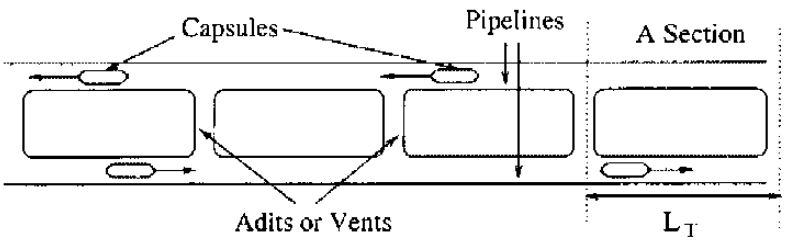

Figure 4.1 Layout of A Two-Bore Pipeline System

4.1 Derivations

Equations of motion for a pipeline system consist of equations for capsule motions as well as for fluid motions in the pipeline. The following assumptions are made to make the analysis tractable.

1. The flow inside pipetube is incompressible turbulent flow. This requires that capsule velocities be small enough and the spacing between tube and capsule be large enough that choking can not occur in the gap. Under these circumstances the drag on a capsule is little affected by density variations, even though there may be uncomfortably high noise levels in the tubes.

2. The capsule length is short compared to the distance between adits (or section length). As a result, the volume of air occupied by the capsules in a section can be neglected.

3. Adits are assumed to be ideal and lossless. In other words, pressures across adits are assumed constant.

The drag on a capsule is given by

$$D = \frac{1}{2}\rho(V-w)^2 \mathrm{sgn}(V-w) A C_D(\beta, V, w) \tag{4.1}$$

where V is the capsule speed, w is the velocity of the air in the tube, ρ is the gas density, and A is the capsule cross-sectional area. The sgn function indicates the algebraic sign; if w is greater than V the drag becomes thrust. An expression for the drag coefficient C_D has been derived in Appendix B. The result is

$$C_D(\beta, V, w) = \frac{\beta}{(1-\beta)^2} + \frac{(1+\beta^{1/2})}{(1-\beta)^3}\frac{4l}{d} C_{fg}(V, w) \tag{4.2}$$

where $\beta = A/A_T$ is the blockage ratio, A_T the tube area, l and d the length and hydraulic diameter of the capsule, and C_{fg} is a friction coefficient. The first term in Eq. (4.2) is a large pressure drag caused by separation at the rear of an (assumed) unstreamlined capsule. The second term is a viscous effect caused by the flow in the gap.

The friction coefficient is a function of the Reynolds number of the turbulent flow in the gap between the capsule and the tube. According to the Blasius formula, the friction coefficient is given approximately by

$$C_{fg}(V, w) = \frac{.316}{4R_{eg}^{1/4}} \tag{4.3}$$

where

$$R_{eg} = \frac{2(R_T - R)v}{\nu} = \frac{2R_T|V-w|}{\nu(1-\beta^{1/2})}. \tag{4.4}$$

and ν is the kinematic viscosity of the air inside the pipetube. The concept of hydraulic diameter is discussed further in Appendix B.

Let us assume there are N sections (or $N-1$ adits or vents) in the two-bore pipeline. The pressure change across a capsule is seen by the air in the tube as a pressure rise in the direction of motion and pushes the air through the tube as if it were produced by a pump. When there are a number of capsules in a bore section, each with different velocities in general, the sum of the pressure rises causes flow in each bore according to the following

momentum equation, which is based on the fact that the rate of change of air momentum must equal the sum of the forces acting on the air. For $i = 1, 2, \ldots, N$,

$$\frac{d}{dt}(\rho A_T\ L_T\ w_{ri}) = \sum_{\text{all cap. in } i \text{ th sect.,r}} .5\rho(V_{rj} - w_{ri})^2 \text{sgn}(V_{rj} - w_{ri}) A C_D(\beta, V_{rj}, w_{ri})$$
$$- .5\rho\ w_{ri}^2\ \text{sgn}(w_{ri})\ 2\pi R_T\ L_T\ C_f(w_{ri}) + A_T(p_i - p_{i+1}) \tag{4.5}$$

$$\frac{d}{dt}(\rho A_T\ L_T\ w_{li}) = \sum_{\text{all cap. in } i \text{ th sect.,l}} .5\rho(V_{lk} - w_{li})^2 \text{sgn}(V_{lk} - w_{li}) A C_D(\beta, V_{lk}, w_{li})$$
$$- .5\rho\ w_{li}^2\ \text{sgn}(w_{li})\ 2\pi R_T\ L_T\ C_f(w_{li}) - A_T(p_i - p_{i+1}) \tag{4.6}$$

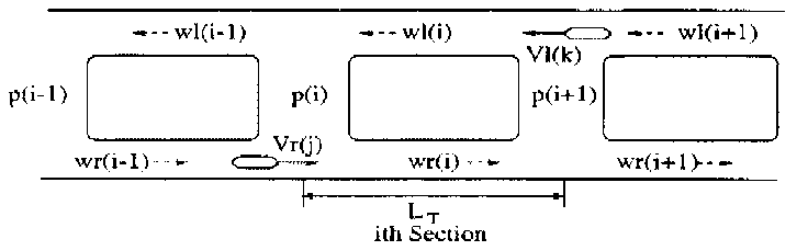

Figure 4.2 Notations in Pipeline System Analysis

Referring to Figures 4.2 and 4.3, here subscript i indicates the ith bore section, j indicates the jth capsule in the right bore, and k indicates the kth capsule in the left bore. Furthermore, w_{ri} and w_{li} are the air velocities in the right and left bores respectively, V_{rj} is the velocity of the jth capsule in the right bore, and V_{lk} is the velocity of the kth capsule in the left bore. $C_D(\beta, V, w)$ is given by Eqs. (4.2) through (4.4) with the dependence on the velocities indicated by the notation. The sums are over **all the capsules** in the appropriate bore of the ith section, which has length L_T.

The jth capsule in the right bore is currently in the ith section if

$$(i-1)\ L_T \leq x_{rj} \leq i\ L_T \tag{4.7}$$

Similarly, the kth capsule in the left bore is currently in the ith section if

$$(N-i)\ L_T \leq x_{lk} \leq (N-i+1)\ L_T \tag{4.8}$$

The friction coefficient $C_f(w_i)$ is again given by the Blasius formula but with Reynolds number based on the average tube air velocity and the tube diameter;

$$C_f(w_i) = \frac{.316}{4R_{ei}^{1/4}} \tag{4.9}$$

where

$$R_{ei} = \frac{2R_T|w_i|}{\nu} \tag{4.10}$$

The variables p_i and p_{i+1} are the pressures at the ends of the ith bore section, assumed constant through an idealized lossless adit. Figure 4.2 shows some of the notations.

The tube flow velocities must conserve mass at the junctions of bore sections with adits. Flow through an adit which decreases the flow rate in the right bore must be accounted for as an increased flow rate in the left bore. Mathematically,

$$w_{ri} - w_{li} = w_{r,i+1} - w_{l,i+1}. \tag{4.11}$$

The negative signs occur here because the w_l variables are defined to be positive for flow to the left (in the direction of traffic there). There is a condition like Eq. (4.11) for each adit, $i = 1, 2, \ldots, N-1$.

Based on Appendix A, the equations of motion for the jth capsule in the right bore are

$$\frac{dx_{rj}}{dt} = V_{rj} \tag{4.12}$$

$$\begin{aligned} M_{rj}\frac{dV_{rj}}{dt} &= F_{rj} - .5\rho(V_{rj} - w_{rI})^2 \mathrm{sgn}(V_{rj} - w_{rI}) A C_D(\beta, V_{rj}, w_{rI}) \\ &\quad - M_{rj} g \sin\theta_r(x_{rj}) - f_r(M_{rj} g \cos\theta_r(x_{rj}) + F_{N_{rj}}) - \Delta F_{rj} \end{aligned} \tag{4.13}$$

where w_{ri} refers to the flow velocity of the section in which the jth capsule is currently in. Mathematically,

$$(I-1)L_T \leq x_{rj} \leq I\ L_T \tag{4.14}$$

In these equations, T_{rj} is the thrust force applied to the jth capsule in the right bore by the motor, θ_r is the slope of the pipetube seen by moving capsules in the right bore, g the gravitational constant, f_r the coefficient of rolling friction discussed in Section 2.3, $F_{N_{rj}}$ is the normal force on the jth capsule in the right bore by the motor, and ΔF_{rj} is the miscellaneous force on this capsule. Furthermore, x_{rj} and V_{rj} are taken as positive in the direction of traffic in the appropriate bore (Figure 4.3). In particular, $x_r = 0$ at the left end of pipeline.

Similarly, the equations of motion for the kth capsule in the left bore are

$$\frac{dx_{lk}}{dt} = V_{lk} \tag{4.15}$$

$$\begin{aligned} M_{lk}\frac{dV_{lk}}{dt} &= F_{lk} - .5\rho(V_{lk} - w_{lI})^2 \mathrm{sgn}(V_{lk} - w_{lI}) A C_D(\beta, V_{lk}, w_{lI}) \\ &\quad - M_{lk} g \sin\theta_l(x_{lk}) - f_r(M_{lk} g \cos\theta_l(x_{lk}) + F_{N_{lk}}) - \Delta F_{lk} \end{aligned} \tag{4.16}$$

where w_{li} refers to the flow velocity of the section in which the jth capsule is currently in. Mathematically,

$$(N - I)L_T \leq x_{lk} \leq (N - I + 1)L_T \tag{4.17}$$

In these equations, the notations have similar meanings as those in Eqs. (4.12) and (4.13). In particular, θ_l is the slope of the pipetube seen by capsules in the left bore. As a result

$$\theta_l(x_l) = -\theta_r(L_P - x_l) \tag{4.18}$$

where L_P is the total pipetube length.

This set of equations is strongly coupled since the drag force on the jth capsule depends on w_i for the section and bore it is in, and w_i in turn depends on the velocities of all the capsules in the system. In addition, there is also coupling through the pressure variables.

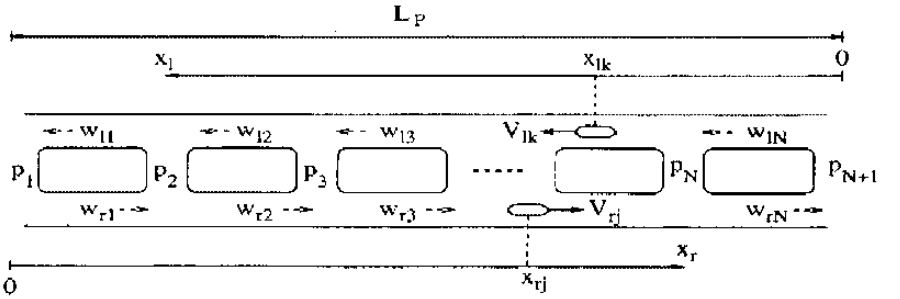

Figure 4.3 Section Indexing For Equations of Motion

In summary, we have considered a two-bore pipeline system with N sections. The right bore contains N_{cr} capsules whereas the left bore contains N_{cl} capsules. A complete solution to the system analysis would require the determination of the following variables:

(1) Flow velocities for the right bore

$$w_{ri} \qquad \text{for } i = 1, 2, \ldots, N$$

(2) Flow velocities for the left bore

$$w_{li} \qquad \text{for } i = 1, 2, \ldots, N$$

(3) Positions and speeds of capsules in the right bore

$$x_{rj} \qquad \text{for } j = 1, 2, \ldots, N_{cr}$$

$$V_{rj} \qquad \text{for } j = 1, 2, \ldots, N_{cr}$$

(4) Positions and speeds of capsules in the left bore

$$x_{lk} \qquad \text{for } k = 1, 2, \ldots, N_{cl}$$

$$V_{lk} \qquad \text{for } k = 1, 2, \ldots, N_{cl}$$

(5) Pressure variables at the adits/vents and at stations

$$p_i \qquad \text{for } i = 1, 2, \ldots, N, N+1$$

Therefore, there are a total of $(2N + N_{cr} + N_{cl}) + (N + 1)$ variables. Figure 4.3 shows the location and variables. To solve for these variables, one needs the same number of differential and/or algebraic equations as the number of unknowns, and appropriate initial conditions. In the above, we have derived $(2N + N_{cr} + N_{cl})$ differential equations for flow

velocities, capsule positions, and capsule velocities. We need additional $(N+1)$ relations to determine the pressure variables.

Before these variables can be determined, a set of system design parameters need to be specified. These parameters include dimensions of pipeline system and capsules: blockage ratio β, pipetube interior cross-sectional area $A_T = \pi R_T^2$, total pipeline length L_P, number of sections N which in turn determines the length of a section $L_T = L_P/N$, pipeline grade geometry $\theta(x)$, capsule length ℓ, capsule hydraulic diameter d so that $A = \beta A_T$. In addition, some parameters are needed to specify the physical environment of pipeline operations, such as air density ρ, kinematic viscosity ν, and acceleration of gravity g. Finally, models of LIM thrust force F and normal force F_N as functions of pipeline operation conditions are needed.

4.2 System of Normalized Equations

For good numerical accuracies, the above equations are normalized as follows. We first select three fundamental variables:

V_d	design speed of steady-state capsule operation
L_T	section length for equally spaced adits/vents
M_d	nominal capsule weight at steady-state operation

Choices of these design variables will be discussed in the next Chapter. Two useful variables derived from these fundamental variables are

$F_b = M_d V_d^2 / L_T$	benchmark thrust at steady-state operation
$t_b = L_T / V_d$	benchmark time

In addition, capsule payload M_p is needed to estimate the potential cost of transporting the payload.

All other variables can be normalized by these variables or their combinations. Denoting normalized variables by $\bar{(\ )}$, we have,

$$\bar{x}_{rj} = x_{rj}/L_T$$

$$\bar{V}_{rj} = V_{rj}/V_d$$

$$\bar{M}_{rj} = M_{rj}/M_d$$

$$\bar{F}_{rj} = T_{rj}/F_b$$

$$\bar{F}_{N_{rj}} = F_{N_{rj}}/F_b$$

$$\Delta\bar{F}_{rj} = \Delta F_{rj}/F_b$$

$$\bar{x}_{lk} = x_{lk}/L_T$$

$$\bar{V}_{lk} = V_{lk}/V_d$$

$$\bar{M}_{lk} = M_{lk}/M_d$$

$$\bar{F}_{lk} = T_{lk}/F_b$$

$$\bar{F}_{N_{lk}} = F_{N_{lk}}/F_b$$

$$\Delta\bar{F}_{lk} = \Delta F_{lk}/F_b$$

$$\bar{w}_{ri} = w_{ri}/V_d$$

$$\bar{w}_{li} = w_{li}/V_d$$

$$\bar{p}_i = p_i/\rho {V_d}^2$$

$$\tau = t/t_b = tV_d/L_T$$

$$\bar{M}_p = M_p/M_d$$

We also have

$$\frac{d(\ )}{d\tau} = \frac{L_T}{V_d}\frac{d(\ )}{d\tau}$$

Define

$$g_{ri} = \frac{1}{2}\beta \sum_{\forall j,\ i-1 \le \bar{x}_{rj} < i} C_D(\beta, V_{rj}, w_{ri})(\bar{V}_{rj} - \bar{w}_{ri})^2 \mathrm{sgn}(\bar{V}_{rj} - \bar{w}_{ri})$$
$$- (L_T/R_T) C_f(w_{ri})\ \bar{w}_{ri}^2\ \mathrm{sgn}(\bar{w}_{ri}) \tag{4.19}$$

$$g_{li} = \frac{1}{2}\beta \sum_{\forall k,\ N-i \le \bar{x}_{lk} < N-i+1} C_D(\beta, V_{lk}, w_{li})(\bar{V}_{lk} - \bar{w}_{li})^2 \mathrm{sgn}(\bar{V}_{lk} - \bar{w}_{li})$$
$$- (L_T/R_T) C_f(w_{li})\ \bar{w}_{li}^2\ \mathrm{sgn}(\bar{w}_{li}) \tag{4.20}$$

$$m_d = M_d/(\rho A_T L_T) \tag{4.21}$$

$$\bar{g} = g L_T / V_d^2 \tag{4.22}$$

where m_d compares the design mass with the mass of air in one adit length, and $\bar{g}$ is a dimensionless gravitational constant. Then, the set of normalized differential equations become for $i = 1, 2, \ldots, N$, $j = 1, 2, \ldots, N_{cr}$, and $k = 1, 2, \ldots, N_{cl}$

$$\frac{d\bar{w}_{ri}}{d\tau} = g_{ri} + \bar{p}_i - \bar{p}_{i+1} \tag{4.23}$$

$$\frac{d\bar{w}_{li}}{d\tau} = g_{li} - \bar{p}_i + \bar{p}_{i+1} \tag{4.24}$$

$$\frac{d\bar{x}_{rj}}{d\tau} = \bar{V}_{rj} \tag{4.25}$$

$$\bar{M}_{rj}\frac{d\bar{V}_{rj}}{d\tau} = \bar{F}_{rj} - \frac{\beta}{2m_d} C_D(\beta, V_{rj}, w_{rI})(\bar{V}_{rj} - \bar{w}_{rI})^2 \mathrm{sgn}(\bar{V}_{rj} - \bar{w}_{rI})$$
$$- \bar{M}_{rj}\bar{g}\sin\theta_r(\bar{x}_{rj}) - f_r(\bar{M}_{rj}\bar{g}\cos\theta_r(\bar{x}_{rj}) + \bar{F}_{N_{rj}}) - \Delta\bar{F}_{rj} \tag{4.26}$$
$$\text{where } (I-1) \le \bar{x}_{rj} < I$$

$$\frac{d\bar{x}_{lk}}{d\tau} = \bar{V}_{lk} \tag{4.27}$$

$$\bar{M}_{lk}\frac{d\bar{V}_{lk}}{d\tau} = \bar{F}_{lk} - \frac{\beta}{2m_d} C_D(\beta, V_{lk}, w_{lI})(\bar{V}_{lk} - \bar{w}_{lI})^2 \mathrm{sgn}(\bar{V}_{lk} - \bar{w}_{lI})$$
$$- \bar{M}_{lk}\bar{g}\sin\theta_l(\bar{x}_{lk}) - f_r(\bar{M}_{lk}\bar{g}\cos\theta_l(\bar{x}_{lk}) + \bar{F}_{N_{lk}}) - \Delta\bar{F}_{lk} \tag{4.28}$$
$$\text{where } (N-I) \le \bar{x}_{lk} < (N-I+1)$$

This set contains $(2N + N_{cr} + N_{cl})$ differential equations for $\bar{w}_{ri}, \bar{w}_{li}, i = 1, 2, \ldots, N$, for $\bar{x}_{rj}, \bar{V}_{rj}, j = 1, 2, \ldots, N_{cr}$, and for $\bar{x}_{lk}, \bar{V}_{lk}, k = 1, 2, \ldots, N_{cl}$. These equations make

a complete statement of the problem and can be solved numerically. Appropriate initial conditions are needed to start the numerical integrations. In addition, the $(N+1)$ pressure variables must be solved at each integration step.

To solve for the $(N+1)$ pressure variables at each integration step, additional relations are needed. We consider three scenarios.

1. If open vents are used at every connections between the two pipetubes, pressures at these connections are the same as external pressures. We have for $i = 1, 2, \ldots, N, N+1$

$$p_i = p_{\text{external}} \tag{4.29}$$

   Because pressure effects are relative, we assume in the numerical simulations

$$\bar{p}_i = 0 \tag{4.30}$$

2. If pipetubes are connected with adits, the pressure variables need to be solved based on the continuity relation in Eq. (4.11). In this case, pressure variables are solved as functions of flow speeds, capsule positions, and capsule speeds. Mathematically, for $k = 1, 2, \ldots, N+1$,

$$\bar{p}_k = \bar{p}_k(\bar{x}_{rj}, \bar{V}_{rj}, \bar{x}_{lk}, \bar{V}_{lk}, \bar{w}_{li}, \bar{w}_{ri}) \tag{4.31}$$

   Details are discussed in the next subsection.

3. In the special case of no adits or vents, the two pipetubes would be independent. This scenario can be considered as the limiting case of just two vents at loading/unloading stations at the ends, or $N = 1$.

Numerical solutions to the above set of equations have been implemented independently using Fortran and C programs, and the results are consistent. These programs apply to a two-bore tube system of any length connecting warehouse terminals, where capsules are removed and unloaded and new loaded capsules are set in motion in the opposite direction. There are any number of capsules in each bore and the system can have any number of equally spaced adits or vents.

Appropriate initial conditions need to be specified in order to solve the system equations. These initial conditions include the initial values of flow speeds, capsule positions, and capsule speeds. Arbitrary initial conditions of flow speeds, capsule positions and speeds can be specified to simulate given scenarios. In particular, the insertion of new capsules into the system can be done according to any schedule.

4.3 Determination of Pressures With the Use of Adits

When pipetubes are connected with adits, the pressure variables can be determined from the continuity equation in Eq. (4.11). The normalized version of Eq. (4.11) becomes

$$\bar{w}_{r,i-1} - \bar{w}_{l,i-1} = \bar{w}_{ri} - \bar{w}_{li} \tag{4.32}$$

for $i = 2, 3, \ldots, N$.

Subtracting Eq. (4.24) from Eq. (4.23) gives

$$\frac{d(\bar{w}_{ri} - \bar{w}_{li})}{d\tau} = g_{ri} - g_{li} + 2(\bar{p}_i - \bar{p}_{i+1}) \ . \tag{4.33}$$

Write the same equation with i replaced by $i - 1$:

$$\frac{d(\bar{w}_{r,i-1} - \bar{w}_{l,i-1})}{d\tau} = g_{r,i-1} - g_{l,i-1} + 2(\bar{p}_{i-1} - \bar{p}_i) \tag{4.34}$$

Using Eq. (4.32), one obtains

$$\bar{p}_{i-1} - 2\bar{p}_i + \bar{p}_{i+1} = f_i \ , i = 2, 3 \ldots, N \tag{4.35}$$

where

$$f_i = .5(g_{ri} - g_{li} - g_{r,i-1} + g_{l,i-1}) \tag{4.36}$$

The difference equation (4.35) requires specification of end conditions because there are $(N - 1)$ equations and $(N + 1)$ pressure variables. We use two kinds of conditions.

1. Open ends. In this case the values of the pressures at the ends are taken to be zero; $\bar{p}_1 = 0$, $\bar{p}_{N+1} = 0$. Thus we have $(N-1)$ equations for the remaining $(N-1)$ pressures. Appendix D presents an analytical solution to the resulting tridiagonal system.

2. Periodic ends. It is convenient sometimes to imagine that the ends are connected, as if the right end is taken around a large circle and connected to the left end; inserting another adit at the join. Now we have $\bar{p}_1 = \bar{p}_{N+1}$ and we assume also that $\bar{w}_{r0} = \bar{w}_{rN}, \bar{w}_{l0} = \bar{w}_{lN}$ in order to evaluate f_i for $i = 1$. This gives N equations for the N pressures (we have added $\bar{p}_1$). However, now the matrix equation which results from Eq. (4.35) is singular; it can be easily verified that the coefficient matrix has zero determinant. This fact corresponds to nonunique solutions, as an arbitrary constant can be added to each of the pressure variables. Therefore we can subtract $\bar{p}_1$ from each of the pressures, effectively setting $\bar{p}_1 \equiv 0$, and throwing out the $i = 1$ equation. The result is $(N-1)$ equations for the remaining $N-1$ pressures. But this is exactly the same as the open ended case, and may be solved in the same way.

Based on Appendix D, one needs to specify $\bar{p}_1$ and $\bar{p}_{N+1}$. The rest pressure variables can be found from

$$\bar{p}_2 = \frac{N-1}{N}\bar{p}_1 + \frac{1}{N}\bar{p}_{N+1} + \sum_{k=2}^{N}\left(\frac{k-1}{N} - 1\right) f_k \tag{4.37}$$

and for $k = 3, \ldots, N$,

$$\bar{p}_k = f_{k-1} - \bar{p}_{k-2} - 2\bar{p}_{k-1} \tag{4.38}$$

4.4 Operating Cost

Total cost of a pipeline system consists of initial construction cost, maintenance cost, and operating cost. Figure 4.4 shows the energy flow in a pipeline system during operation.

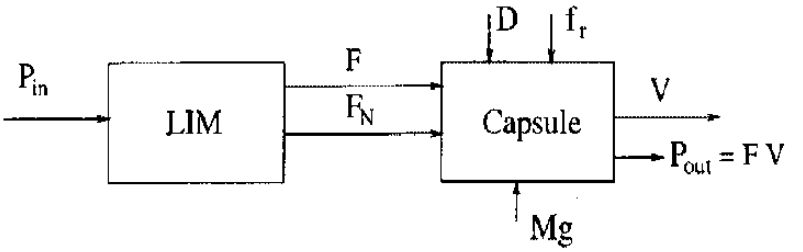

Figure 4.4 Operating Cost Flow

The following cost parameter can be devised to describe the operating cost of a pipeline system. It is defined as the amount of electrical energy required to transport one unit of payload over one unit of distance. This is a useful parameter for comparison with other modes of freight movement, since it can be converted to a dollar cost per ton-mile. Mathematically,

$$\begin{aligned}\mu &= \frac{1}{M_p g\ L}\int_0^{t_f} P_{\text{in}}\ dt \\ &= \frac{1}{M_p g}\frac{\int_0^{t_f} P_{\text{out}}/\eta_e\ dt}{\int_0^{t_f} V\ dt} \\ &= \frac{1}{M_p g L}\int_0^{t_f} FV/\eta_e\ dt \end{aligned} \tag{4.39}$$

where t_f is the amount of time required to travel over distance L, η_e is the efficiency of the linear electric motor, and

$$P_{\text{out}} = FV \tag{4.40}$$

In terms of normalized variables

$$\mu = \frac{1}{\bar{M}_p \bar{g} \bar{L}}\int_0^{\tau_f} \bar{F}\bar{V}/\eta_e\ d\tau \tag{4.41}$$

During steady-state operations,

$$V = \text{constant}, \quad P_{\text{in}} = \text{constant}, \quad L = Vt_f$$

Therefore

$$\mu = \frac{P_{\text{in}}\ t_f}{M_p g L} = \frac{P_{\text{in}}}{P_{\text{out}}}\frac{P_{\text{out}}}{M_p g V} = \frac{1}{\eta_e}\frac{F}{M_p g} = \frac{1}{\eta_e}\frac{\bar{F}}{\bar{M}_p \bar{g}} \tag{4.42}$$

The cost parameter defined above can be put into monetary terms by the following conversion. The operating cost in terms of dollars required to move a one-ton load over a distance of one mile (cost per ton-mile) is

$$\begin{aligned} C &= \mu \times (9.81 \times 907.18) \times 1609.3 \quad \text{joule} \\ &= \mu \times (9.81 \times 907.18) \times 1609.3 \cdot \frac{1}{1000 \times 3600} \quad \text{kilowatt} \cdot \text{hour} \\ &= 3.98\ \mu \quad \text{kw.hr} \end{aligned} \tag{4.43}$$

Assuming 7 cents per kw.hr. (the electrical rate in Minneapolis), we get a conversion factor of 28:

$$C = 28 \times \mu \quad \text{cents/ton} \cdot \text{mile} \tag{4.44}$$

5. System Operation Design

This chapter presents designs of nominal pipeline system operation parameters. We again consider a two-bore pipeline system. Under optimum operating conditions, there is balanced traffic in each bore. At steady-state operating conditions, an equal number of capsules are moving in each direction; each with the same load and velocity and with the same spacing between them. Under such "design conditions" there are the same number of capsules in each bore section and therefore

$$w_{ri} = w_{li} = w_d = \text{constant} \tag{5.1}$$

$$V_{rj} = V_{lk} = V_d = \text{constant} \tag{5.2}$$

$$p_i = \text{constant} \tag{5.3}$$

The basic parameters which need to be specified in system design include

V_d	capsule velocity at steady-state operation
q_d	number of capsules per second. Therefore, $1/q_d$ is headway time, V_d/q_d is spatial headway
M_d	design mass of capsule plus payload
M_p	capsule payload
A_T	pipetube cross-sectional area
A	capsule cross-sectional area
ℓ	capsule length
V_s	synchronous speed of the linear induction motor
F_R	rated motor thrust force
s_{cr}	critical slip corresponding to maximum LIM thrust

5.1 An Operation Scenario

The design and analysis methods presented in this report can be applied to a general pipeline system powered by linear electric motors. In order to obtain some specific comparisons, we now define a freight pipeline transportation scenario.

Blockage is defined as the ratio of the capsule cross sectional area over the area of the tube. Blockage is a critical design parameter. Since tunneling is expensive the first thought is to make the capsule of circular section and as large as possible for a given tube diameter. However, general freight is often palletized into rectangular units, which would leave packing voids in circular capsules. This suggests the use of capsules of square section. These would have smaller blockage, since the voids would then be on the outside. As an added advantage square capsules could be more conveniently stacked onto trucks for final destinations. A square section capsule which just fits a circular tube has a blockage of .64. If some additional clearance were allowed at corners a blockage of .5 is realistic. (This is the blockage of a channel shuttle.)

The tube diameter itself is also an important parameter, which must be kept as small as possible to minimize boring costs. For general freight transport it would be difficult to have a diameter smaller than about two meters; we adopt this value when it is necessary to be specific about size. One might consider tubes of smaller diameter for parcel or document delivery.

We have adopted Vandersteel's model [41] which has a 2m diameter tube carrying 10ton capsules (of which 8 tons are payload), propelled at 25m/s. At these design conditions, a 2 sec headway would give a continuous freight rate of 4 tons/sec, or 100 million tons per year, which is about 10 times the annual truck freight tonnage carried between Minneapolis and Chicago, but is not an unreasonable rate for some heavily used corridors.

The design speed $V_d = 25$ m/s would allow a capsule to travel from coast to coast in about two days. For comparison, the design speed of $V_d = 50$ m/s is also used. Actually, an electrical pipeline system with a wheel-on-rail configuration can allow capsules to travel much faster, up to 250 miles/hour (or about 110 m/s). An electrical pipeline concept can certainly accommodate one-day or faster capsule deliveries from coast to coast. Further increase in capsule speeds would result in much higher maintenance cost with a wheel-on-rail configuration, and would require the use of magnetic suspension for economic feasibility.

The following table summarizes the base line operation design parameters. Values of overall pipeline length, number of adits, and number of capsules need to be specified in the studies of off-design conditions. These values are used in simulations in the next chapter and are included here for convenience.

Table 5.1 Baseline Pipeline Design Parameters

$R_T = 1$ m	interior radius of the pipetube
$\theta_d = 0$	pipeline average grade
$V_d = 25$ m/s	steady state capsule speed
$\ell = 3$ m	capsule length
$d = 1.25$ m	capsule hydraulic diameter
$\beta = A/A_T = 0.5$	blockage ratio
$1/q_d = 2$ sec	capsule headway times
$M_d = 10$ tons $= 9071.8$ kg	capsule weight
$M_p = 8$ tons $= 7257.4$ kg	capsule payload
$L_T = 250$ m	section length
$L_P = 20$ km	total pipeline length
$N = 80$	number of sections (adits)
$V_d/q_d = 50$ m	spatial headway
$N_{cl} = N_{cr} = 400$	number of capsules in each bore
$N_c/N = 5$	number of capsules in each section

5.2 Steady-State Speed Relations

The steady-state versions of Eqs. (4.5) and (4.13) are now used to determine steady relations between flow and capsule speed under design conditions. During steady state operations under design conditions, the number of capsules per unit length is q_d/V_d, which is the reciprocal of the headway length. Therefore, the number of capsules in a bore section is $L_T q_d/V_d$. Eq. (4.5) at steady-state conditions becomes

$$(L_T q_d/V_d)\frac{1}{2}\rho(V_d - w_d)^2 A C_{Dd} = \frac{1}{2}\rho w_d^2 2\pi R_T L_T C_{fd} \tag{5.4}$$

where

$$C_{Dd} = C_D(\beta, V_d, w_d) \tag{5.5}$$

$$C_{fd} = C_f(w_d) \tag{5.6}$$

Solving Eq. (5.4) for w_d gives

$$\frac{w_d}{V_d} = \frac{\phi}{1+\phi} \tag{5.7}$$

where ϕ is defined by

$$\phi = \sqrt{\frac{\beta R_T q_d C_{Dd}(\beta, V_d, w_d)}{2 V_d C_{fd}(w_d)}} = \phi(\beta, V_d, w_d, q_d) \tag{5.8}$$

The parameter ϕ represents the relative effects of drag and wall friction. When C_{Dd} is very large, ϕ is large and w_d can become nearly as large as V_d, while if β is small, ϕ and therefore w_d are small.

It is interesting to examine the ratio of flow speed over capsule speed at steady-state operations under design conditions. We have

$$\alpha = \frac{w_d}{V_d} = \frac{\phi}{1+\phi} = \alpha(\beta, V_d, q_d) \in (0,1) \tag{5.9}$$

Since C_{fd} and C_{Dd} depend on w_d, it is necessary to iterate numerically in order to solve for this ratio α for given (β, V_d, q_d). Specifically, α can be determined as roots to

$$f = \alpha(1+\phi) - \phi = \alpha + (\alpha - 1)\phi = 0 \tag{5.10}$$

A bisection method is found to be feasible for this problem. One starts a bisection by guessing two values of α: α_1 and α_2, such that

$$f(\alpha_1) < 0 \qquad f(\alpha_2) > 0 \tag{5.11}$$

This is always possible because

$$\lim_{\alpha \to 0} f(\alpha) = -\phi < 0 \qquad \lim_{\alpha \to 1} f(\alpha) = 1 > 0 \tag{5.12}$$

For example,

$$\alpha_1 = 0.0001 \qquad \alpha_2 = 0.9999 \tag{5.13}$$

Then, the bisection algorithm proceeds as follows

1. $\alpha_0 = (\alpha_1 + \alpha_2)/2$

2. Evaluate $f(\alpha_0)$

3. If $f(\alpha_0) = 0$, α_0 is the solution.

4. Otherwise,

5. If $f(\alpha_0) \cdot f(\alpha_1) > 0$, $\alpha_1 = \alpha_0$

6. Else if $f(\alpha_0) \cdot f(\alpha_2) > 0$, $\alpha_2 = \alpha_0$

7 Stop the iteration if $|\alpha_1 - \alpha_2| < \epsilon$. Otherwise go back to 1.

A computer program based on the above bisection procedure is coded. Figure 5.1 shows α as a function of the capsule speed V_d with β as a parameter at specified pipeline design conditions, for $q_d = 0.5$ sec^{-1}.

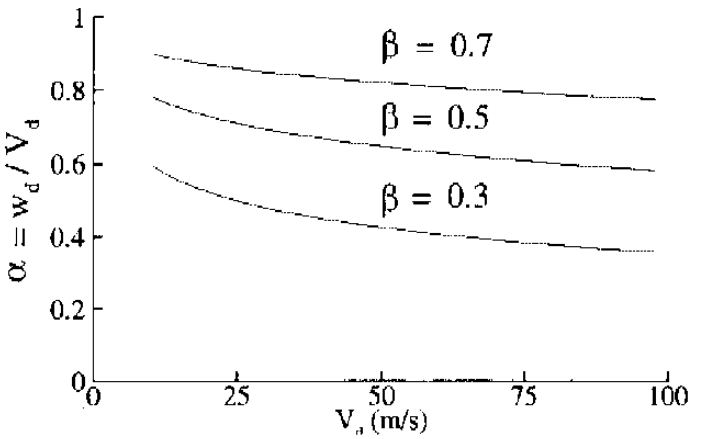

Figure 5.1 Steady-State Relation Between w_d and V_d, $q_d = 0.5$ sec^{-1}.

5.3 Linear Motor Thrust for Overcoming Aerodynamic Resistance

Based on Eq. (4.13), the motor thrust required for steady-state operation at design conditions is given by

$$\begin{aligned} F_d &= \frac{1}{2}\rho(V_d - w_d)^2 A C_{Dd} + M_d g \sin\theta_d + f_r(M_d g \sin\theta_d + F_N) + \Delta F \\ &\approx F_d^a + M_d g(\sin\theta_d + f_r \cos\theta_d) \end{aligned} \tag{5.14}$$

where it is assumed that $F_N \ll M_d g$ and the miscellaneous forces are negligible. The first term represents the thrust required to overcome aerodynamic resistance.

$$\begin{aligned} F_d^a &= \frac{1}{2}\rho(V_d - w_d)^2 A C_{Dd} = \frac{1}{2}\rho V_d^2 A_T C_{Dd} \frac{\beta}{(1+\phi)^2} \\ &= \frac{1}{2}\beta\rho V_d^2 A_T (1-\alpha)^2 C_{Dd}(\beta, V_d, \alpha V_d) \\ &= F_d^a(\beta, V_d, q_d) \end{aligned} \tag{5.15}$$

Figure 5.2 plots the required thrust to overcome aerodynamic resistance at steady-state as a function of capsule speed with blockage as a parameter, for $q_d = 0.5$ sec^{-1}. As the blockage increases, the required thrust force increases.

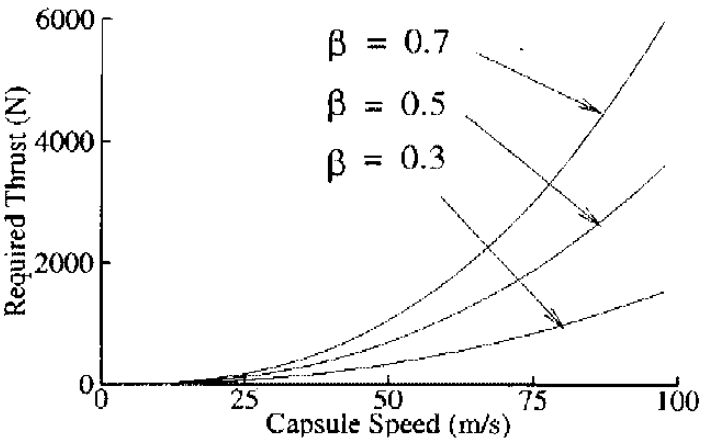

Figure 5.2 Thrust Required to Overcome Aerodynamic Resistance

To compare a pipeline system with trains or trucks, an effective drag coefficient can be defined as

$$C_{\text{Deff}} = \frac{C_{Dd}}{(1+\phi)^2} = C_{\text{Deff}}(\beta, V_d, w_d; q_d) \tag{5.16}$$

This effective drag coefficient represents the equivalent drag coefficient if the capsules were operating out in the open without the pipelines. During steady-state operations at design conditions, $w_d = \alpha V_d$. Therefore,

$$C_{\text{Deff}} = (1-\alpha)^2 C_{Dd}(\beta, V_d, \alpha V_d) = C_{\text{Deff}}(\beta, V_d, q_d) \tag{5.17}$$

Figure 5.3 plots effective drag coefficient as a function of blockage ratio at two speeds: $V_d = 25$ m/s and $V_d = 50$ m/s, for $q_d = 0.5$ sec^{-1}. Despite the apparent differences, the *effective* drag coefficient for the electrical pipeline system is of the same order as for trucks.

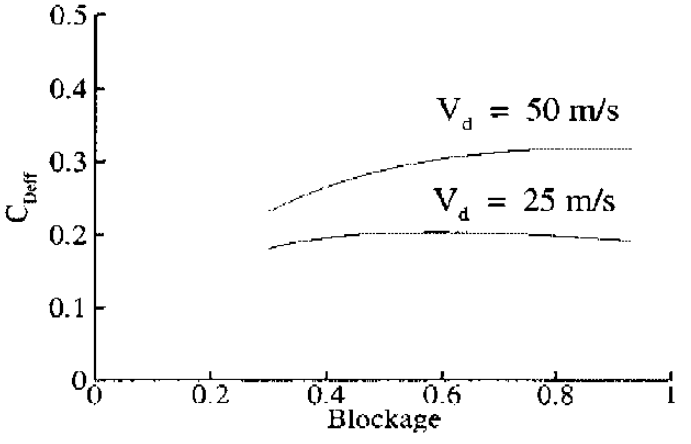

Figure 5.3 Effective Drag Coefficient for Pipeline Capsules, $q_d = 0.5$ sec^{-1}.

A comparison can be made between the proposed electrical pipeline system and a pneumatic pipeline system. In a pneumatic propulsion system, air is forced through the pipetubes by external pumps to drive the capsules, while for an electrical pipeline system air is forced by the motion of the capsules themselves. In the **ideal** pneumatic case, blockage is large and the air velocity is equal to the capsule velocity V_d; there is no drag or thrust on the capsule. In the real world the air velocity would have to be greater than V_d, passing over the capsule from behind to provide enough thrust to overcome rolling friction. The pneumatic pumps in the ideal case would have to produce a pressure force

$$F_p = .5\rho V_d^2 2\pi R_T C_f(V_d) V_d / q_d \tag{5.18}$$

for each capsule in order to overcome wall friction in the headway length between capsules. This force should be compared with the electrical motor thrust required to overcome aerodynamic resistance, F_d^a given in Eq. (5.15). The ratio of the latter to the former,

η, represents the aerodynamic efficiency of an electrical pipeline system over a pneumatic propulsion system with the same capsule velocity and pipetube diameter:

$$\eta = \left(\frac{\phi}{1+\phi}\right)^{7/4} = \alpha^{7/4} = \eta(\beta, V_d, q_d) \tag{5.19}$$

Clearly η is less than one, so the electrical pipeline system always requires less power. In Figure 5.4, η is plotted versus β for a particular case: 2m diameter tube and $1/q_d = 2$ sec. As $\beta \rightarrow 1$ the two systems become equivalent, but at $\beta = .5$ (which is close to the actual feasible design blockage ratio), there is nearly a 50% improvement. In other words, the electrical pipeline concept is inherently better than the pneumatic pipeline concept from an aerodynamic point of view.

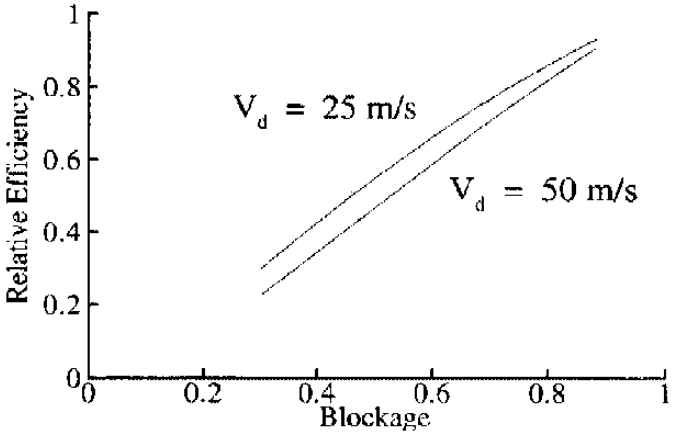

Figure 5.4 Efficiency of Electrical Propulsion Relative to Pneumatic Propulsion

5.4 Operating Cost Under Design Conditions

The cost parameter μ defined in Section 4.4 is plotted versus β in Figure 5.5 for the above design case. In these calculations, a rolling friction coefficient of $f_r = 0.01$ is used. Two grade levels are studied: $\theta = 0$ deg and $\theta = 2$ deg. Clearly, there is a **best operating speed** that corresponds to the lowest cost parameter for a given linear induction motor.

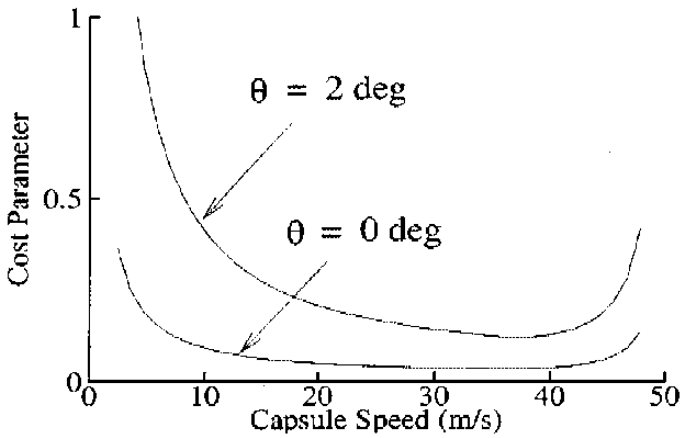

Figure 5.5 Steady-State Cost Parameter, $V_s = 50$ m/s, $\beta = 0.5$, $f_r = 0.01$.

Specifically, the cost parameter in Eq. (4.42) comes from four sources: aerodynamic resistance, grade slope, rolling friction, and linear electric motor loss. We have

$$\mu \sim \frac{aV^2 + Mg(\sin\theta + f_r \cos\theta)}{\eta_e(V)} \tag{5.20}$$

where a represents the aerodynamic resistance effect. Simulations show that the best operating speed is equal or close to the speed for optimal LIM efficiency, $V_{\max,e}$ (see Appendix C). Therefore, a linear induction motor should be designed such that

$$V_{\max,e} = V_d \tag{5.21}$$

If $V_{\max,e}/V_s \triangleq u_{\max}$ is known for a given LIM, the synchronous speed is given by

$$V_s = \frac{V_d}{u_{\max}} \tag{5.22}$$

5.5 Sizing of Linear Motor Thrust

A linear electric motor must provide sufficient thrust force at all ranges of capsule speeds, load conditions, and variations in the pipeline environment. The required thrust force at steady-state is comparable to the sum of aerodynamic drag, gravity component due

to pipeline grade, rolling friction force, and miscellaneous forces. Referring to discussions in Section 5.3, Eq. (5.15) and Figure 5.2, the required motor thrust during steady state operations to overcome aerodynamic resistance **does not** depend on capsule weight; it only depends on capsule/pipeline dimensions and traveling speed. Increase in traveling speed requires an increase in motor thrust to overcome aerodynamic resistance, as shown in Figure 5.2. In comparison, thrust forces required to overcome rolling friction depend on the capsule weight, but do not depend on capsule speed. For a 10-ton capsule (9071.8 kg) with rolling friction coefficient of $f_r = 0.01$, the thrust required to overcome rolling friction is on the order of 889 N. The thrust required to overcome a 3 degree grade is $4,653$ N.

In addition, the motor thrust must be able to accelerate a capsule into motion. An acceleration rate of $0.1g$ for the above capsule would require an **additional** thrust of $0.1M_d g = 8,890$N. This large required thrust during initial acceleration may be provided by a down-grade pipeline geometry. In Chapter 3, a concept of grade braking is proposed to slow a capsule down toward a loading/unloading station. This concept can also be used to accelerate a capsule into motion using gravity force, as shown in Figure 2.17. For example, a 6-deg down slope can effectively produce a propulsion force of $9,300$N. Because the pipelines are buried underground while loading/unloading stations are above ground, this change of pipeline grades can be naturally implemented.

Therefore, we assume that a 6 deg downslope is used at stations to assist electric motors in accelerating capsules into motion. Similarly, a 6 deg up slope is used to slow down capsules near loading/unloading stations. This choice will make the required thrust during initial acceleration and the required steady-state thrust comparable.

Let's now use the required steady-state thrust to size an electric motor. The LIM thrust can be predicted using Kloss' formula,

$$F = \frac{2F_{\max}}{s/s_{cr} + s_{cr}/s} \tag{5.23}$$

where the slip is defined as

$$s = 1 - \frac{V}{V_s} \tag{5.24}$$

and $F_{\max}$ is a maximum thrust under a specific input voltage/frequency condition. Roughly, $F_{\max}$ is proportional to the ratio of input voltage over input frequency

$$F_{\max} \propto \frac{U}{f} \tag{5.25}$$

Therefore, the maximum thrust $F_{\max}$ can be varied by changing input voltage and/or frequency and can be used to control capsule speed. In sizing an electric motor, we need to determine an **upper bound** of the maximum thrust, called rated thrust.

$$F_{\max} \leq F_{\mathrm{R}} \quad \text{for all } V \tag{5.26}$$

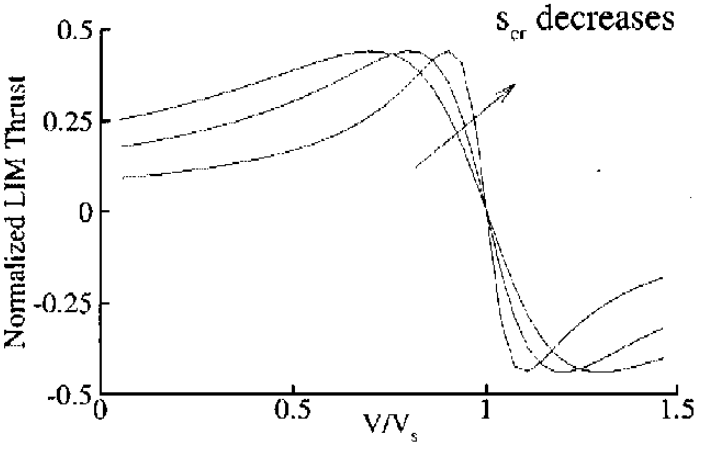

Figure 5.6 Effect of Critical Slip on LIM Thrust

It appears on the surface that capsule speed can also be controlled through the variations of synchronous speed V_s and critical slip s_{cr}. Physically, however, there are only two independent controls once a linear induction motor design is fixed: input voltage U and input frequency f. The input frequency directly controls the synchronous speed,

$$V_s = 2\tau f \tag{5.27}$$

This synchronous speed should be selected so that a desired capsule speed offers the best energy efficiency (i.e. Eq. (5.22)). In comparison, a specific LIM design fixes the value

of the critical slip s_{cr} at specified conditions of V_s and $F_{\max}$. To understand the effect of the critical slip on LIM thrust performance, Figure 5.6 shows the LIM thrust force as a function of normalized speed V/V_s at various values of s_{cr}.

A smaller critical slip results in steeper thrust variations around the synchronous speed. This would produce a larger thrust change for a given amount of speed variation. Too small a critical slip would produce jerky capsule motions, whereas too large a critical slip would result in slow capsule responses to perturbations that cause capsule speed variations. In this report, it is assumed that

$$s_{cr} = 0.3 \tag{5.28}$$

The required maximum motor thrust $F_{\max}$ corresponding to a certain capsule speed at design conditions can be determined as roots to the following nonlinear equation.

$$f = F(V_d; F_{\max}, s_{cr}, V_s) - F_d^a(\beta, V_d, q_d) - M_d g(\sin\theta_d - f_r \cos\theta_d) = 0 \tag{5.29}$$

where s_{cr}, β, and q_d are specified, and V_s is determined from Eq. (5.22). In addition, it is necessary that the maximum thrust satisfy the following requirement to ensure natural speed stability;

$$\frac{\partial f}{\partial V} < 0 \quad \text{at } V = V_d \tag{5.30}$$

This is true as long as

$$1 - s_{cr} < \frac{V_d}{V_s} = u_{\max} < 1 + s_{cr} \tag{5.31}$$

For example, this relation is satisfied by our choice of $u_{\max} = 0.75$ and $s_{cr} = 0.3$. A functional dependence of the maximum thrust is given by

$$F_{\max} = F_{\max}(V_d; \beta, q_d, s_{cr}, f_r, \theta_d, u_{\max}) \tag{5.32}$$

A computer program is coded that determines the maximum motor thrust.

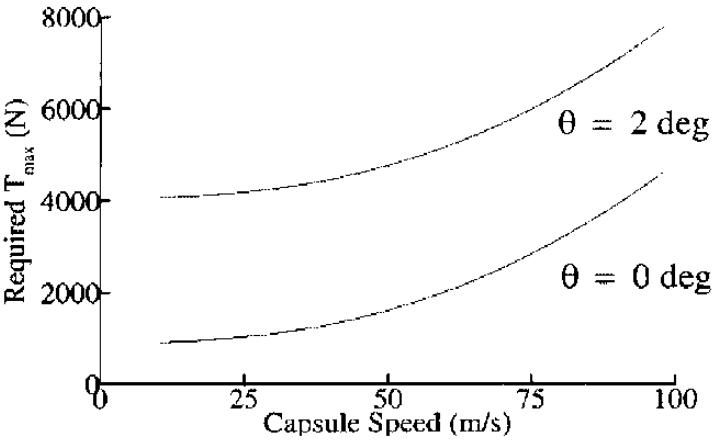

Figure 5.7 Rated Maximum LIM Thrust

As shown in Figure 5.7, the maximum motor thrust requirement at a specific capsule speed is a strong function of pipeline grade. Table 5.2 shows values of required maximum thrust and the corresponding input power requirement at several conditions of capsule steady-state speed and continuous pipeline grade (1 HP = 745.7 W = 745.7 Nm/s).

Table 5.2 Maximum Required LIM Thrust

Speed (m/s)	Grade (deg)	$F_{\max}$ (N)	$P_{\max} = F_{\max}V/\eta_e$ (HP)
25	0	1,030	70
50	0	1,650	220
25	2	4,180	280
50	2	4,800	650

The rated thrust F_R should be large enough so that the electric motor can maintain steady capsule motions at specified speed range and conditions, and can start capsule motions initially. On other other hand, too large a F_R would cause unnecessary energy losses. The rated motor thrust should be at least larger than this required steady-state thrust, plus some extra thrust force reserved for feedback control of capsule motions in the presence of various uncertainties and perturbations. For the pipeline geometry and capsule

operation conditions stated in Table 5.1, the rated thrust is selected to be $F_{\mathrm{R}} = 6,000$N, for an average pipeline grade of $\theta_d = 0$ deg. Table 5.3 summarizes the LIM design parameters selected so far.

Table 5.3 Baseline LIM Design Parameters

$s_{cr} = 0.3$	LIM critical slip corresponding to $T_{\max}$
$F_{\mathrm{R}} = 6,000$ N	rated maximum LIM thrust
$V_{\max,e} = V_d$	speed at maximum LIM efficiency, assumed
$V_s = V_{\max,e}/0.75$m/s	LIM synchronous speed
$\eta_e = 0.5$	maximum LIM efficiency, assumed

6. Computer Simulation Studies

A comprehensive computer program is coded using C language to simulate pipeline operations. This computer program essentially solves the differential/algebraic equations developed in Chapter 4. A major challenge to the development of this simulation program is that capsules must be allowed to enter and/or leave the pipeline system with **arbitrary** schedules. As a result, the number of capsules in the pipeline system and thus the number of solution variables can change from time to time. In numerical implementations, a set of logics has to be devised that can detect when a new capsule enters into the pipeline system, and when a capsule exits the system. An array of variable dimensions is implemented with dynamic memory allocations.

Because of the flexibility in the simulation program, it can be used to study a wide range of pipeline operation scenarios. In this chapter, numerical simulations are used to compare the efficiencies of different pipeline system configurations such as adits and vents under off-design conditions. The relative merits of intermittent versus platoon operations under off-design conditions are also compared. Then, capsule stabilities are discussed and feedback control of capsule motions are designed. Finally, simulations are used to demonstrate the working of feedback control laws.

6.1 Configurations and Operational Strategies

Normally, a practical pipeline system needs two bores for transporting capsules in two directions. These two bores can be kept independent, or connected at intervals with short cross tunnels (adits). There are some economic advantages to connecting these pipetubes with adits [42], to allow pressure relief. The channel tunnel is an example of an existing long two-bore system with adits [43]. These adits can also be opened up to the external environment. In this case, these connecting tunnels are called vents.

The idea behind adits is to allow the high pressure difference that builds up across a moving capsule to divert air through a cross tunnel into the other pipetube, thus producing

circulation around an adit loop (consisting of both pipetubes and two successive adits) and limiting the length of air column a capsule must push. Under ideal operating conditions in which there is uniform capsule traffic in each direction, each capsule with the same velocity and load and with the same headway between each, the cross tunnels have no effect. Each capsule pushes its own measure of tube air and there is no pressure imbalance to induce flow through the cross tunnels. However, when there is light or intermittent traffic the added flexibility in allowing air to be routed through a path of less resistance can reduce the drag. As an extreme example, if there were only one tightly fitting capsule in a long tube, with no adits or air vents for relief, the capsule would have to push the entire column of tube air against the frictional resistance of the tube walls.

There are also some negative aspects to the use of adits, besides the obviously higher capital costs of construction. When the capsule blockage is fairly large, very high tube air speeds can result, nearly as large as the capsule velocity, and there is a potential for high speed flow through the cross tunnels to produce damaging jet flow into the other tube. The side force could derail an unrestrained capsule or damage loose freight. Bernard reports that in the channel tunnel this possibility necessitated design changes in the cross tunnels and limitations on shuttle speeds [44]. In an electrical pipeline system, capsule blockage is fairly small to reduce aerodynamic resistance. The use of adits or vents is mainly advantageous.

The previous chapter has shown that the economics of tube freight transport are quite favorable at the tonnage rates (4 ton/sec) and under the design conditions. However, it is inevitable that there will be periods of light traffic when it is not possible to inject fully loaded capsules into the pipetube at the design headway interval. There are two operating strategies one can consider: intermittent operation, in which loaded capsules are inserted as they become available, and platoon operation in which capsules are held back at the warehouse until there is a sizeable number, which are then each inserted at the design headway forming a compact group, to be followed by a, perhaps lengthy, period while a sufficient number are collected for the next platoon. We now evaluate these two strategies

using numerical simulations of the pipeline system operation. The relative merits of adits versus vents are also compared. Because system configurations are concerned only with aerodynamic aspects of the pipeline system, a combined cost parameter $\mu \cdot \eta_e$ is used (Eq. (4.42)).

In this simulation analysis, the insertion of new capsules into the system was done by a simple freight periodicity condition for convenience. With this assumption, capsules entering a warehouse were reinserted into the same tube at the warehouse at the other end of the system.

6.1.1 Intermittent operation

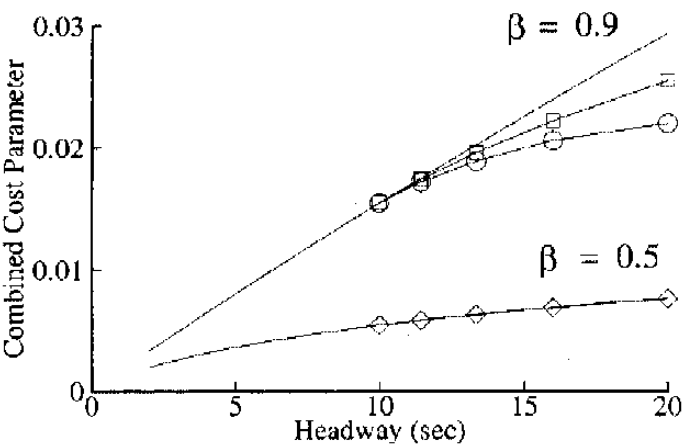

Figure 6.1 Cost Parameter vs. Headway

Circle for Vents, Square for Adits, Diamond for Both

Solid Line for Without Adits or Vents

We consider the cost of transporting the standard 10 ton capsules, with 8 ton payloads, without adits, in an off-design situation in which the capsules are evenly spaced but the headway between the capsules is greater than the 2 second design value. We consider two blockage values, $\beta = .5$ and $\beta = .9$. It is assumed that the motor force is available to keep

the speed of each capsule at 25 m/s. In Figure 6.1, the combined cost parameter $\mu \cdot \eta_e$ is plotted versus headway time for the range 2 seconds to 20 seconds, i.e., the tonnage rate varies from 4 ton/sec on the left side of the figure to .4 ton/sec on the right. For $\beta = .9$ the cost increases by a factor of 9 over this range, while for $\beta = .5$ it increases by a more moderate factor of 4. At the higher blockage value the cost increases almost linearly with headway time, most of the resistance coming from air friction in the linearly lengthening distance between capsules.

When adits (or vents) are considered it is necessary to specify both the adit spacing and the total length of the pipeline. We have computed for a 20 km pipeline with 80 adits; the adit spacing is 250 m (Table 5.1). Under design conditions, there would be 400 capsules in each tube and 5 capsules between adits in each tube. As we increase the headway between capsules there is no effect on cost as long as there is at least one capsule in each adit section. That is, no effect up to a headway time of 10 sec, and this is also the case if there is no traffic in the other tube; at longer headways we begin to see an effect. The results for adits are disappointing. For $\beta = .5$ there is no effect over the range shown, while for $\beta = .9$ there is only a small improvement. When the capsules are spaced out like this there is only a small opportunity for air to be shunted through the other tube. For simple lossless vents to the atmosphere, at the same spacing as for the adits, the results are somewhat better for the larger blockage, but still have no effect for $\beta = .5$.

6.1.2 Platoon operation

We consider platoons of from one to 80 capsules, with 25 m/s speed and 2 sec headway in a 20 km pipeline with 250 m between adits or vents. The other tube is empty. The results are shown in Figure 6.2 as relative cost versus platoon length for $\beta = .5$ and $\beta = .9$. Relative cost is the cost divided by the cost under design conditions. If the platoon length were increased to 400 for this pipeline the relative cost would be one. If the capsules in a 40 capsule platoon were spaced out evenly they would have headway of 20 seconds; the situation would be the same as the right hand side of Figure 6.1. The advantage of platoon

operation over intermittent operation is clear from these figures. The physical reason is that with a platoon it is not necessary to pump air through the entire tube; the adits work as intended, circulating the air through the other tube. Vents work even better. Vents are also preferred from a heat circulation point of view. It is interesting that the *relative* results are almost independent of blockage.

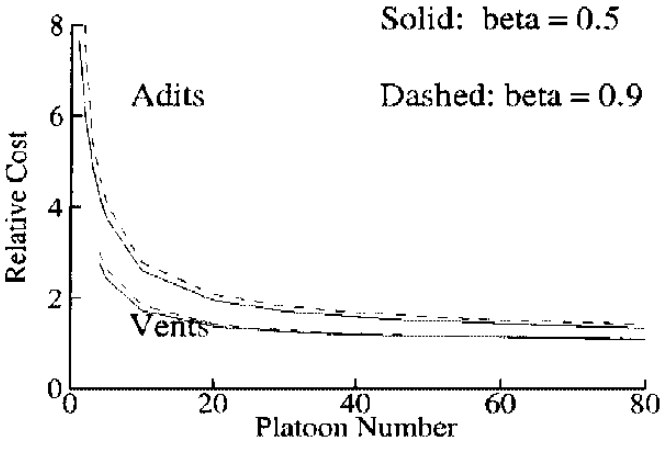

Figure 6.2 Relative Cost vs. Platoon Number

The forces required to keep all the capsules moving at the design speed are much larger for the lead capsules in the platoon, which must accelerate the air as they enter a new adit section, thus providing drafting for the following capsules. For $\beta = .5$ the (time average) force on the lead capsule in a long platoon is about 3.5 times average force; for $\beta = .9$ it is about 5.5 times the average. This requirement can be handled in one of two ways. Sufficient reserve forces can be designed into each capsule. Alternatively, a special "lead capsule" can be designed that has a larger LIM thrust force capability than other follower capsules.

6.2 Capsule Stabilities and Feedback Control

Capsules are designed to operate at a certain speed. In addition, capsules should not run into each other. As a result, it is often desirable that capsules follow specified time

histories of position inside the pipetube. On the other hand, actual systems are always different from models that are used in system design and analysis. Modeling uncertainties and disturbances can cause capsule motions to deviate from the designed speed or locations.

The concept of stability represents capsules' inherent ability to follow a specified speed or time history of position in the presence of uncertainties and disturbances. Stability of capsule motion depends on the overall pipeline system design, configurations of electrical motors, pipeline geometry, and other factors.

6.2.1 Stabilities of Capsule Motions

In the proposed system configuration, a capsule's operating speed is determined by the balance of its linear induction motor thrust force, aerodynamic drag, rolling friction, weight thus pipeline grade, and miscellaneous forces on the capsule. This speed, called an equilibrium speed for the capsule, differs from the designed capsule speed due to modeling uncertainties and disturbances. It also differs from capsule to capsule, because different capsules will have different payloads, and experience different aerodynamic drags and rolling frictions. Efforts to load capsules evenly can make the equilibrium speeds of different capsules close to each other, and close to designed capsule steady-state speed.

In actual operations, an individual capsule can maintain its speed in a certain range around the equilibrium speed, which is hopefully close to the designed steady-state speed. This is due to the nature of linear induction motor force. An increase in capsule speed results in a decrease in motor thrust and vice versa. As a result, individual capsules are expected to travel within a small range of speeds around the equilibrium speed without active feedback control.

However, the capsule positions in the pipetube are expected to deviate from the position history corresponding to the equilibrium speed. This is because positions are integrations of capsule speed, and deviations of capsule speeds from the designed value can cause a finite change in capsule position from designed time history. These deviations will cause

a capsule to arrive early or late at a specified location in the pipetube. For a train of capsules without physical connections, the relative distance between any pair of capsules will either increase or decrease gradually over time. Because of the low pressure region behind each capsule, a capsule approaching from behind will be sucked into the wake region of the lead capsule if the relative separation becomes sufficiently small. Therefore, the motion of a train of capsules is not stable without active feedback control.

A train of capsules can be chained together with physical connections. Then, the train of capsules behavior like a single capsule. Special connectors are allowed in the capsule design discussed in Chapter 3. This arrangement will necessarily require a platoon operation and can limit the freedom of individual capsules. Alternatively, active feedback control of capsule speed and position can be used to force capsules travel at specified speed or position history. To control a capsule speed to a prescribed value, for example, the feedback control logic can reduce the linear motor thrust force if the actual speed is larger than the desired speed, and increase the linear motor thrust force otherwise.

6.2.2 Design of Feedback Control Laws

The specific logic that determines the amount of change of linear motor thrust force based on differences between actual and desired speed is called feedback control law. A feedback control law determines how fast and how much the motor thrust force is changed.

For any feedback control law to be successful, accurate measurements of capsule speed and position must be obtained. Because of the flow motion inside a pipetube, measurement of capsule speed and position must be obtained from inertial references rather than aerodynamic equipment (such as pitot-static tube). Furthermore, the concealed pipeline environment would precludes the use of satellite-based inertial measurement such as the Global Positioning System (GPS). We propose two types of sensing devices. As discussed in Chapter 3 for capsule design, magnetic plates can be placed on individual capsules that can detect the relative speed and position with respect to a fixed reference mounted on the interior of pipetubes. The importance of position measurement really lies in collision

avoidance. Therefore, a radar unit can be placed on the head of a capsule that can measure the relative distance between the own capsule and a nearby capsule.

Assuming accurate measurements can be made on capsule speed and position, feedback control laws can be designed that vary motor thrust force to regulate capsule speed and position based on measurements. The capsule motion system is a nonlinear dynamical system with fairly large ranges of speed change. As a result, **nonlinear** feedback control laws must be used. Over the last decade, a method known as feedback linearization has been successfully used for many nonlinear systems [52].

Capsule feedback control laws are now designed using the feedback linearization method. Eqs. (4.25) and (4.26) represent a second-order dynamic system, repeated here for convenience.

$$\frac{d\bar{x}_{rj}}{d\tau} = \bar{V}_{rj} \tag{6.1}$$

$$\begin{aligned}\frac{d\bar{V}_{rj}}{d\tau} &= \frac{\bar{F}_{rj}}{\bar{M}_{rj}} - \frac{\beta}{2m_d\bar{M}_{rj}} C_D(V_{rj}, w_{rI})(\bar{V}_{rj} - \bar{w}_{rI})^2 \mathrm{sgn}(\bar{V}_{rj} - \bar{w}_{rI}) \\ &\quad - \bar{g}\sin\theta_{rI} - f_r\left(\bar{g}\cos\theta_{rI} + \frac{\bar{F}_{N_{rj}}}{\bar{M}_{rj}}\right) \quad \text{where } (I-1) \le \bar{x}_{rj} \le I \qquad (6.2) \\ &\triangleq \frac{\bar{F}_{rj} - \bar{D}_{rj}}{\bar{M}_{rj}}\end{aligned}$$

where $\bar{D}_{rj}$ contains all other forces. Suppose that we want the capsule speed $\bar{V}_{rj}$ to follow a desired speed $\bar{V}^*$ (which can be the design speed $\bar{V}_d$). We first need to define desired dynamics. Here, the LIM thrust force is a control variable because it can be directly changed, whereas the capsule speed $\bar{V}$ is a first-order state variable because it takes one differentiation of the speed to reach control. In comparison, the capsule position is a second-order state variable because it takes two differentiations of the position to reach control. Correspondingly, a desired closed-loop dynamics for speed response can be defined by a first-order model with a selected time constant. Mathematically

$$\dot{\bar{V}}_{rj} + K_V(\bar{V}_{rj} - \bar{V}^*) = 0 \tag{6.3}$$

where the feedback gain K_V can be selected for desired responses. The required LIM thrust force that can guarantee Eq. (6.3) is determined by substituting Eq. (6.3) into Eq. (6.2). We have

$$\begin{aligned}\bar{F}_{rj} &= \bar{D}_{rj} - K_V \bar{M}_{rj}(\bar{V}_{rj} - \bar{V}^*) \\ &= \frac{\beta}{2m_d} C_D(V_{rj}, w_{rI})(\bar{V}_{rj} - \bar{w}_{rI})^2 \mathrm{sgn}(\bar{V}_{rj} - \bar{w}_{rI}) \\ &\quad + \bar{M}_{rj}\bar{g}\sin\theta_{rI} + f_r(\bar{M}_{rj}\bar{g}\cos\theta_{rI} + \bar{F}_{N_{rj}}) \\ &\quad - K_V \bar{M}_{rj}(\bar{V}_{rj} - \bar{V}^*) \quad \text{where } (I-1) \le \bar{x}_{rj} \le I \end{aligned} \tag{6.4}$$

In essence, Eq. (6.4) represents a nonlinear feedback control law.

If we want the position variable $\bar{x}_{rj}$ to follow a prescribed history $\bar{x}^*(t)$, a similar procedure can be used. Since x is a second-order state, a desired closed-loop dynamics must be specified as,

$$\ddot{\bar{x}}_{rj} - \ddot{\bar{x}}^* + K_1(\dot{\bar{x}}_{rj} - \dot{\bar{x}}^*) + K_2(\bar{x}_{rj} - \bar{x}^*) = 0 \tag{6.5}$$

and the feedback control action is given by

$$\begin{aligned}\bar{F}_{rj} &= \bar{D}_{rj} - K_1 \bar{M}_{rj}(\dot{\bar{x}}_{rj} - \dot{\bar{x}}^*) - K_2 \bar{M}_{rj}(\bar{x}_{rj} - \bar{x}^*) \\ &= \frac{\beta}{2m_d} C_D(V_{rj}, w_{rI})(\bar{V}_{rj} - \bar{w}_{rI})^2 \mathrm{sgn}(\bar{V}_{rj} - \bar{w}_{rI}) \\ &\quad + \bar{M}_{rj}\bar{g}\sin\theta_{rI} + f_r(\bar{M}_{rj}\bar{g}\cos\theta_{rI} + \bar{F}_{N_{rj}}) \\ &\quad - K_1 \bar{M}_{rj}(\dot{\bar{x}}_{rj} - \dot{\bar{x}}^*) - K_2 \bar{M}_{rj}(\bar{x}_{rj} - \bar{x}^*) \quad \text{where } (I-1) \le \bar{x}_{rj} \le I \end{aligned} \tag{6.6}$$

Feedback control laws for capsules in the left bore can be similarly determined. We have for capsule speed control,

$$\begin{aligned}\bar{F}_{lk} &= \frac{\beta}{2m_d} C_D(V_{lk}, w_{lJ})(\bar{V}_{lk} - \bar{w}_{lJ})^2 \mathrm{sgn}(\bar{V}_{lk} - \bar{w}_{lJ}) \\ &\quad + \bar{M}_{lk}\bar{g}\sin\theta_{lJ} + f_r(\bar{M}_{lk}\bar{g}\cos\theta_{lJ} + \bar{F}_{N_{lk}}) \\ &\quad - K_V \bar{M}_{lk}(\bar{V}_{lk} - \bar{V}^*) \quad \text{where } (N-J) \le \bar{x}_{lk} \le (N-J+1) \end{aligned} \tag{6.7}$$

and for capsule position control,

$$\begin{aligned}\bar{F}_{lk} = & \frac{\beta}{2m_d} C_D(V_{lk}, w_{lJ})(\bar{V}_{lk} - \bar{w}_{lJ})^2 \mathrm{sgn}(\bar{V}_{lk} - \bar{w}_{lJ}) \\ & + \bar{M}_{lk}\bar{g}\sin\theta_{lJ} + f_r(\bar{M}_{lk}\bar{g}\cos\theta_{lJ} + \bar{F}_{N_{lk}}) \\ & - K_1\bar{M}_{lk}(\dot{\bar{x}}_{lk} - \dot{\bar{x}}^*) - K_2\bar{M}_{lk}(\bar{x}_{lk} - \bar{x}^*) \\ & \text{where } (N-J) \le \bar{x}_{lk} \le (N-J+1) \end{aligned} \tag{6.8}$$

There are two control issues: regulation of capsule speed or position, and optimization of capsule operation efficiency. In Chapter 5, it was explained that the capsule speed should be at the optimal electrical efficiency speed for a given synchronous speed V_s. In other words, the synchronous speed V_s should be varied so that the desired speed is always the optimal speed for LIM electrical efficiency. We can then vary the maximum thrust force $F_{\max}$ to maintain a desired speed. The above feedback control laws can be easily computed assuming the current level of computer technologies.

6.3 Examples of Numerical Simulations

The simulation program can be used to simulate essentially any schedules of capsule operation. For example, capsules' entering times into pipeline systems, and capsule speeds, weights, and payloads can all be specified individually for different capsules. Here, we use a specific scenario to show the working of capsule feedback control laws.

In this scenario, the pipeline length is $L_P = 10,000$ m, and there are $N = 40$ sections. Two capsules are injected into the right bore with 10 second intervals. Initial capsule speeds are both zero. A zero level pipeline grade is assumed, and the rated thrust is $F_R = 6000$ N. Gross weights and payloads are the same as in Table 5.1. In these simulations, open vents are assumed. As a result, flow speeds on the left bore are zero.

Figure 6.3 shows the speed history of the leading capsule. It shows the feedback control of capsule speed is working. Figure 6.4 shows the corresponding thrust history. Initially, the required thrust is large and the rated thrust is used. After the capsule establishes the

steady operating speed at $V_d = 25$ m/s, the LIM thrust reduces to about 3000 N. Note this thrust is higher than the steady-state thrust at design conditions. This is because in the current simulation, the left bore is empty and the flow speeds are smaller than steady-state design value; causing the drag on capsules to be larger. Figure 6.5 shows the corresponding capsule position history.

Figure 6.6 plots the flow velocity at the first section. There are 40 sections in this simulation and the first section is arbitrarily selected. It shows that entering capsules increase flow speed at the first section. But after the capsules pass, the flow speed decays to zero.

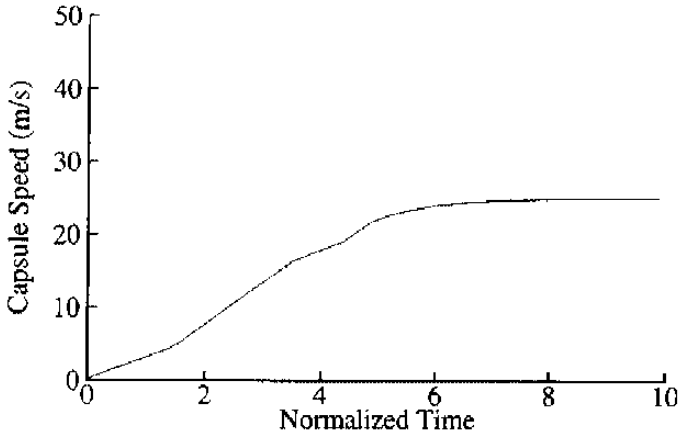

Figure 6.3 Speed History of Leading Capsule

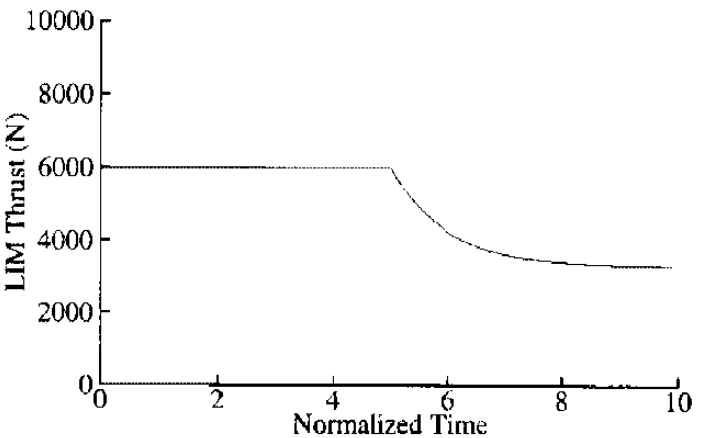

Figure 6.4 Thrust History of Leading Capsule

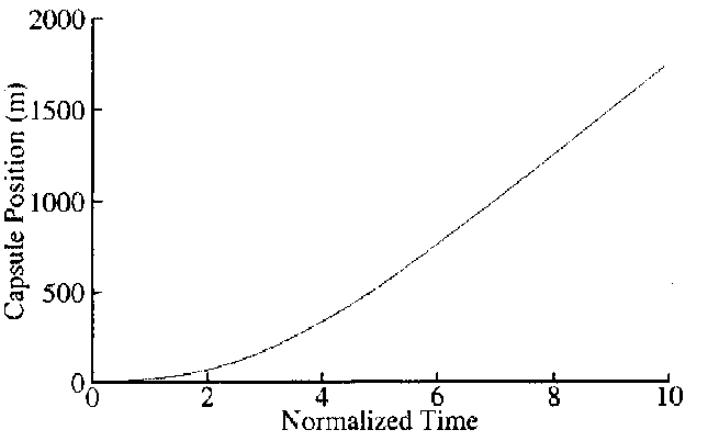

Figure 6.5 Position History of Leading Capsule

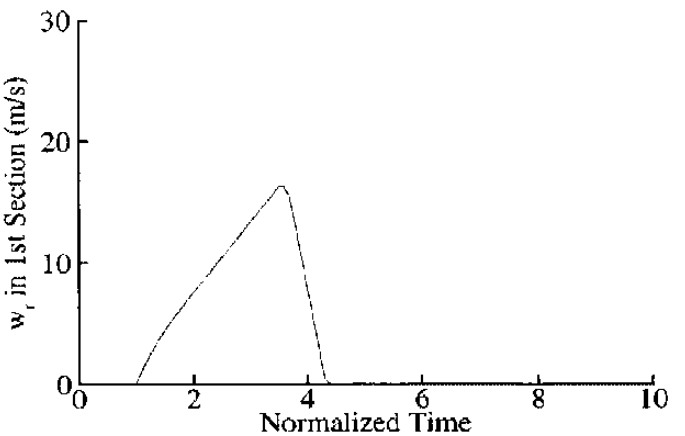

Figure 6.6 Flow Speed at the First Section

7. Conclusions and Recommendations for Future Research

7.1 Summary of Results

In this report, related work on pneumatic pipelines and electrical pipelines are first reviewed. The inherent advantage of an electrical pipeline system over a pneumatic pipeline system is established. Then, models of individual components in an electrical pipeline system are studied. In particular, an expression for the drag coefficient of capsule motion inside pipetube is developed. An overview of principles of linear electric motors are provided, followed by performance models of linear induction motors. Coefficient of rolling friction is examined.

Based on the results of component modeling, several concepts of electrical freight pipeline system configuration are presented and compared. Each configuration specifies the choice of linear electric motors, locations of primary and secondary units, and power supply needs. A linear induction motor pipeline system with moving primaries are selected. Based on this configuration, designs of capsule and pipetubes are conducted. A wheel-on-rail configuration is used.

Then, equations for capsule motions and pipeline flow are developed. An analysis and computational method for use in the design of electrical freight pipeline systems are developed. The methods can be used for two-bore systems, of any length and diameter, connected at intervals by adits or vented. A comprehensive computer simulation program is developed that allows for arbitrary schedules of capsule entrance into and/or departure from a pipeline system. In addition, feedback control laws are designed for capsule speed and position control. Numerical simulations are conducted using the computer program to demonstrate the working of feedback control laws. During the numerical simulations, specific examples are used. Our examples have centered on 2 m diameter tubes, a size which is suitable for general freight, carrying 10 ton capsules at the relatively low speed of 25 m/s with 2 sec headway. When the tubes are operating at capacity we refer to this as "design conditions" and relate off-design operational costs to this ideal.

7.2 Conclusions

Conceptual analysis demonstrates that the electrical freight pipeline concept is feasible and offers a list of potential benefits in terms of safety, reduction of ground traffic, environmental impact, and cost. Necessary technologies for such a system have already existed. Potential problems to construct such a system are initial capital investment and heating. The heating problem can be alleviated by the use of open vents, which also result in low operating costs.

Theoretical analysis shows that there is an intrinsic advantage, in terms of energy use, of this kind of system over pneumatically propelled systems if the capsules have moderate blockage, since some of the air set in motion by the capsules can pass over the capsules. For a blockage of .5, which can be achieved without making the tube larger, by using capsules of square section, the aerodynamic cost is about half that for pneumocapsules.

Potential cost problems arise when the system is not operating at full capacity; the aerodynamic cost per ton-mi would be 4 to 9 times the optimum if the traffic were at 10% of capacity. This situation is much improved if the tubes are connected by adits or are vented, provided the traffic management strategy is to run platoons of capsules at the design headway, followed by long intervals with no traffic. If the physical length of the platoons is much longer than the spacing between adits the cost per ton-mi is only 50% greater than the optimum, and only 10% greater if vents are used instead. The advantage comes from circulating the driven air through the other tube, or diverting it to atmosphere, eliminating the necessity of pushing it at high speed all the way through the tubes.

7.3 Recommendations for Future Research

This report represents one of very few technical studies on the concept of electrical freight pipeline systems. As a result, system analysis and system design are inevitably mixed together. In this report, necessary design decisions are made in order to facilitate the development of theoretical analysis methods. Studies on system configurations not pursued in this report as well as issues for advanced studies on the proposed configuration

would provide further details on the concept, design, and operation of electrical freight pipeline systems. Some recommendations for further research include the following issues.

1. Examination of the use of other linear electric motors. In this study, the use of linear induction motor is assumed for its low cost and robustness. Other transportation needs may require the use of different types of linear electric motors. Further conceptual studies of various motors can provide in-depth comparisons of relative merits of different motors.

2. Further studies of system component modeling may be needed if such an electrical freight pipeline system were to be built. In particular, three-dimensional modeling of capsule and flow motions are needed for an actual system design that consists of large angle turns.

3. Modeling and control of heat generated by linear electric motors as well as aerodynamic resistance need to be studied for underground pipeline systems that are buried deeply underneath the ground.

4. Stochastic simulation of capsule motions is an important way of studying pipeline system performance in actual operations. In this type of studies, capsule schedules are randomly generated on a computer and operating performances are stochastically averaged.

5. A specific electrical pipeline system can be designed for a specified transportation corridor, tonnage requirement, and preferred speeds. A small-scale prototype experimental pipeline system should be developed and studied before an actual system can be built.

References

[1]. U.S. Department of Transportation, Bureau of Transportation Statistics, *National Transportation Statistics*, Annual Report, September, 1993, Historical Compendium, 1960-1992.

[2]. U.S. Congress, *Intermodal Surface Transportation Efficiency Act of 1991*, Public Law 102-240, December 18, 1991.

[3]. Medhurst, George A., *A New System of Inland Conveyance for Goods and Passengers*, London, 1827.

[4]. U.S. Department of Transportation, *Tube Transportation*, RSPA/VNTSC-SS-HW495-01, February 1994.

[5]. Wheatstone, C., British Patent No. 9022, 1841.

[6]. Laithwaite, Eric R., *A History of Linear Electric Motors*, McaMillian Education Ltd., 1987.

[7]. McLean, G. W., "Review of Recent Progress in Linear Motors," *IEE Proceedings*, Vol. 135, Part B, No. 6, November 1988, pp. 380-416.

[8]. Gibbon, M. A. and Parker, J. H., "Operational Experience with a LIM-Drive Transit System," *Proceedings of International Conference on Maglev and Linear Drives*, 1986, pp. 135-140.

[9]. Menadovic, V., "Maglev Transit Link for Birmingham Airport," *Proceedings of International Conference on Maglev Transport*, Birmingham, IMechE, UK, 1984, pp. 169-176.

[10]. McGeough, P. A., and Sutton, A., "Birmingham Airport Maglev Vehicle Construction," ibid, pp. 177-184.

[11]. Linacre, H., Chahal, J. S., Crawshaw, J. S., and Rawlinson, B., "Birmingham Airport Propulsion System," ibid, pp. 193-201.

[12]. Suzuki, S., Murai, M., Kawashima, M., and Hosoda, Y., "HSST-03 System Operational Summary at Expo '85 and Operational Outline at Expo '86," *Proceedings of International Conference on Maglev and Linear Drives*, 1986, IEEE Cat. 86CH2276-4, pp. 217-230.

[13]. Friedrich, R., Dreiman, K., and Leistikow, R., "The Power Supply and the Propulsion System of the Transrapid 06 Vehicle Results of Trials," ibid, pp. 243-249.

[14]. Washington Post, "Germany's Magnetic Levitation Train Fuels Environmental Fears," published by Star Tribune, Sunday, April 26, 1998, Page 15.

[15]. Vandersteele, W., "The Future of Our Transportation Infrastructure," Ampower Corporation, North Bergen, N. J., 07047, 1993. Also, U.S. Patent No. 4,458,602 - Pneumatic Capsule Pipeline System, 1984.

[16]. "Vacuum Technology Weighed for Swiss Maglev Proposal", *Maglev News*, Vol. 1, No. 15, May 17, 1993.

[17]. "New Millennium Seeks Support From NMI Officials." *Maglev News*, Vol. 1, March 22, 1993.

[18]. Email communication with a researcher in the Netherlands, 1997.

[19]. Fujisawa, T., Misago, T. Araki, O. & Goriki, T. (1994) "Development of Linear Tube Transportation System," *NKK Technical Review*, No. 70, pp. 25-32. (Available from National Technical Information System, Springfield, VA)

[20]. Fujisawa, Tomoji, et al., "Linear Tube Transportation System – Second Report," *NKK Technical Review*, No. 76, July 1997, pp. 49-55.

[21]. *First National Conference on Street and Highway Safety*, Hon. Herbert Hoover Secretary of Commerce, Chairman, Washington, D.C., December 15-16, 1924.

[22]. Fox, Robert, and McDonald, Alan, *Introduction to Fluid Mechanics*, John Wiley & Sons Inc., 4th edition, 1992.

[23]. Schlichting, H, *Boundary Layer Theory*, 7th edition, McGraw-Hill, 1979.

[24]. Tsuji, Y., "Fluid Mechanics of Pneumatic Capsule Transport," *Bulk Solids Handling*, Vol. 5, No. 3, June, 1985, pp. 653 - 661.

[25]. Anderson, John D., *Fundamentals of Aerodynamics*, second edition, McGraw-Hill, Inc., 1991. pp. 516-518.

[26]. Hammitt, A. G., "Unsteady Aerodynamics of Vehicles in Tubes," *AIAA Journal*, Vol. 13, No. 4, April, 1975, pp. 497-503.

[27]. Tsuji, Y., Morikawa, Y., and Seki, W., "Velocity Control in a Capsule Pipeline by Changing the Area of the End-Plate," *Journal of Pipelines*, Vol. 5, 1985, pp. 147-153.

[28]. Sen, P. C., *Principles of Electric Machines and Power Electronics*, second edition, John Wiley & Sons, Inc., 1997.

[29]. Boldea, I. and Nasar, S. A., *Linear Electric Machines*, John Wiley & Sons, 1976.

[30]. Cory, S. A., "The Nature of Linear Induction Motors," *Machine Design*, August 23, 1984, pp. 111 - 113.

[31]. Gieras, Jacek F., *Linear Induction Drives*, third edition, Oxford Science Publications, 1994.

[32]. Poloujadoff, M., *The Theory of Linear Induction Machinery*, Oxford University Press, 1980.

[33]. Nasar, S. A., editor, *Handbook of Electric Machines*, McGraw-Hill Book Company, 1987.

[34]. Laithwaite, E. R., editor, *Transport Without Wheels*, Westview Press, Inc., 1898 Flation Court, Boulder, Colorado 80301, 1977.

[35]. Ludema, Kenneth C., *Friction, Wear, Lubrication*, A Textbook in Tribology, CRC Press, Inc., 2000 Corporate Blvd., NW, Boca Raton, Florida 33431, 1996.

[36]. Glaeser, William A., *Characterization of Tribological Materials*, Manning Publications Co., 3 Lewis Street, Greenwich, CT 06830, 1993.

[37]. Williams, J. A., *Engineering Tribology*, Oxford University Press, 1994, Chapter 3.

[38]. Blau, Peter J., *Friction Science and Technology*, Marcel Dekker, Inc., 1996.

[39]. Avallone, E. A., and Baumeister, T., III, editors, *Mark's Standard Handbook for Mechanical Engineers*, 9th edition, McGraw-Hill, New York, 1987.

[40]. Edminister, J. A., *Electromagnetics*, second edition, Schaum's Outline Series, McGraw-Hill, 1993, Chapter 14.

[41]. Ampower Corporation (1984), "Pneumatic Capsule Pipeline System," U.S. Patent No. 4,458,602.

[42]. Gawthorpe, R. G., Pope, C.W. & Green, R.H. (1979), "Analysis of train drag in various configurations of long tunnels," Proc. 3rd Int. Symposium on the Aerodynamics and Ventilation of Vehicle Tunnels, BHRA Fluid Engineering, Cranfield,Bedford, England, 257-280.

[43]. Henson, D.A. and Bradbury,W.M.S. (1991),"The aerodynamics of channel tunnel trains", Int. Symp. on Aerodynamics and Ventilation of Vehicle Tunnels (7th: 1991: Brighton, England) ed. Haerter, A. , 927–956. Elsevier.

[44]. Bernard, K. (1993) " Eurotunnel - design and implementation" High Speed Ground Transportation Systems I: Proc. First Int. Conf. on High Speed Ground Transportation (HSGT) Systems. ed. Bondada, M.V.A. and Wayson, R.L., ASCE N.Y., 405–416.

[45]. Assadollahbaik, M. and Liu, H. (1986), "Optimum Design of Electrodynamic Pump for Capsule Pipelines," *Journal of Pipelines*, **5**, 157-169.

[46]. Assadollahbaik, M. Liu, H. and Hoft, R. G. (1986), "Experiments on an Electromagnetic Capsule Pump," *Journal of Energy Resources Technology*, **108**, 262-268.

[47]. Hammitt, A. G. (1972), "Aerodynamic Analysis of Tube Vehicle Systems," *AIAA Journal*, **10**, 1972, 282-290.

[48]. Liu, H. and Rathke, J. E. (1976), "Electromagnetic Capsule Pumps," International Symposium on Freight Pipelines, Washington, D.C.

[49]. Round, G.F. & Marcu, M.I. (1987),"Pneumocapsule Pipelines: Potential for North America," *J. Pipelines*, **6**, 221-238.

[50]. Vance, L. & Mills, M.K. (1994), "Tube Freight Transportation," *Public Roads*, **58**, 21-27. (U.S. Dept. of Transportation, ISSN 0033-3736; USPS 516-690)

[51]. Zandi, I. (1976), "Transport of Solid Commodities via Freight Pipelines," U.S. DOT Report No. DOT-TST-76T-39.

[52]. Slotine, J. -J., and Li, Weiping, *Applied Nonlinear Control*, Prentice Hall, 1991.

APPENDIX A

CAPSULE EQUATIONS OF MOTION

Capsule Equations of Motion

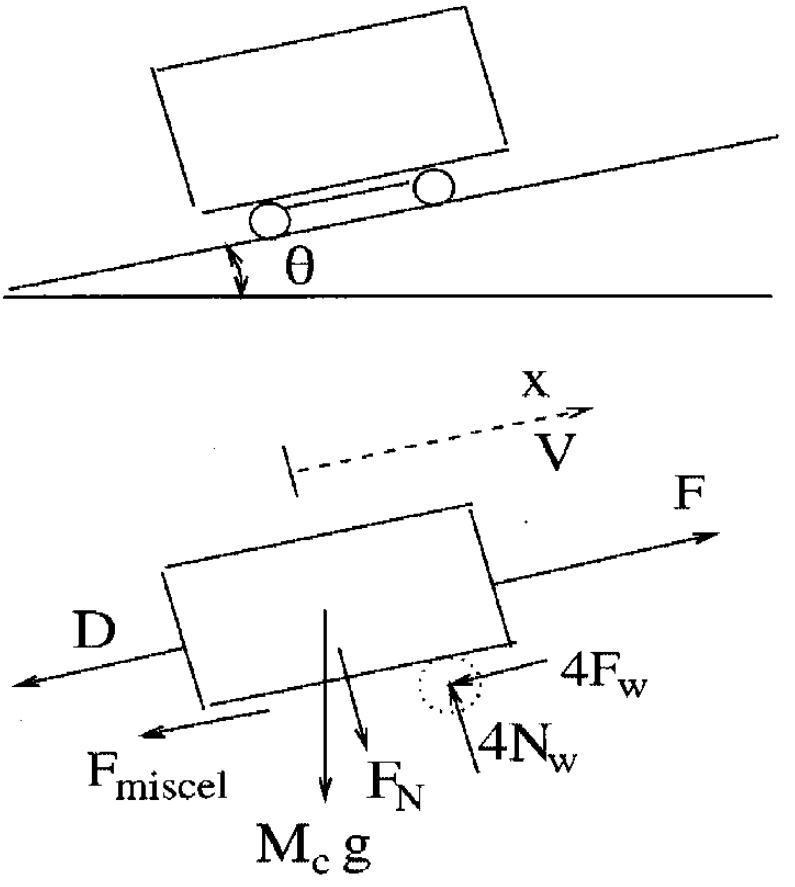

Figure A.1 Capsule Free-Body Diagram

Figure A.1 shows the free-body diagram of a capsule in motion. It is assumed that the capsule has four wheels and forces on the four wheels are balanced. In other words, the four wheels support the capsule weight equally and produce the same amount of rolling frictions. The linear induction motor exerts both a thrust force F and a normal force F_N on the capsule. The normal force is attractive if $F_N > 0$, and is repulsive if $F_N < 0$.

Based on Newton's Second Law, we have

$$M_c\ddot{x} = F - D - M_c g \sin\theta - 4F_w - \Delta F \qquad (A.1)$$

Vertical force balance gives

$$M_c g \cos\theta + F_N = 4N_w \tag{A.2}$$

Therefore,

$$N_w = \frac{1}{4}(M_c g \cos\theta + F_N) \tag{A.3}$$

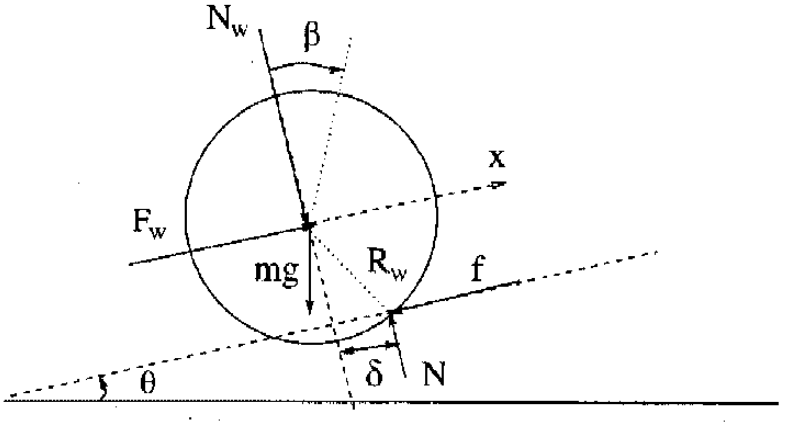

Figure A.2 Free-Body Diagram of an Individual Wheel

Figure A.2 shows the free-body diagram of an individual wheel. Balances of forces and moment give

$$m\ddot{x} = F_w - mg\sin\theta - f \tag{A.4}$$

$$I_w\ddot{\beta} = fR_w - N\delta \tag{A.5}$$

$$N = N_w + mg\cos\theta \tag{A.6}$$

where δ is caused by rolling friction on the wheel.

Because thrust forces produced by linear induction motors do not depend on adhesions, it is assumed that the wheels roll without sliding (no traction). Therefore

$$\dot{x} = R\dot{\beta} \tag{A.7}$$

We have from Eqs. $(A.5)$ and $(A.7)$,

$$\frac{I_w}{R_w^2}\ddot{x} = f - \frac{\delta}{R_w}N \tag{A.8}$$

Adding Eq. $(A.8)$ to Eq. $(A.4)$ and using Eq. $(A.6)$ result in

$$\left(m + \frac{I_w}{R_w^2}\right)\ddot{x} = F_w - mg\sin\theta - \frac{\delta}{R_w}(N_w + mg\cos\theta) \tag{A.9}$$

or

$$4F_w = 4\left(m + \frac{I_w}{R_w^2}\right)\ddot{x} + 4mg\sin\theta + \frac{\delta}{R_w}(M_c g\cos\theta + F_N + 4mg\cos\theta) \tag{A.10}$$

Substituting Eq. $(A.10)$ into Eq. $(A.1)$, we obtain

$$\left(M + \frac{4I_w}{R_w^2}\right)\ddot{x} = F - D - Mg\sin\theta - \Delta F - \frac{\delta}{R_w}(Mg\cos\theta + F_N)\mathbf{1}(Mg\cos\theta + F_N) \tag{A.11}$$

where $\mathbf{1}(z)$ is a step function

$$\mathbf{1}(z) = \begin{cases} 1 & z > 0 \\ 0 & z \leq 0 \end{cases} \tag{A.12}$$

Capsule weight is usually much larger than the normal force F_N, and than the rolling contribution $4I_w/R_w^2$, we have

$$M\ddot{x} = F - D - Mg\sin\theta - \Delta F - f_r(Mg\cos\theta + F_N) \tag{A.13}$$

where

$$f_r = \frac{\delta}{R_w} = \text{rolling friction coefficient}$$

APPENDIX B

CAPSULE DRAG COEFFICIENT

Capsule Drag Coefficient

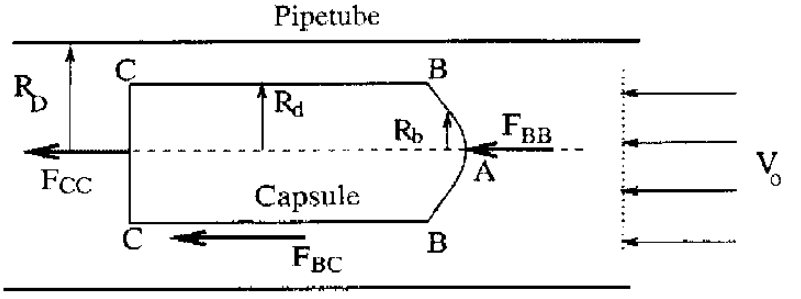

Figure B.1 Determination of Capsule Aerodynamic Drag

Figure B.1 shows the drag determination method used in this analysis. The total aerodynamic drag on a capsule inside a pipetube is divided into three components: the inviscid pressure drag caused by high pressure on the capsule nose and low base pressure at the rear, a viscous contribution caused by shear stresses in the high speed gap region between the capsule and the tube wall, and a contribution due to a viscous pressure drop in this gap which causes an additional decrease in the base pressure. These effects are now studied term by term.

(1) The momentum integral theorem provides a formula for inviscid drag. For steady flow in a reference frame attached to the capsule

$$D_i = \int_{upstream,a} (p + \rho u^2) dA - \int_{rear face,e} (p + \rho u^2) dA$$

$$= A_T(p_a + \rho V^2) - (p_e A_T + (A_T - A)\rho w^2) \qquad (B.1)$$

where w is the velocity in the gap, V is the approach velocity at the upstream station a, A_T is the tube area, A is the capsule area, and p_e is the pressure in the gap which is assumed to be the same over the whole capsule rear face, where the velocity is zero. By the Bernoulli equation [22],

$$p_a + \frac{1}{2}\rho V^2 = p_e + \frac{1}{2}\rho w^2 \qquad (B.2)$$

and by conservation of mass

$$VA_T = w(A_T - A) \tag{B.3}$$

By eliminating w from the last two equations, we find

$$p_a - p_e = \frac{1}{2}\rho V^2 \left(\frac{A_T^2}{(A_T - A)^2} - 1 \right) \tag{B.4}$$

Using this and w from Eq. $(B.3)$ gives

$$D_i = \frac{1}{2}\rho V^2 A C_{Di} \tag{B.5}$$

with

$$C_{Di} = \beta/(1-\beta)^2 \tag{B.6}$$

where β is the blockage area ratio.

$$\beta \triangleq A/A_T \tag{B.7}$$

(2) The shear stress contribution may be obtained by assuming that the gap is small compared to the length l of the capsule and that the flow in the gap is like a turbulent channel flow. In this case

$$D_f = C_f \frac{1}{2}\rho w^2 2\pi R l \tag{B.8}$$

where C_f is a friction coefficient (per Schlichting [23]). Using Eq. $(B.3)$ for w gives

$$D_f = C_f \frac{1}{2}\rho V^2 \left(\frac{A_T}{A_T - A} \right)^2 2\pi R l \tag{B.9}$$

and therefore

$$C_{Df} = \frac{C_f}{(1-\beta)^2} \frac{2l}{R} \tag{B.10}$$

(3) The pressure drop in the annular channel is given by

$$\Delta p(A_T - A) = C_f \frac{1}{2}\rho w^2 2\pi (R + R_T) l \tag{B.11}$$

or

$$\Delta p = \frac{1}{2}\rho V^2 \left(\frac{A_T}{A_T - A}\right)^2 \frac{2l}{R_T - R} C_f \qquad (B.12)$$

Since this lower pressure is felt over the whole rear face, the additional drag is

$$D_{\Delta p} = A\Delta p = \frac{1}{2}\rho V^2 A \left(\frac{1}{1-\beta}\right)^2 \frac{2l}{R_T - R} C_f \qquad (B.13)$$

and this gives

$$C_{D\Delta p} = \frac{1}{(1-\beta)^2} \frac{2l}{R_T - R} C_f \qquad (B.14)$$

Combining these into a single drag coefficient one finds

$$\begin{aligned} C_D &= C_{Di} + C_{Df} + C_{D\Delta p} \\ &= \frac{\beta}{(1-\beta)^2} + \frac{(1+\beta^{1/2})}{(1-\beta)^3} \frac{2l}{R} C_f \end{aligned} \qquad (B.15)$$

where C_f depends on the Reynolds number in the gap.

When applied to a situation where the capsule has velocity V and the tube carries air with velocity w one should calculate the drag using the relative velocity, i.e.

$$D = C_D \frac{1}{2}\rho (V - w)^2 A \qquad (B.16)$$

using Eq. $(B.15)$ for the drag coefficient.

In the above, the concept of hydraulic diameter is used. For a given cross section, the hydraulic diameter is defined as four times the cross-sectional area divided by wetted perimeter. For a cylindrical vehicle, the hydraulic diameter is the same as the diameter

$$D_H = \frac{4\pi R^2}{2\pi R} = 2R = D$$

For a capsule with a rectangular cross-section of width w and height h,

$$D_H = \frac{4wh}{2(w+h)} = \frac{2wh}{w+h}$$

which reduces to $w = h$ for a square cross section.

APPENDIX C

MODELING OF LINEAR INDUCTION MOTOR EFFICIENCY

Modeling of Linear Induction Motor Efficiency

This Appendix provides a simple model of linear induction motor efficiency in the form of

$$\eta_e = \eta_e(V; V_s, \eta_{\max}, V_{\max,e}) \tag{C.1}$$

This model is valid for LIM operation in the motor mode. In other words

$$V \leq V_s \tag{C.2}$$

Figure C.1 shows a typical LIM efficiency. We approximate the first part by a linear function of speed, and the second part by a quadratic function.

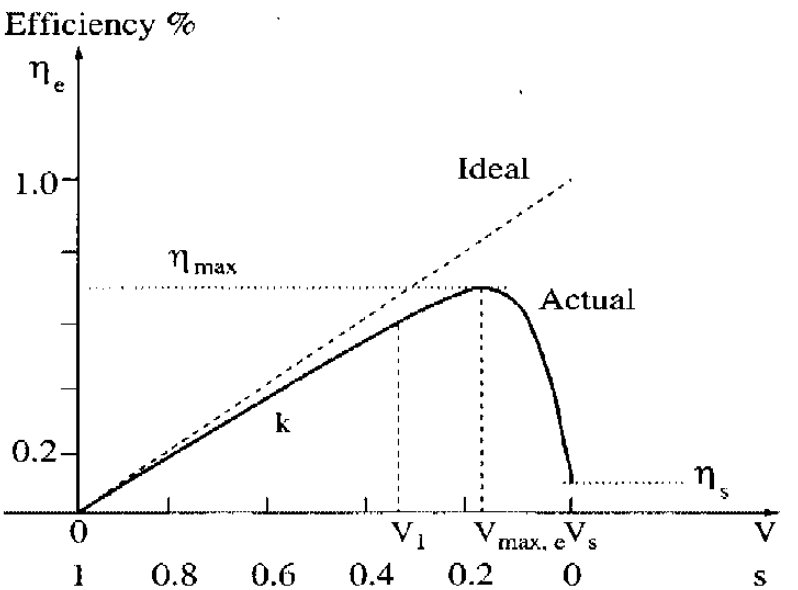

Figure C.1 LIM Operational Efficiency

Define a normalized speed

$$u = \frac{V}{V_s} \qquad u_{\max} = \frac{V_{\max,e}}{V_s} \tag{C.3}$$

The above LIM operating efficiency can be expressed mathematically as follows.

$$\eta_e(u) = \begin{cases} ku & 0 \leq u \leq u_1 \\ \eta_{\max} - c(u - u_{\max})^2 & u_1 \leq u \leq 1 \end{cases} \tag{C.4}$$

where $k > 0$ is the slope of the linear part, and $c > 0$.

Let us first assume that $\eta_{\max}$, $u_{\max}$, and u_1 are given and we need to determine k and c from continuity conditions. To insure that the linear part and the quadratic part are smoothly connected, we require that values of the function as well as first-order derivatives match at $u = u_1$, Mathematically,

$$ku_1 = \eta_{\max} - c(u_1 - u_{\max})^2$$

$$k = -2c(u_1 - u_{\max})$$

Solving these two equations for k and c, we obtain

$$k = \frac{2\eta_{\max}}{u_1 + u_{\max}} \tag{C.5}$$

$$c = \frac{\eta_{\max}}{u_{\max}^2 - u_1^2} \tag{C.6}$$

At $V = V_s$ or $u = 1$,

$$\eta_e(1) = \eta_{\max} - c(1 - u_{\max})^2 = \eta_{\max}\frac{2u_{\max} - 1 - u_1^2}{u_{\max}^2 - u_1^2} \triangleq \eta_s \tag{C.7}$$

If we require that $\eta_s = 0$, u_1 is also determined. In this case, one only needs to specify $\eta_{\max}$ and $u_{\max}$, and all other parameters are determined. Specifically,

$$u_1 = \sqrt{2u_{\max} - 1} \tag{C.8}$$

$$k = \frac{2\eta_{\max}}{u_1 + u_{\max}} \tag{C.5}$$

$$c = \frac{\eta_{\max}}{(1 - u_{\max})^2} \tag{C.9}$$

With typical performance numbers

$$u_{\max} = 0.7 \sim 0.8$$

$$\eta_{\max} = 0.5$$

we have

$$u_1 = 0.632 \sim 0.775$$

$$k = 0.75 \sim 0.63$$

$$c = 5.56 \sim 12.5$$

APPENDIX D

SOLUTION OF A TRIDIAGONAL SYSTEM OF EQUATIONS

Solution of A Tridiagonal System of Equations

With $\bar{p}_1$ and $\bar{p}_{N+1}$ given, the pressure equations become

$$\bar{p}_1 - 2\bar{p}_2 + \bar{p}_3 = f_2 \qquad (D.1)$$

$$\bar{p}_2 - 2\bar{p}_3 + \bar{p}_4 = f_3 \qquad (D.2)$$

$$\bar{p}_3 - 2\bar{p}_4 + \bar{p}_5 = f_4 \qquad (D.3)$$

$$\bar{p}_4 - 2\bar{p}_5 + \bar{p}_6 = f_5 \qquad (D.4)$$

$$\vdots$$

$$\bar{p}_{N-3} - 2\bar{p}_{N-2} + \bar{p}_{N-1} = f_{N-2} \qquad (D.N\text{-}3)$$

$$\bar{p}_{N-2} - 2\bar{p}_{N-1} + \bar{p}_N = f_{N-1} \qquad (D.N\text{-}2)$$

$$\bar{p}_{N-1} - 2\bar{p}_N + \bar{p}_{N+1} = f_N \qquad (D.N\text{-}1)$$

Adding all equations together, we obtain

$$\bar{p}_1 - \bar{p}_2 - \bar{p}_N + \bar{p}_{N+1} = \sum_{k=2}^{N} f_k$$

or

$$\bar{p}_2 + \bar{p}_N = \bar{p}_1 + \bar{p}_{N+1} - \sum_{k=2}^{N} f_k \qquad (D.N)$$

Adding $(D.1) + 2(D.2)$, we obtain

$$-3\bar{p}_3 + 2\bar{p}_4 = f_2 + 2f_3 - \bar{p}_1 \qquad (D.2)'$$

Adding $(D.2)' + 3(D.3)$, we obtain

$$-4\bar{p}_4 + 3\bar{p}_5 = f_2 + 2f_3 + 3f_4 - \bar{p}_1 \qquad (D.3)'$$

Adding $(D.3)' + 4(D.4)$, we obtain

$$-5\bar{p}_5 + 4\bar{p}_6 = \sum_{k=2}^{5}(k-1)f_k - \bar{p}_1 \qquad (D.4)'$$

Repeating these steps, we have

$$-j\bar{p}_j + (j-1)\bar{p}_{j+1} = \sum_{k=2}^{j}(k-1)f_k - \bar{p}_1 \qquad (D.j\text{-}1)'$$

and by induction, for $i = 2, \ldots, N-1$,

$$-i\bar{p}_i + (i-1)\bar{p}_{i+1} = \sum_{k=2}^{i}(k-1)f_k - \bar{p}_1$$

In particular, for $i = N-1$,

$$-(N-1)\bar{p}_{N-1} + (N-2)\bar{p}_N = \sum_{k=2}^{N-1}(k-1)f_k - \bar{p}_1 \qquad (D.N\text{-}2)'$$

From Eq. $(D.N\text{-}1)$,

$$(N-1)\bar{p}_{N-1} - 2(N-1)\bar{p}_N + (N-1)\bar{p}_{N+1} = (N-1)f_N \qquad (D.N\text{-}1)'$$

Adding the previous two equations together, we have

$$-N\bar{p}_N = \sum_{k=2}^{N}(k-1)f_k - \bar{p}_1 - (N-1)\bar{p}_{N+1}$$

or

$$\bar{p}_N = \frac{1}{N}\left(\bar{p}_1 + (N-1)\bar{p}_{N+1} - \sum_{k=2}^{N}(k-1)f_k\right) \qquad (D.N\text{+}1)$$

Combining with Eq. $(D.N)$, we obtain

$$\bar{p}_2 = \frac{N-1}{N}\bar{p}_1 + \frac{1}{N}\bar{p}_{N+1} + \sum_{k=2}^{N}\left(\frac{k-1}{N} - 1\right)f_k$$

Solutions

Therefore, the solution to the original tridiagonal system of equations is

$$\bar{p}_2 = \frac{N-1}{N}\bar{p}_1 + \frac{1}{N}\bar{p}_{N+1} + \sum_{k=2}^{N}\left(\frac{k-1}{N} - 1\right)f_k \qquad (D.N\text{+}2)$$

and for $k = 3, \ldots, N$,

$$\bar{p}_k = f_{k-1} - \bar{p}_{k-2} + 2\bar{p}_{k-1} \qquad (D.N\text{+}3)$$

APPENDIX E

PIPELINE DOWNSLOPE AND UPSLOPE

Pipeline Downslope and Upslope

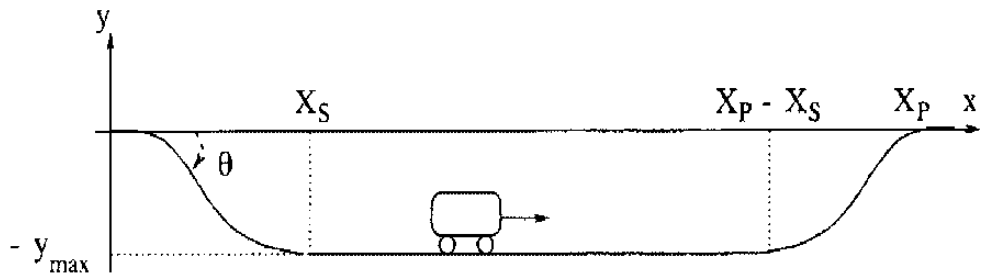

Figure E.1 Pipeline Grade Design

The pipeline grade at the start of capsule motion can be approximated as

$$y = \frac{1}{2} y_{\max} \left[\cos\left(\frac{\pi x}{X_S} \right) - 1 \right] \tag{E.1}$$

for $0 \le x \le X_S$, where $y_{\max} > 0$ is the pipeline depth under the ground. The slope angle can be determined from

$$\tan\theta = \frac{dy}{dx} = -\frac{\pi y_{\max}}{2X_S} \sin\left(\frac{\pi x}{X_S} \right) \tag{E.2}$$

In particular, the maximum slope angle is achieved at $x = 0.5X_S$ and is

$$\tan\theta_{\max} = -\frac{\pi y_{\max}}{2X_S} \tag{E.3}$$

Therefore, one only needs to specify two of the three variables: $y_{\max}$, $\theta_{\max}$, and X_S.

The pipeline grade at the arrival side of a pipeline can be designed by symmetry. We have

$$y = \frac{1}{2} y_{\max} \left[\cos\left(\frac{\pi(X_P - x)}{X_S} \right) - 1 \right] \tag{E.4}$$

for $X_P \ge x \ge X_P - X_S$.

In summary, the vertical pipeline profile is specified by

$$y = \begin{cases} 0.5 y_{\max} \left[\cos\left(\frac{\pi x}{X_S} \right) - 1 \right] & 0 \le x \le X_S \\ -y_{\max} & X_S \le x \le X_P - X_S \\ 0.5 y_{\max} \left[\cos\left(\frac{\pi (X_P - x)}{X_S} \right) - 1 \right] & X_P - X_S \le x \le X_P \end{cases} \tag{E.5}$$

The slope curve is defined as

$$\tan\theta = \begin{cases} -0.5\frac{\pi y_{\max}}{X_S}\sin\left(\frac{\pi x}{X_S}\right) & 0 \le x \le X_S \\ 0 & X_S \le x \le X_P - X_S \\ 0.5\frac{\pi y_{\max}}{X_S}\sin\left(\frac{\pi(X_P - x)}{X_S}\right) & X_P - X_S \le x \le X_P \end{cases} \tag{E.6}$$

For example, $X_S = 40\text{m}$, $y_{\max} = 3\text{m}$, and $\theta_{\max} = 6.7^o$.

The speed command can be

$$V_c = \begin{cases} V_d & x \le X_P - X_S \\ V_d\frac{X_P - x}{X_S} & X_P - X_S \le x \le X_P \\ 0 & x \ge X_P \end{cases} \tag{E.7}$$

The second part of the speed command can also be set to zero.

Office of Research & Strategic Services
395 John Ireland Blvd., Mail Stop 330
Saint Paul, Minnesota 55155

(651) 282-2274